IMPROVED EEG SIGNAL ANALYSIS TECHNIQUES FOR EPILEPTIC SPIKE DETECTION AND ARTIFACT EXCISION

A THESIS

SUBMITTED IN FULFILLMENT OF THE REQUIREMENT

FOR THE AWARD OF DEGREE OF

DOCTOR OF PHILOSOPHY

IN

ELECTRONICS AND COMMUNICATION ENGINEERING

SUBMITTED BY

GARG HARISH KUMAR

SUPERVISOR

DR. AMIT KUMAR KOHLI

(ASSOCIATE PROFESSOR)

ELECTRONICS AND COMMUNICATION ENGINEERING DEPARTMENT

THAPAR UNIVERSITY, PATIALA-147004, PUNJAB, INDIA

2016

CERTIFICATE

I, **Garg Harish Kumar,** hereby declare that the thesis entitled, **"Improved EEG Signal Analysis Techniques for Epileptic Spike Detection and Artifact Excision,"** submitted to Thapar University, Patiala, in partial fulfillment of the requirement for the award of the Degree of **Doctor of Philosophy** in **the Electronics and Communication Engineering** is a record of original and independent research work done by me during 2011-2016. This thesis has been conducted under the guidance of **Dr. Amit Kumar Kohli**, Associate Professor, Electronics and Communication Engineering Department, Thapar University. Moreover, it has not formed the basis for the award of any Degree/Diploma/Associateship/Fellowship or other similar title to any candidate of any university.

Harish Garg

Garg Harish Kumar

(Signature of Candidate) Date: December, 2016

This is to certify that above statement made by the candidate is correct to the best of my knowledge.

Amit Kohli 30/12/16

Dr. Amit Kumar Kohli

(Signature of Supervisor)

Associate Professor,

Electronics and Communication Engineering Department,

Thapar University, Patiala-147004,

Punjab, India.

ABSTRACT

Electroencephalography is the most common noninvasive technique utilized for monitoring the electrical brain activity and inferring brain function, in which the recorded signal traces represent an electric signal from a large number of neurons. The main goal of electroencephalogram (EEG) signal analysis is to infer functional connectivity between different brain areas, which is directly useful for neuroscience and clinical investigations. Due to its potentially complex nature and due to the presence of epileptic-spikes (ESs), ocular-artifacts (OAs) and inevitable additive-white-Gaussian-noise (AWGN), the electroencephalogram signal processing poses some great challenges for researchers. These challenges can be tackled, by using the epileptic spike detection, artifact suppression and noise removal techniques, in a principled manner via adaptive signal processing approach.

We first present the evaluation of nonstationary epileptic spike detection algorithm for the electroencephalogram signal using the smoothed-nonlinear-energy-operator (SNEO) based on the different time-domain window functions. However, the incorporation of adaptive threshold determination procedure enhances the performance of proposed ES detector. The detection procedure exploits the fact that the presence of instantaneous ES corresponds to the high instantaneous energy content at the high frequencies. In addition to the stochastic amplitude, sign and the location of appearance of triangular spikes in the synthetic EEG signal, its base-width is also considered to be variable for the nonstationary signal analysis. The five pairs of EEG signals, obtained from electrodes placed on the left and right frontal cortex of male adult WAG/Rij rats, are used for the testing of proposed adaptive scheme in the real-time environment, which is a genetic animal model of human epilepsy. The simulation results are presented to demonstrate that the choice of window function plays a pivotal role in the efficient detection of ESs. Its computational complexity is found to be in trade-off relationship with the detection accuracy of algorithm. However, it may be inferred

that the real-time EEG signals (rat-data) can be processed and analyzed using the proposed adaptive scheme for the ES detection, which supersedes the conventional techniques.

We next propose a technique for the electroencephalogram spike enhancement and detection, which uses the Kalman-filtering (KF) approach based on the output correlation method for the nonstationary signal enhancement. We describe the nonstationary EEG signal in terms of the general Markov-model, in which the parameters are considered to be time-varying. In the proposed methodology, neither the process- and measurement-noise statistics nor the initial Kalman blending factor are stringently required. The EEG epileptic spikes are pre-emphasized using the output correlation method, and subsequently the detection is performed using the decision threshold based on the output of same adaptive filter. We have tested the proposed scheme on the synthetic EEG signal corrupted with randomly occurring triangular spikes. The presented simulation results manifest significant improvement in the signal-to-noise-ratio (SNR) due to the modified estimation of time-varying parameters of the general Markov-model, which in turn leads to the alleviated number of false-positives (FPs). It is apparent that the real-time EEG signal (rat-data) can be analyzed using the proposed EEG epileptic spike enhancement and detection adaptive scheme, which outperforms the conventional KF technique under the different SNR conditions. At 10dB SNR, the output correlation method provides approximately 40 % reduction in FPs for the triangular spikes in synthetic EEG signal and approximately 27.5 % reduction in FPs for ESs in the rat-data as compared to the conventional KF scheme.

Further, we present a technique for the removal of ocular artifacts from the electroencephalogram by using the adaptive filtering. The major concern is electrooculogram (EOG) signal present in the recorded EEG signal, which appears due to the abrupt eye movements. The conventional regression based methods for removing the EOG artifacts require various procedures for the pre-processing and calibration, which are inconvenient and

time-consuming. However in the presented method, we use separately recorded horizontal-EOG (HEOG) and vertical-EOG (VEOG) signals as two reference inputs, which are processed using the finite-impulse-response (FIR) filters. The linear filter coefficients are adaptively updated using the numeric-variable-forgetting-factor (NVFF) recursive-least-squares (RLS) algorithm, which track the nonstationary EOG signals. Subsequently, the processed HEOG and VEOG signals are subtracted from the recorded EEG signal to obtain the artifact-free EEG signal. The most appealing feature of this artifact and noise excision technique is its ability to remove the EOG artifacts without any pre-processing and calibration. The weight-vector of FIR filters can be automatically adapted to a new state without losing its effectiveness. Simulation is conducted using the synthetic EEG signal corrupted by the noise, synthetic HEOG and VEOG signals. The real-time recorded EEG signal (corrupted by EOG and noise) is also refined using the separately recorded reference EOG signals and an FIR filter. The linear generalized-variable-step-size normalized-least-mean-square (GVSS-NLMS) algorithm based artifact and noise suppression scheme is found to be suitable only under the high signal-to-noise-ratio conditions, due to its low computational complexity. However for the synthetic as well as real-time signals, the simulation results are presented to demonstrate that the linear NVFF-RLS algorithm based artifact and noise excision technique outperforms the conventional fixed-forgetting-factor (FFF) RLS, fixed-step-size (FSS) NLMS and GVSS-NLMS algorithms, in terms of the reduction in mean squared error, under the low as well as high SNR conditions.

In the presented research work, we are incorporating different adaptive algorithms to formulate improved EEG signal analysis techniques for the epileptic spike detection and artifact/noise excision, which only represents the tip of the iceberg in the domain of biosignal processing and biomedical engineering.

LIST OF PUBLICATIONS

1. H.K. Garg and A.K. Kohli, "Nonstationary-epileptic-spike detection algorithm in EEG signal using SNEO," *Springer, Biomedical Engineering Letters*, vol. 3, no. 2, pp. 80 – 86, June 2013.
2. H.K. Garg and A.K. Kohli, "EEG spike detection technique using output correlation method: A Kalman filtering approach," *Springer, Circuits, Systems, and Signal Processing*, vol. 34, no. 8, pp. 2643 – 2665, August 2015.
   (SCI indexed by Thomson Reuters; Impact factor = 1.18)
3. H.K. Garg and A.K. Kohli, "Excision of ocular artifacts from EEG using NVFF-RLS adaptive algorithm," *Springer, Circuits, Systems, and Signal Processing*, pp. 1 – 16, Online Published, March 2016.
   (SCI indexed by Thomson Reuters; Impact factor = 1.18)
4. H.K. Garg, P.G. Gakhar, and A.K. Kohli, "A review of neural signal processing paradigms based on physiological models for EEG," *Journal of Artificial Intelligence*, vol. 3, no. 2, pp. 56 – 73, February 2012. (Bioinfo Publications)
5. H.K. Garg, P.G. Gakhar, and A.K. Kohli, "Signal processing aspects in epileptic spike detection schemes: A review," *World Research Journal of Bioinformatics*, vol. 2, no. 1, pp. 41 – 48, April 2014. (Bioinfo Publications)

CONFLICT OF INTEREST STATEMENT

I (Garg Harish Kumar) hereby declare that I have no conflict of interest in relation to the research work presented in the abovementioned publications.

ACKNOWLEDGEMENT

The real spirit of achieving a goal is through the way of excellence and austere discipline. I would have never succeeded in completing my task without the cooperation, encouragement and help provided to me by various personalities. First of all, I would like to render my gratitude to the Almighty, and I bow before him for his umpteen blessings and bestowing in me the grit and confidence to carry out my thesis work successfully. It is my privilege to express my sincere thanks to our Hon'ble Director **Dr. Prakash Gopalan** and Esteemed Dean RSP **Dr. O.P. Panday,** for giving me this opportunity to undertake the Ph.D.

With deep sense of gratitude, I express my sincere thanks to my esteemed and worthy supervisor, **Dr. Amit Kumar Kohli,** Associate Professor, ECED for his valuable guidance in carrying out work under his effective supervision, encouragement, enlightenment and cooperation. Most of the novel ideas and solutions found in this thesis are the result of our numerous stimulating discussions. His feedback and editorial comments were also invaluable for writing of this thesis. I am aslo thankful to **Dr. Poonam Gakhar Kohli**, Associate Professor, Physiology Department, Punjab Institute of Medical Science Jalandhar, affiliated to Baba Farid University, Punjab, India for her fruitful suggestions and motivational discussions regarding Physiology and Neurology. The EEG signal-sets (publicly available) can be downloaded from a web page entitled with EEG, ERP and single cell recordings database by **R. Q. Quiroga**, on **https://www.vis.caltech.edu/~rodri/data.htm.** In addition, the EEG signal-sets (publicly available) can be downloaded from a web page entitled with EEG recordings database on **https://www.physionet.org.** I am appreciative to all the concerned researchers associated with both websites.

I would also like to acknowledge **Dr. Sanjay Sharma,** Professor & HECED, Thapar University, Patiala**, Dr. Mandeep Singh**, Associate Professor, EIED, and **Dr. Ravi Kumar**,

Assistant Professor, ECED, Thapar University, Patiala, Punjab, India, who have been a constant source of inspiration for me throughout this dissertation. I also thank the technical education department, Haryana, India for countenancing me to pursue Ph.D. at Thapar University, Patiala, Punjab, India.

I am greatly indebted to all my friends**,** who constantly supported and encouraged me all the time. I also express my sincere gratitude, deep love, and fondness to my wife **Mrs. Anju Garg,** my children **Krithik** and **Bhavya** for enduring a seemingly endless ordeal, for sacrificing some of their best years. Their love, patience and persistent encouragement enabled me to finally finish this research work.

At last but not the least my gratitude towards my parents, who always supported me in doing the things my way and whose everlasting desires, selfless sacrifice, encouragement, affectionate blessings and help made it possible for me to complete my thesis.

Garg Harish Kumar

Place: Thapar University, Patiala, India Date: December, 2016

TABLE OF CONTENTS

LIST OF FIGURES

LIST OF TABLES

ACRONYMS AND ABBREVIATIONS

AAR	:	Adaptive Autoregressive
AC	:	Alternating Current
AF	:	Adaptive Filtering
AFOP	:	Adaptive Filtering by Optimal Projection
AI	:	Artificial Intelligence
ANC	:	Adaptive Noise Canceller
ANFIS	:	Adaptive Neuro Fuzzy Inference System
ANN	:	Artificial Neural Network
ApE	:	Approximate Entropy
APF	:	Adaptive Predictor Filter
AR	:	Autoregressive
AWGN	:	Additive White Gaussian Noise
BCI	:	Brain Computer Interface
BLUE	:	Best Linear Unbiased Estimator
BPNN	:	Backpropagation Neural Network
BSS	:	Blind Source Separation
COB	:	Cepstrum of Bispectrum
CTM	:	Convolution-based Template Matching
DWT	:	Discrete Wavelet Transform
ECG	:	Electrocardiogram
ECoG	:	Electrocorticogram
ED	:	Epileptiform Discharge
EEG	:	Electroencephalogram
EFA	:	Epileptiform Activity

EM	:	Electromagnetic
EMG	:	Electromyogram
EOG	:	Electrooculogram
ERP	:	Event Related Potential
ES	:	Epileptic Spike
EV	:	Epileptiform Event
FF	:	Forgetting Factor
FFF	:	Fixed Forgetting Factor
FFF-RLS	:	Fixed Forgetting Factor RLS
FFNN	:	Feedforward Neural Network
FIR	:	Finite Impulse Response
FN	:	False Negative
FNR	:	False Negative Ratio
FP	:	False Positive
FPR	:	False Positive Ratio
FRLS	:	Fast Recursive Least Squares
FSS	:	Fixed Step Size
FSS-NLMS	:	Fixed Step-Size Normalized Least Mean Square
GVSS	:	Generalized Variable Step-Size
GVSS-LMP	:	Generalized Variable Step-Size Least Mean *p*th Power
GVSS-NLMS	:	Generalized Variable Step-Size NLMS
HEOG	:	Horizontal EOG
HOS	:	Higher Order Statistics
ICA	:	Independent Component Analysis
IFR	:	Infinite Frequency Response
KF	:	Kalman Filter

k-NEO	:	k-Nonlinear Energy Operator
LFM	:	Lead Field Matrix
LMS	:	Least Mean Square
LS	:	Least Squares
MLP	:	Multilayer Perceptron
MSE	:	Mean Squared Error
MWT	:	Multi Wavelet Transform
NCED	:	Normalized Cumulative Energy Difference
NEO	:	Nonlinear Energy Operator
NLMS	:	Normalized LMS
NN	:	Neural Network
NVFF	:	Numeric Variable Forgetting Factor
NVFF-RLS	:	Numeric Variable Forgetting Factor Recursive Least Squares
OA	:	Ocular Artifact
PCA	:	Principal Component Analysis
RBFN	:	Radial Basis Function Network
REOG	:	Radial EOG
RK-LMS	:	Reduced Kalman LMS
RLS	:	Recursive Least Squares
SAA	:	Sharp Alpha Activity
SEO	:	Squared Energy Operator
SNEO	:	Smoothed Nonlinear Energy Operator
SNR	:	Signal to Noise Ratio
SSD	:	Sum of Squared Differences
STEO	:	Smoothed Teager Energy Operator
STFT	:	Short Time Fourier Transform

SVD	:	Singular Value Decomposition
SVM	:	Support Vector Machine
TEO	:	Teager-Kaiser Energy Operator
TF	:	Time Frequency
TFR	:	Time Frequency Representation
TMS	:	Transcranial Magnetic Stimulation
TV	:	Time-Varying
TVAR	:	Time Varying Autoregressive
TWPF	:	Time Warped Polynomial Filter
VEOG	:	Vertical EOG
VFF	:	Variable Forgetting Factor
w.r.t.		With Respect To
WD	:	Wavelet Denoising
W-LMS	:	Wiener-LMS
WNN	:	Wavelet Neural Network
WT	:	Wavelet Transform

CHAPTER 1

INTRODUCTION BASED ON LITERATURE REVIEW

1.1 Brief Introduction About Electroencephalography

Electroencephalography (EEG) is a famous noninvasive scheme utilized to observe the traces of electric signals received from a huge number of neurons, which are inferred to understand functioning of brain as well as neurophysiology. The physiology of brain can be expressed using a paradigm, which consists of neuronal population of "cortex as well as thalamus". Moreover, cerebral cortex encompasses a great volume of brain, which lies nearest to measurement electrodes of electroencephalography. In fact, cortex is outermost layer of brain, and it makes a major contribution to scalp potentials; it is also a site of termination for a number of electric signals that reach to brain. Therefore, electroencephalogram signals offer a unique way to measure brain activity at a fine temporal resolution, generating a number of opportunities to address substantial neuroscience issues. The central aim of EEG is to extract a wealth of spatiotemporal spectral patterns of brain activity and functional connectivity from the large and complex time-series data to address enormous questions in neuroscience, neural engineering, and clinical studies. Since 1929, the analysis of EEG signals posed noteworthy challenges in the field of signal processing and statistical methods because of their inherent high dimensionality, large or sparse sample-size, low signal-to-noise-ratio (SNR), nonstationarity (across time/trials/conditions/subjects/groups), nonlinearity (of the feature space *w.r.t*. signal channel space), and other structures afforded by different signal types (e.g., event-related-potentials (ERPs) and oscillations).

The modelling of brain electric activity and the modelling of head volume conduction process for linking the neuronal electric activity (electroencephalogram recording) lead to a solution of the well-known electroencephalography forward problem, which details the

distribution of electrical potentials for particular source locations, orientations and waveforms. However, reconstructing the brain electric activity from measured electroencephalogram signal (from scalp potentials) helps in solving the inverse of previous ones; which is often called electroencephalography inverse problem solution. A paradigm of brain electric activity (in short "source-model") is consisting of bioelectrical units distributed within whole brain volume or over certain brain surfaces or confined to some particular brain locations. Here, one source unit is usually modelled as a current dipole, which efficiently approximates synchronized synaptic currents at the columnar level. In cerebral cortex, orientation of these current dipoles may be either free or constrained to be orthogonal to cortical surface. Linkage of source paradigm to physical electromagnetic (EM) signal recordable at the sensor positions on scalp (forward paradigm) needs the detailing of a volume conductor paradigm that describes the propagation of currents throughout human head in terms of geometry as well as conductivity of medium. The modeling imperfections generated by difference between actual head and volume conductor paradigm affects precision of electroencephalography forward problem solution and also inverse problem remedy, as the measured scalp potentials are obtained not only by the location and strength of neural signal generators, but also by the geometry as well as conductive properties of head. Such modeling imperfections consist of differences in actual head tissues.

Neural activity also gives rise to extracellular electrical and magnetic fields, which are detected in electromyography (EMG) and EEG [1]. Electrical current contribution due to active cellular processes within a volume of brain tissues gets superimposed at a particular location in extracellular medium and generates an electric potential, V_e (a scalar observed in volts), *w.r.t.* a reference potential. The difference in V_e between two locations generates an electrical field (a vector, whose amplitude is observed in "volts per unit of distance"). EEG measures the summation of synchronous activity (i.e., population V_e in voltage) of millions

of neurons that have similar spatial orientation, which can be detected on the scalp surface by utilizing conductive electrodes and sensitive bioelectric amplifiers. Importantly, EEG measurements have an excellent temporal resolution (~ 1 millisecond) in sampling the rich temporal dynamics of neuronal population activity. The spatial sampling precision of EEG signals is particularly around 1 – 2 centimeters outside the head, but ultimate spatial resolution of such methods depends on the algorithms and applications.

The clinical interpretation of bioelectric signalling waveforms plays a significant role in diagnosis of diseases. Here, substantial information is frequently contained by low amplitude bioelectrical signalling waveforms. Electroencephalography is also a clinical tool utilized in diagnosis, monitoring and management of neurophysiological disorders corresponding to epilepsy, which exhibits features like abrupt recurrent as well as transient disturbances of mental functions, and movement of body because of an unbridled electric discharge in brain. During seizures (ictal activity), electroencephalography is featured by large amplitude synchronized periodical waveforms in case of epilepsy. Such periodical signals reflect abnormal discharge from a huge number of neurons. Between, before and after seizures (interictal activity), electroencephalography may exhibit occasional epileptiform transient signals. Epileptiform-activity (EFA) indicates waves measured during interictal activity, and those may be categorized as spikes, sharp-waves, spike-and-slow-wave-complexes, and multiple spike-and-slow-wave-complexes. The signal-modeling techniques can be utilized to detect such epileptic-spikes (ESs) in electroencephalography recordings. However, electroencephalography in patients differs from day-to-day, and it encompasses substantial nonstationarities even in one measurement [2] – [6]. Moreover, the second-order nonstationarities lead to a time-variant auto-covariance function. Here, related power spectral density is therefore also time-variant. Stationary time-series analysis tools, like Fourier-transform, may not be utilized. Therefore, joint time-frequency analysis is needed.

Furthermore, EEG signal can also be viewed as the electric activity of brain, which is quite stochastic in nature. In such scenario, electroencephalography forward problem deals with the mapping of current dipoles utilizing lead-field-matrix (LFM) of observation paradigm and determines potential at different electrodes. However, hypothetical dipoles inside the head gives scalp potentials. Electroencephalography inverse problem tackles the estimation of spatially extended sources of EEG from related scalp measurements, i.e., for estimation of current distribution within human brain. Electroencephalogram signals consist of the underlying background activity with superimposed transient nonstationarities, like ESs. Moreover, quantitative detailing of amplitude as well as spectrum of spikes differ from signal-to-signal, subject-to-subject; and this even differs from time-to-time for a single patient. This is precisely why detection and pathological implications of spikes appear to be tedious. As spike base-width gets increased, the energy gets concentrated much in low-frequency band, where the energy of background signalling waveform is situated, and therefore detecting a signal is tedious in frequency-domain. Here, electroencephalogram signal is modelled as time-variant-autoregressive (TVAR) paradigm. Kalman filtering can be utilized for estimation of parametric values of TVAR paradigm. A threshold function is traditionally incorporated for the estimation of electroencephalogram signal to detect ESs.

Adaptive signal processing methods for the removal of artifactual activities from newborn electroencephalogram signals are presented in [7]. Here, a pre-processing is essential before attempting a fine time-frequency analysis of electroencephalography rhythmical events, such as electric seizures contaminated by large amplitude signals. Such short-time high amplitude artifacts are known as intra-artifacts. However, the artifacts generated due to surrounding EM field are known as extra-artifacts. The EEG has proven to be superior to clinical examination and prognosis of brain dysfunction [2].

However, electroencephalography is a set of information recorded by electrodes placed on scalp, and it is inevitably affected by artifactual signals. There are different kinds of noise

and artifactual signals in the electroencephalogram signal. Furthermore, electroencephalogram signal is also susceptible to different large-signal contaminations, such as baseline wander, powerline interference, muscle activity or electromyogram (EMG), electrooculogram due to eye-blinking (EOG), electrocardiogram (ECG), electrode displacement and other brain background activities (sharp-alpha-activity or SAA). However, the scalp electroencephalography is critically contaminated by low-frequency artifactual signals (baseline wander) exhibiting large amplitude generated due to movement of patient and due to variation in electrode-skin impedance. Moreover, spurious signals from AC power supplies may contaminate electroencephalography data in between scalp electrodes and recording equipment. Actually EMG, EOG and ECG are generated due to activities in various muscle groups like neck and/or facial muscles, due to reorientation of retinocorneal dipoles; and when an electrode is placed close to blood vessel, which generates pulses or beats. Such measurements are processed by low-pass filter to eliminate low-frequency artifactual signals (often in range 0.5 Hz to 1 Hz) and also processed by high-pass filter to eliminate large-frequency artifactual signals (often between 35 Hz and 70 Hz). Usually, electroencephalography equipment exhibit configurable noise cancellation alternatives already built-in. Moreover, independent-component-analysis (ICA) technique or cascaded adaptive filtering method can be utilized effectively to eliminate artifacts and interference.

It is well-known fact that the forward problem estimates scalp potentials i.e., electroencephalogram signal, in which scalp potentials can be expressed in terms of time-variant autoregressive process. The parametric values of underlying paradigm can be approximated by Kalman filtering. The usage of time-variant AR paradigm boosts spikes. Electroencephalography inverse problem is incorporated to localize the source of an epileptic spike pursuit in real-time EEG dataset. But, inverse problem reconstructs electroencephalogram signal source by mapping potential back on scalp, and also locates current dipole location on scalp (exact position of source). Subsequently, filter can be utilized

to approximate dynamical neuronal activity from electroencephalogram signals for the cases of linear as well as nonlinear models having either time-invariant or time-variant parametric values. Kalman filter-based technique utilizing physiological paradigms can be incorporated for linear paradigm, in which both spatial as well as temporal dynamics are utilized to approximate the dynamical neuronal activity from the recorded electroencephalogram waveforms. The appropriate estimation is attained by utilizing a nonlinear paradigm with time-variant parametric values. For robust automatic system, Kalman filtering procedure assumes estimation errors and paradigm uncertainties to enhance performance. Kalman filter-based procedure is found to be optimal for estimation under time-variant scenarios [8], [9], but its computation burden and need of the information about system paradigm may usually preclude its usage. To circumvent on-line Riccati updating in conventional Kalman automation procedure, Authors have reported a Wiener-LMS strategy for tracking-mode features in [10], [11]. The main drawback of such scheme is that it needs prior knowledge regarding the paradigm of dynamics of time-variant parametric values (hypermodel).

However, recursive-least-squares (RLS) procedure is vastly utilized in adaptive signal processing, self-tuning adjustment appliances and parameter-identification. Moreover, traditional RLS is popular for its high quality convergence-mode features and low mean-squared-error (MSE) under stationary conditions. But, RLS procedure utilizing a fixed-forgetting-factor (FFF) can't give acceptable performance under time-variant conditions. A lot of efforts are made towards the progress of an enhanced RLS procedure. The fundamental principle of such procedures is either to vary forgetting-factor (FF) or to perturb covariance-matrix. Though these procedures may exhibit excellent tracking ability, but their outputs are actually deteriorated under low SNR scenarios. In [12], a novel control strategy for the forgetting factor in recursive least squares procedure is mentioned. It relies on a time-varying equation of gradient of MSE rather than gradient of immediate squared error. This recursive least squares procedure is revealed to possess fast tracking ability and low MSE. Particularly,

this scheme can alleviate the impact of disturbance/noise; and it generates suitable variations in the value of FF, which are proportionate to paradigm changes. In [13], a tuning strategy for variable-forgetting-factor (VFF) of an RLS adaptive procedure is introduced. This control strategy is principally a gradient-based procedure, in which gradient is governed by a modified MSE analysis of recursive least squares algorithm. This investigation leads to a dynamical-equation of MSE, that may be utilized to get a dynamical-equation of the gradient of MSE to manage FF. Its dynamical-equation may yield a positive-gradient in case error is high; and a negative-gradient in case error reaches to its steady state. In comparison to other VFF procedures, this control strategy bestows fast tracking and low mean squared paradigm error for various values of SNR. But, it is also computationally complex. Subsequently, numeric-variable-forgetting-factor (NVFF) RLS procedure has been mentioned in [14], [15] for linear as well as nonlinear signal processing applications (it may include biosignal processing and biomedical engineering applications), which exhibits relatively lower computational complexity, under nonstationary environment [16]. Further, generalized-variable-step-size (GVSS) normalized-least-mean-square (NLMS) adaptive procedure is detailed in [17], which supersedes the fixed-step-size (FSS) NLMS algorithm, as far as the adaptation characteristics are concerned, at lower computational burden relative to different types of RLS procedures [9], [16], [18].

In the light of aforementioned facts, Kalman, RLS, NLMS and LMS adaptive algorithms can play a pivotal role in formulating improved electroencephalogram signal analysis schemes for the epileptic spike detection and artifact/noise excision, which is the main objective of the presented research work. Therefore, interest has peaked in the application of adaptive techniques to process or refine EEG signalling waveforms (nonstationary biomedical signals/biosignals) in the presence of artifacts and noise signals.

1.2 Conventional EEG Refining Techniques to Combat Artifacts/Noise

The electroencephalogram signal is subject to interference from various other signals, which are collectively called artifactual signals, and these basically originate either from concerned patient or from external sources (i.e., noncortical). Various artifactual signals come into picture due to eye blinks (source of EOG signals in EEG), electrical activity due to muscle movements (source of residual EMG signals in EEG [19] – [20]), electrical potential generated by cardiac activity (source of spiky activity because of residual ECG in EEG [19], [21]), electrical line-noise and other background noise/interference signals [22]. Typically, EEG recordings are contaminated by relatively strong artifactual signals caused by the eyes [19], [21], [23], [24]. These can either be eye blinks (picked up mostly by vertical EOG) contaminating typically the lower frequencies or be saccades (visible mostly in horizontal EOG) also interfering at higher frequency ranges, where certain saccadic spike artifactual signals resemble high-frequency muscular artifacts [21]. However, the muscular artifacts may also be caused by mastication (chewing), deglutition (tongue movement), and respiration.

Recordings of evoked-responses with electroencephalography are widely used methods in cognitive and clinical neuroscience [25]. One of the major challenges in research and clinical applications of evoked-responses is the prevalent strong interfering electromagnetic (EM) signals from external objects and devices in the surrounding EEG measurement environment as well as due to nearby mechanical and biological EM sources originating from the head and other parts of the body of subject. Since the interfering environmental-noise from, for example, laboratory mechanics and electronic devices may be several orders of magnitude stronger than the brain signals of interest [26], therefore it is necessary to eliminate this noise from recordings. Moreover, nonencephalic electromagnetic activity can be up to a thousand times stronger than the encephalic signal of interest [26]. Since some of these interfering artifactual signals can be synchronous with the brain signal of interest, therefore significant parts of the continuous measurement can be contaminated by artifactual signals. Hence to

ensure a reliable measurement, it is necessary to omit or correct the data contaminated with artifacts, which is required in addition to employing an average measure of an evoked-response across multiple time-locked data segments. These artifactual signals deteriorate the quality of electroencephalogram signal recordings; and their elimination is one of the most challenging problems in electroencephalography research. Usually, this recorded signal is segmented into trials, and every trial is visually examined by an expert. Trials, which are found to be encompassing artifactual signals, are then excluded. However, the removal of a trial that encompasses an artifact also eliminates all beneficial information in that trial. Moreover, visual examination is slow. It is also observed that visual examination involves making judgments according to the visual characteristics of data, and it is therefore subject to human error. It occasionally leads to missed artifacts, and sometimes the factual non-artifact contaminated data may also be abolished from analysis. Hence, there is a requirement to exclude artifactual signals automatically according to fixed, reproducible and rigorous criteria. A PC-based system is designed and reported in [27], which integrates both spatial as well as temporal contextual information to automatically detect definite and probable epileptiform events, and to reject non-epileptiform (background activity) events.

In [28], researchers have proposed an ECG artifact detection technique using the energy interval histogram elimination scheme. A smoothed nonlinear energy operator is incorporated to refine the corrupted EEG signal. It emphasizes ECG artifacts more in comparison to the background EEG signal, which in turn leads to an efficient detection and elimination of periodic artifacts. However, the properties of Teager-Kaiser-energy-operator (TEO) and squared-energy-operator (SEO) are examined in the presence of additive noise, as a function of short-term averaging window-length, in [29]. The robustness of energy estimation process is explored when TEO and SEO are applied to the derivatives of the true signal. TEO is proven superior to SEO, for the shorter window-length. However, it is found for the medium and longer window-lengths that TEO outperforms SEO only when the spectral content of

desired signal is high-pass relative to the spectral content of noise. The presented analysis in [29] showcases some guidelines for selecting an appropriate energy operator *w.r.t*. the minimization of short-term energy estimation error. This technique has found applications in the field of artifact (like epileptic spike) detection and excision.

The electromyogram signals originated from head and neck muscles are usually comparable to the high-frequency brain activity. Therefore, the frequency spectra of EEG and EMG overlap, which leads to highly inefficient frequency-domain filtering. In [30], Masherov *et al*. have detailed cross-regression method for signal segregation based on regression analysis. This cross-regression procedure is an effective tool for removing uncorrelated EEG components, such as EMG and artifactual signals present due to the movement of electrodes and its connecting wires. Subsequently, a fully automated EMG elimination technique is proposed in [31] by introducing a reasonable threshold, which is based on a canonical correlation analysis method. It considers that the underlying sources are mutually uncorrelated, but maximally auto-correlated under realistic environment. But, drawback of these methods is the partial elimination of the natural/true EEG signals corresponding to individual electrodes.

In [32], Clercq *et al*. have developed a subspace-based method, in which artifactual signals are removed, when epileptiform activity appears in a large number of channels and the muscle artifacts appear in a few channels. In [33], Jung *et al*. have explored an extended type of independent-component-analysis (ICA) based on statistics of recorded field maps, without relying on accessibility of clear reference channels. It segregates and removes contaminated artifacts from a verity of artifactual sources in EEG records. ICA conserves and regains higher brain activation information than principal-component-analysis (PCA) by decomposing both simulated as well as real-time EEG data. In [34], line-noise and EOG artifacts are abolished from EEG signal by means of ICA technique. It is apparent that its

performance is more accurate in locating noise frequency in comparison with wavelet packet analysis for removing line-noise. An effort is made in [35] to eliminate all types of artifactual signals using global filtering of records by utilizing ICA method. However, high-frequency components can't be segregated due to non-synchronization. A substantial reduction in amplitude is observed during slow-waves and paroxysms. It also combats ECG based interfering signals present in measured EEG, and gives promising outcomes [36]. For detection of independent components that relates to electrooculogram, Milijkovic *et al*. [37] have utilized a linear correlation method. Though ICA has been utilized for electroencephalogram signal decomposition in order to extract ECG artifact, but it has ignored the presence of noise component that may be significant. However, two-step identification of spurious contents before and after ICA utilizing Kurtosis parameter results in automation of artifactual signal excision process [38]. In [39], a combination of ICA and Stockwell-transform is utilized to eliminate ECG artifactual signals. In [40], robust PCA has been introduced for automatic noise cancellation and artifact eradication using wavelet denoising technique. In [41], ICA and PCA are utilized to combat line-noise. An ICA method is also capable to cooperate with wavelet-transform (WT) to boost electroencephalogram artifact suppression efficiency [42]. The lifting WT in combination with ICA has ability to eliminate ocular as well as muscular artifactual signals from multichannel electroencephalography brain signals in clinical scenario [43]. This is noteworthy that it requires high complex computations. ICA performs a better decorrelation of signal having higher-order statistical dependencies [44]. It can efficiently identify and isolate the artifactual signals present in magneto encephalographic recordings [45]. But, its major drawback is that the performance of ICA is dependent on the size of dataset.

In [46], Ferdousy *et al*. have presented a scheme for the suppression of electrooculogram artifactual signals based on the second-order blind-source-separation (BSS) scheme, and also presented a procedure to remove muscle artifacts based on the canonical correlation analysis.

A number of EOG artifacts can be eliminated without altering the measured ictal activity. This technique is found to be beneficial for accurate seizure zone localization and for the reduction of false-positive-ratios in the automatic epileptic seizure detection. In [22], BSS is reported to be best approach for artifactual signal removal under high SNR conditions, when it is applied to a dataset containing mixtures of artifactual signals. Further in [47], a potential solution for high amplitude artifact elimination is presented using BSS. However, a second-order blind identification can also be applied to suppress EOG and EMG artifactual signals [48]. Unfortunately, it can't provide information about the order of source. A brain-computer-interface (BCI) system permits user (particularly patients with motor disabilities) to communicate, via computer, through electroencephalogram signals. To enhance the efficiency of BCI procedures, it is required to look for a scheme to enhance SNR of observed electroencephalogram signals. The purpose of using BCI is for assisting or repairing human cognitive or sensory motor function [47]. A survey on artifact suppression schemes has been given in [49]. In [50], Chadwick *et al*. have presented the usage of machine learning procedures for the classification of artifactual signals present in electroencephalography. This study is focused on the classification of eye and head movement corresponding to artifacts present in electroencephalogram signals, without the usage of EOG and EMG measurements rather than trying to suppress general artifacts. In [51], Ma *et al*. have suggested a BCI technique by taking benefit of electroencephalogram artifactual signals, produced due to a number of intentionally developed voluntary facial muscle movement. The success of these techniques depends on the efficiency of artifact classification methods. However, artificial-intelligence (AI), in particular knowledge-based techniques, is being developed in [52] to recognize and subsequently classify the pathological waves and artifacts, based on knowledge of their characteristics, in order to suppress artifactual signals present in EEG signals when necessary. A system is presented in [53], which boosts transient nonstationarities and epileptiform discharges. It relies on the method of multi-reference automatic noise canceling,

which reduces background electroencephalogram signal present in primary channel by utilizing spatial as well as temporal data obtained from adjacent channels in multichannel electroencephalography measurements. It is incorporated by using a three-layer perceptron artificial-neural-network (ANN) trained by a backpropagation procedure. The results depict that enhancement in SNR is substantial in comparison to same techniques utilizing a linear model, due to nonlinear nature of neural-networks (NNs).

An automated methodology based on four-stage procedure for the detection as well as classification of transient events in EEG recording is reported in [54]. However in [55], the EEG signals are pre-processed using ICA for suppression of artifactual signals. After this pre-processing step, a time-frequency-representation (TFR) of signals is determined to exploit the time-variant characteristics of electroencephalogram signals. Subsequently, wavelet-based texture characteristics are extracted from TFR and utilized to classify signals. Eventually, these characteristics are fed into a multilayer feedforward backpropagation NN. In [56], two methods have been utilized for artifact denoising: the first method uses WT, and second method is based on adaptive linear NNs. A novel nonlinear adaptive denoising technique is proposed in [57] by applying a backpropagation NN ensemble, which not only attenuates additive as well as multiplicative white-noise inside signals, but also preserves signal features. In [57], Chen *et al*. have proposed that electromyography is a type of shot-noise in terms of EMG generation. The limitation of AI [52] in this particular application is that, when used in real-time, it may take an unacceptability long time to arrive at a decision whether or not to remove an ocular artifact.

In [44], WT conducts a correlation analysis; therefore outcome is expected to be optimal, when input signal resembles mother-wavelet considerably. Moreover, artifacts may dramatically vary signals measured at entire scalp sites, particularly those nearest to source of noise. Wavelet denoising band-pass filtering for pre-processing and robust PCA procedure for feature extraction are presented in [40] to suppress the artifacts. However, a drawback

observed in wavelet-based transformations is that if the EEG signal and artifacts have similar amplitudes, then the wavelet faces difficulty in distinguishing between them.

Shigemura *et al*. have proposed a NN with non-recursive second-order Volterra filter in [58] that consists of the terms of linear as well as nonlinear combinations for elimination of artifacts from EEG signal. The comprehensive classification rule [59] is derived from clinical electroencephalograms recorded from sleeping newborns by combining the polynomial NN and decision tree. Philips has presented time-warped-polynomial-filter (TWPF) in [60], which is an adaptive filter to suppress stationary noise present in nonstationary biomedical signalling waveforms. TWPF has exclusive benefits over conventional adaptive noise excision schemes; as former reacts instantaneously to variations in signal's characteristics, independent of desired noise alleviation. Moreover, this doesn't need a reference signal, and it may be incorporated in case of non-periodical signalling waveforms also. The main limitation of this adaptive filter is the requirement of significantly large nonstationary constituents in comparison to the stationary constituents. Moreover, it is unsuitable for filtering nonstationary signals corrupted by nonstationary noise. A Volterra filtering procedure based on a multichannel structure for noise reduction is reported in [61]. This procedure may maintain natural true shape of electroencephalogram signal under small SNR scenarios. In [62], nonlinear autoregressive algorithm for artifact removal from EEG signals in connection with the choice of model structure (order) and computation of the system coefficients is proposed. It has introduced an intelligent method for EEG artifactual signal removal, which can substantially boost prominence of spikes in the clean EEG signals. A multistep extraction procedure to segregate maternal electrocardiogram, fatal electrocardiogram, fatal electroencephalogram and interfering baseline wander transabdominal recordings is reported in [63].

In [64], Schachinger *et al*. have reported a procedure for the decomposition of signal into various sub-bands in order to isolate various types of artifactual signals into typical frequency

bands. Subsequently, an adaptive threshold is engaged to exclude components with large variance related to the significant artifactual activity. As the ECG is periodic signal and exhibits lack of correlation with EEG signal, therefore in [65], Dewan *et al*. have presented a scheme for automatic detection and elimination of ECG artifactual signals. A global artifact suppression scheme related to the evolution of adaptive-filtering-by-optimal-projection (AFOP) method is presented in [66]. This technique excludes ocular as well as muscular artifactual signals, but it can't combat electrode artifactual signals. Transcranial-magnetic-stimulation (TMS) impulse produces large amplitude and long-lasting artifactual signals that contaminate the electroencephalogram traces. The off-line Kalman filtering procedure to suppress TMS-induced artifactual signals present in electroencephalogram recordings is reported in [67].

Linear filtering-based artifact removal is considered as the most simple and practical approach for the purpose of artifact eradication, which could span over a particular range of frequencies on spectrum [44]. Princy *et al*. have mentioned a method for reducing the eye blink artifact in EEG using FIR filter in [68], which enhances SNR. GuruvaReddy and Narava [69] have shown that linear filtering can also be utilized to combat artifacts present in EEG signals. However, the usage of adaptive filtering provides more promising outcomes, as far as the artifact removal is concerned. Moreover, a limitation noticed in the usage of least-mean-square (LMS) filtering is that it fails to distinguish between EEG and EOG signals; and as a consequence, it removes part of the EEG along with EOG signal removal. However, least mean square procedure reduces computations by approximating gradient from immediate values of correlation-matrix of filter input sequence and cross-correlation vector between the desired output and filter weights [70] – [73]. Dhiman *et al*. [74] have demonstrated a comparative evaluation between adaptive filtering procedures, such as LMS, NLMS and RLS. A trade-off between complexity and convergence is observed. The performance of RLS

procedure is at its best in the time-varying environment. The RLS procedure has been implemented for off-line artifact excision in [75]. The RLS procedure utilizes a tapped-delay-line transversal filter configuration. It depends upon matrix inversion lemma, which leads to reduced numeric robustness and unnecessary numerical complexity [75] – [78].

RLS could be the best option for recovering EEG signal or denoising it during the transmission through telemedicine system [79]. In [80], the investigators have presented different digital filtering algorithms to predict electroencephalogram signal from previous samples for premature diagnosis of any patient, suffering from recurrent epileptic seizure, for psychotherapeutic cure of psychiatric subjects. Such investigation includes variation of filter-order, sample-size, and eventually reaffirms Kalman filtering approach as a remedy for the small root-mean-square prediction error as compared to LMS, NLMS and RLS filtering procedures. However, LMS and NLMS filtering algorithms demonstrate lower performance than Kalman and RLS filtering procedures. But, Kalman filter performs exceptionally well under nonstationary environment.

1.3 Epileptic Spike Detection and Removal Techniques

In a few cases, when surgery is feasible and recommendable, electrodes are implanted on cerebral cortex to measure electric activity of brain, and recorded signal is called electrocorticogram. Between seizures, EEG may show activity, in the form of transients, referred to as interictal spikes (or sharp-waves). These transients are a sudden burst of electrical activity, which appear in the form of a spike in the EEG record [81]. As per the Committee on Terminology of International Federation of Societies for Electroencephalography and Clinical Neurophysiology definition [82], the electroencephalogram spike is a transient signal, apparently distinguishable from background activity, exhibiting a pointed tip. The difference between sharp-waves and spikes lies in their duration. Spikes usually occur for shorter periods (20 $m\sec$ to 70 $m\sec$), while sharp-waves

last from 70 $m$sec to 200 $m$sec [81]. The major constituent is usually surface negative. ESs can crop up alone, but usually it is followed by a slow-wave, which lasts from 150 $m$sec to 350 $m$sec, generating a "spike" and "slow-wave-complex". The detection of "spike" and the "spike-and-wave-complexes" requires their exclusion from usual electroencephalogram background activity. However, detection as well as classification of sharp transient signals by visual investigation of electroencephalography measurement is a time consuming process. An electroencephalographer, guided by conventional definitions for epileptogenic sharp transient signals, also utilizes some subjective criteria-based on the contextual knowledge as well as heuristics to determine a final conclusion. Hence, visual investigation of electroencephalography measurements needs perfectly trained specialists, which is not always possible. Hence, there is a vital requirement to adaptively detect ESs and seizures.

However, it is very tedious to separate non-pathological processes, which are similar to pathological ones. In some cases, noise as well as instrument artifactual signals may be misinterpreted as spikes. Due to such reasons, different signal processing techniques are popular in this domain. One is the domain of supervised techniques, which corresponds to mimetic, template matching, predictive filtering and ANN. Other one is the domain of unsupervised techniques, which corresponds to SNEO, Kalman filter as well as smoothed Kalman filter. In supervised methods, eminence of classification is dependent on quality of dataset. However, various electroencephalogram enhancement schemes may be separated into three categories: a) time-domain schemes; b) signal-modeling schemes; c) transform-domain methods.

Carrie has suggested a scheme to identify spikes in [83] by using the second-derivatives of EEG. Lopes da Silve *et al*. have processed EEG signals by an autoregressive predictive filter and detected the nonstationary waves by examining the prediction error in [84]. Saltzberg *et al*. have used template matching approach [85], and authors have applied a

pattern recognition technique to detect these waves [86]. However, these methods aim only at the detection of existing nonstationarities. These do not segregate the nonstationarities as signal waves from the stationary waves. Matched filtering has also been used as means for detecting "spike-correlated-activity", but such a technique gives unsatisfactory results in detecting EEG waveforms because of high false alarm rate.

A technique based on cumulative energy has been suggested in [87]. Automatic detection procedures may be categorized in to two broad classes: (i) those that match a desired template to measured signals, and then look for appropriate matches or local maxima in cross-correlation; and (ii) those which look for an event that crosses an amplitude threshold or whose first-derivative, energy or WT coefficients cross a threshold. Template-based procedures need bootstrapping, that approximates true spikes. The convolution-based-template-matching (CTM) is used to pre-emphasize spikes. Sum-of-squared-differences (SSD) template matching is utilized for image matching comparisons. SSD determines Euclidean distance between every point in template pointing the signal section. Normalized-cumulative-energy-difference (NCED) scheme is motivated by a fact that energy content of ES (positive or negative) must be larger in comparison to noise. For spike detection schemes, three thresholding criteria are designed as well as tested on clinical physiological data for comparative evaluation. Vijayalakshmi and Abhishek have proposed a program based on template matching method for the spike determination in a single-channel [88].

In template matching approach [89], templates that correspond to a particular waveform have been utilized as a benchmark. In first-stage of such scheme, a waveform is picked as a template that expresses a particular spike-shape. At second-stage, this procedure locates probable events in signal that approximately match this template. Subsequently, thresholding stage follows with an experimenter recognizing a few good spikes, and utilizing them for training of filter [90]. However, it is found to be impractical, when the number of electrodes is high. El-Gohary *et al*. [91] have described an electroencephalography user-guided

interictal spike recognition procedure, which only needs user to annotate some ESs; and then utilizes mean squared error examination to recognize spikes present in measured signal. This is capable of estimating template morphology adaptively form signals utilizing annotations. This approximates multichannel multitemplate to measure changes in morphology as well as spatial distribution with various subjects, who undergo cycles of wake-sleep during long-term electroencephalogram signal observation. The performance of template matching procedure again gets degraded under the small SNR conditions, as automatic choice of a template in a noise-type signal appears to be tedious. However, overlapping ESs generate a unique waveform of spike, which may spoil its performance. In [92], multichannel template extraction scheme is mentioned for automatic EEG ES recognition.

In [93], Acir and Guzelis have introduced two-stage procedure relying on the support-vector-machines (SVMs) for automatic recognition of ESs in multichannel EEG signal. This proposed classification algorithm displays better performance, while being competent in terms of memory as well as time requirement. To reduce the computation time and to enhance detection performance, a pre-classifier stage classifies peaks into following categories (a) “spike” and “spike like non-spike” (b) trivial non-spike using nonlinear digital filter. In post-classifier stage, a support vector machine with radial basis kernel function is utilized to segregate the spikes from each other. Barreto *et al*. [94] have described a study to detect interictal spikes utilizing EEG and Lagrange-derivatives. Adjouadi *et al*. have introduced an integrated procedure based on-line Walsh-transform to recognize interictal spikes and artifacts related to epileptic subjects utilizing measured electroencephalography data [95]. Orthogonal operators are developed using Walsh-transformation, which are used to formulate and evaluate the morphologic features of interictal spikes. This procedure identifies and localizes interictal spikes, while automatically removing different artifactual signals. A few spike recognition techniques, usually overlooking noise existing in signalling waveforms, use first-derivative of signal [96], [97] or signal’s configuration for developing morphological

filtering procedures [98]. Morphological filter is discussed in [99] for spike detection, which is susceptible to high-frequency noise. The morphological filter also detects a lot of false-positives with epileptic spikes in noisy portion of EEG record. Average weighed grouping of open-closing and close-opening morphological procedure [100], which removes statistical deviation of amplitude, is used to exclude spikes from epileptic electroencephalogram signal. However, proposed method in [101] is applied by simulating epileptic electroencephalography data only. In [102], Shahid *et al*. have proposed a spike detection procedure, which uses cepstrum-of-bispectrum (COB) [103] in case of inverse filter. A procedure for spike detection has been designed in [102] that initializes COB approximated inverse filtering to give blind equalization. Such method is relying on higher-order-statistics (HOS), which looks for event-times of delta sequence. This procedure doesn't need any prior knowledge regarding spike-shape, or maximum/minimum spike-rate and noise-level. COB is implemented to process synthesized signals. This produces relatively lower errors caused by false-positives (under low SNR conditions). In [101], a linear prediction procedure is utilized to examine the presence of spikes and sharp-waves in seizure measurements. It determines an optimal set of coefficients for every window. However, comparative analysis of prediction error with a threshold parameter is needed for decision about an ictal state onset. This threshold parameter is dependent on filter tap-coefficient vector. However, a digital computer described in [104] gives the quantitative value for spike characteristics and determines the parameter values required for the spike detector together with a muscle activity. A nonlinear digital filter poised of an AR prediction filter and a simple nonlinear function are proposed by Arakawa *et al*. [105], which separates nonstationary spikes from the stationary background EEG signal. The nonlinear function segregates a low amplitude constituent and a high amplitude constituent from the predictor error signal.

A microcomputer program is used in [106] for on-line spike detection and analysis. The mean and variability establish the value of adaptive threshold based on SNR. The graphical

and statistical data characteristics of the dynamics of neural spike activity are provided by microcomputer program. Automatic spike detection is justified by the requirement to analyze a large set of dataset corresponding to a particular EEG or electrocorticogram (ECoG) examination and to overcome the unclear description of a spike [107]. ANN is a teachable non-algorithmic data processing system that encompasses densely interconnected neuron-like elements. A number of studies utilizing ANN techniques for recognizing ESs are already mentioned in [108] – [111]. ANN based spike recognition procedure functionally utilizes two independent strategies for input expression: a) extracted EEG coefficients or b) raw electroencephalogram signalling waveform. In first strategy, spike coefficients are approximated from electroencephalogram signalling waveform, like slope as well as sharpness, which are fed to ANNs for training as well as testing [108]. In other approach, raw electroencephalogram signalling waveform is fed to NN after appropriate scaling as well as windowing [109] – [112]. Successful outcomes can be determined by utilizing a sliding input window both in off-line [109] and natural [110], [111] operations. However, multilayer perceptrons trained with backpropagation algorithm [113] are famous because of their flexible nature and high efficiency. Previously, NNs have been utilized to classify a few electroencephalography waveforms, like spikes, sleep-staging, K-complexes [114] – [116] and evoked potentials [117] – [119]. Eberhart *et al*. [114], Principe and Tome [115] have utilized calculated electroencephalography parametric values as inputs to NNs to alleviate input-size. In [120], Eberhart and Dobbins have presented design considerations for incorporating a real-time ES recognition system, such as the selection of spike parameters and NN architecture. Backpropagation neural network for detection of sharp transients i.e., spike and sharp-waves is suggested in [121]. The self-adoption is the unique characteristic of neural network. Vaz and Principe have presented decomposition of orthogonal components of time-varying signals with unsupervised neural networks in [122]. These signal components are used to train another NN to identify the temporal features of the spike. Khan and

Tarassenko [123] have investigated the usage of an ANN for detection of interictal spikes. The feature vectors quantify slope, sharpness and AR parameters extracted from EEG. To improve this method, the features like spike-duration and amplitude may be added to the feature vector. A multichannel system is developed in [124] for spatial analysis of multichannel electroencephalogram signal measurement with fuzzy-logic. The incorporation of spatial-contextual to recognize epileptiform events in electroencephalography reduces the false detection rate. The ANN based recognition by utilizing raw electroencephalogram signals in real-time for spike/EMG excision is developed in [112] by utilizing a sliding window scheme. This method discriminates transient epileptiform waveforms containing "spike" or "spike-and-wave" from EMG signals and background electroencephalogram signals. Wilson and Emerson [125] have reviewed recent approaches including NNs and high-resolution frequency schemes for spike detection. The spike clustering method reduces the burden of false-positives. However, Acir [126] has exploited redundancy in input dataset in [126] for enhancing efficiency of radial-basis-function-network (RBFN) classification procedure. Author has presented a two-stage system based on modifier RBFN classifier for adaptive recognition of epileptiform pattern. Walbran *et al*. [127] have presented a semi-automated scheme for spike detection in the fetal sheep EEG. The spikes are extracted by using short-time-Fourier-transform (STFT) and peak-separation. This scheme detects some spikes, which exhibit amplitude less than $20\mu V$ threshold because high-frequency spikes appear in STFT. This method also distinguishes between spike-waves and sharp-waves.

A hybrid technique for classification of EEG signal for the identification of epilepsy seizure by combining multi-wavelet-transform (MWT), ANN and existing approximate-entropy method (ApE) is presented in [128]. This improved approximate entropy is used to measure irregularities present in the EEG signal. In [129], Kalayci and Ozdamar have reported ANN based EEG spike detection technique by using wavelet-transform (WT) as pre-

processor. A robust system, which uses a combination of multiple signal processing schemes in multistep scenario, integrating WT, is proposed in [130], which relies on a multi-resolution multilevel analysis. The extracted features from EEG during mental task by AR processes are classified by a two-state brain-computer-interface (BCI) using NN in [131]. Burg's procedure and least-squares (LS) procedure are used to find AR coefficients; and LMS procedure computes the coefficients of adaptive-autoregressive (AAR) filter. The linear discriminant analysis provides better classification performance and a lesser amount of computational complexity as compared to multilayer perceptron backpropagation. Dithering is a procedure of deliberately mixing artificially produced noise to an uncorrupted signal. Casson and Villegas in [132] illustrate that a dithering procedure may be utilized to modify performance of an EEG interictal spike recognition procedure in terms of both detection capability as well as hardware requirement. In [133], Melia *et al*. have presented a scheme for removing spike artifactual signals relying on analytical signal envelope, processed by using a low-pass filter.

Transformation as well as decomposition of waveforms are usual techniques in signal processing. ES characteristics can be analyzed in Haar-transform domain [134], which is a type of WT. Here, spike properties can be improved in terms of coefficients of continuous WT [135], [136] and also in the discrete WT [137], [138]. By using WT, it is possible to decompose the EEG signal in sub-bands, capture-frequency and time information from low or fast transients, while disregarding signal's nonstationarities [139]. In other words, the coefficients must discriminate the spike-like events from the signal. The main feature of wavelets is their capability to segregate classified waveforms from noisy signals by thresholding wavelet coefficients, and consequently, this outshines under low SNR scenarios [140]. Nayak *et al*. [141] have described the automated detection of epileptic events based on wavelet analysis of electroencephalogram. The WT considerably alleviates the input-size of ANN. To categorize the epileptic seizure and non-epileptic seizure, three feedforward backpropagation ANNs are considered. In [142], a wavelet-neural-network (WNN) for

automatic detection of epiletptic spikes is presented. This method gives promising results by using ANN as classifier and wavelet analysis as pre-processing. A proper selection of scaling in WNN can be introduced to overcome problem of very long time duration during training. A multi-resolution technique and a nonlinear-energy-operator (NEO) are explored in [143] for detection of spike in electroencephalograms. Any waveform in electroencephalography channel can be decomposed into three sub-bands utilizing a non-decimated wavelet transform. A related technique computes an NEO by utilizing the product of immediate amplitude as well as frequency of extracellular signal, which boosts spike events [144] - [145]. In [146], a two-stage method is reported for ES recognition. First, k-nonlinear-energy-operator (k-NEO) is utilized to recognize all probable spike candidates, and subsequently a spike paradigm with slow-wave characteristics is incorporated to process these candidates for ES recognition. Automatic boosting classifiers are trained and utilized for the classification of electroencephalography patterns into three categories involving “single-spike”, “spike-with-slow-wave” and “non-spike”.

However, spikes can be perceived as small duration broadband processes exhibiting large instantaneous energy. This energy of ESs is rated as localized energy patterns in time-frequency (TF) domain. However, width of localized energy patterns tends to be narrower in high-frequency domain. Eventually, an ES may be viewed as line ridge at large frequencies. To handle noise as well as nonstationary problem hazards, a two-stage spike recognition method is proposed in [147]. First-stage is a pre-processing stage, which attenuates effects of noise in TF by utilizing singular-value-decomposition (SVD) technique [147]. Second-stage is detection phase, which makes use of the characteristics of spikes in TF-domain while emphasizing on capacity of NEO [99]. Neonatal electroencephalogram seizures exhibit traces at both low-frequency (approximately 0.5 Hz) [148] and high-frequency (more than 70 Hz) [149]. The literature presented in [150] focuses on the usage of low-frequency signature for seizure recognition. Detection of electroencephalogram seizures by utilizing the low-

frequency signatures needs less number of data samples, which reduces calculation time. In [149], Hassanpour *et al*. have presented a method for seizure identification in EEG signal of neonates, based on spikes, which is event feature extraction in TF field. To differentiate seizure activity from non-seizure activities, a histogram of consecutive spike intervals is compared with a standard histogram corresponding to seizure activity. In [151], a group of researchers have focused on a scheme to suppress noise in TF-domain by utilizing SVD. The features of spikes in two frequency slices of enhanced TF-domain distribution are classified as well as incorporated in SNEO. To localize position of epileptic spikes in electroencephalogram signal, a threshold is engaged for getting the output of SNEO.

In [152], a technique for epilepsy detection relying on the autoregressive parameters of EEG signal is showcased. In this method, optimum order of autoregressive paradigm is attained by utilizing Bayesian-information-criterion, and further AR parameters of EEG signalling waveforms and its sub-bands are recognized. These parametric values are employed in multilayer-perceptron (MLP) for classification. Liu *et al*. [153] have demonstrated a robust system, which uses spatial as well as temporal contextual information of epileptiform waves for the detection of epileptic activity in EEG. In [154], a noninvasive technique is proposed, which utilizes a "beamformer" spatial filter for boosting of signals from deep sources in brain, which are suspected of encompassing epileptiform-discharges (ED). For detection and localization of epileptigenic sources in the brain, three-dimensional spatial filter i.e., "beamfoming" is used. The further improvement in enhancement can be done by using adaptive algorithmic schemes akin to RLS/NLMS or block processing procedures. Parametric or model-based methods rely on modeling of the EEG signal by linear or nonlinear estimation methods. The parameters (also termed coefficients), that best fit the filter's output to the sample signal under inspection, could be used for spike detection. The usual mathematical models are classified as autoregressive, moving-average and autoregressive-moving-average. In order to consider the nonstationarity of EEG signals,

adaptive models are required (i.e., the parameters are updated according to the next signal samples). However, non-adaptive models can be used to fit quasi-stationary segments (i.e., when the signal is partitioned into short intervals) of EEG time-series (i.e., the parameters are defined to provide the best representation of the data-series) [155]. Acir [126] has deployed a nonlinear digital filter (AR-paradigm) for the purpose of pre-classification of spikes. The constituents are grouped into epileptic spikes and trivial non-spikes (akin to those occurring in background activity). In detection phase, only spike-like components are utilized for SVM classification.

Campbell [156] has proposed a dynamic weight decay, without large filter weight biasing, based LMS adaptive linear predictor. This method discriminates transient events, such as epileptic events or spikes, and in particular, epileptic discharges. This degrades signal-to-noise-ratio of transient events by two-fold with respect to the background activity, which leads to a great selectivity in consequent epileptiform event detection stage. In [157], Oikonomou *et al*. have introduced a technique for spike-like waveform enhancement in electroencephalogram recording utilizing a TVAR-model. Assuming nonstationarity of the epileptiform events, the time-variant coefficients of AR paradigm are approximated by utilizing a Kalman filtering approach. This technique diminishes background activity (modeled as a stationary noise), while emphasizing the spikes. It is assumed that electroencephalography encompasses an underlying background event, that is considered to exhibit stationarity, and which is having superimposed transient nonstationarities. In [157], no dissimilarity is assumed among “spikes”, “sharp-waves”, “spike-and-wave-complexes”; and hence, these are commonly called spikes. Moreover, the sensitivity of spike approximation / estimation process is enhanced in comparison to the case without any pre-processing stage.

1.4 EOG Detection and Removal Techniques

In electroencephalogram signals, the presence of artifacts leads to generation of spikes that may be misinterpreted as neurological rhythms. Therefore, noise as well as spurious signals should be removed from electroencephalogram signal to ensure an accurate analysis as well as diagnosis. Gomez-Herrero *et al*. [158] have proposed a scheme for eliminating ocular artifacts from EEG signals without utilizing an EOG reference channel. In [159], a regression-based electrooculogram alleviation scheme is incorporated to artifactual signals. This regression may be utilized with a number of electroencephalography channels. Moreover, no expert advice is required, and no subjective information is required. This scheme is fully automated, and the outcome is determined based on datasets. Conventional ocular artifact correction algorithms utilize regression-based methods [160], [161], which are utilized to calculate propagation parameters or transmission features for determining relation between different electrooculogram channels and electroencephalography channels. However, correction includes subtraction of approximated proportion of electrooculogram signal from electroencephalogram signalling waveform. One concern usually raised regarding regression method is bidirectional contaminating artifacts. Lins *et al*. [162] have mentioned low-pass filtering of electrooculogram signals utilized to calculate regression parameters. To suppress artifacts in electroencephalogram signals, many regression-based approaches [163], [164] either in time-domain or frequency-domain, are suggested so far. In every regression-based scheme, calibration trials are performed to compute transfer parameters between electrooculogram channel and electroencephalography channel, which are subsequently utilized in correction stage to approximate artifactual signal constituents in EEG recording for elimination [165].

However, exclusion of corrupted electroencephalogram segments leads to an undesired information loss. Karimi *et al*. [166] have presented an adaptive correction scheme relying

on maximum likelihood estimation. Two major techniques are there to rectify electrooculogram artifactual signal. First technique is based on regression with a long history [75], [159], [167], [168]. The second approach is based on blind-source-separation (BSS). This approach has been reported by Vigario [169], in which all channels are assumed to be linear combination of electroencephalogram signal and pure electrooculogram. The limitation of this technique is unknown number of sources, and this technique fails to extract pure EOG component completely. As regression techniques do not take into account the bidirectional contamination between electroencephalography and electrooculogram signals, therefore these not only alleviate artifactual activity, but also the potentially important cerebral information gets suppressed [170]. In order to resolve limitations of regression techniques, Romero *et al*. [171] have presented other techniques using linear decomposition of electroencephalogram and electrooculogram signals into different constituents. Such techniques have shown to play a significant role in electroencephalography signal analysis.

In [172], a statistical approach for the removal of ocular-artifacts (OAs) from electroencephalography recording through thresholding and correlation is proposed. The mean, variance, standard deviation and correlation performance metrics are used. The suppression of ocular artifacts in dBs is improved by utilizing statistical method. An algebraic technique based on numerical differentiation is proposed in [173]. The appearance of an artifactual signal is modelled as irregularity, which occurs explicitly in time-derivative of electroencephalogram signal as delay. Manipulation of this delay is simple with operational calculus, which results in joint detection as well as localization procedure. Chang *et al*. [174] have suggested a scheme for real-time recognition of eye blink artifactual signals in unsupervised way. The presented technique utilizes the first-derivative sum in multiple sliding windows [175] with an automatic thresholding scheme [176]. Both schemes are improved to act in real-time, as these are actually designed for off-line ES signal recognition. The eye blink artifactual signals are reported to affect theta as well as alpha rhythms of

frontal electroencephalogram signals, and hard to be efficiently recognized in an unsupervised manner, because of high level individual variability.

A scheme to identify the OA spike-zones through wavelet-transform (WT) is suggested in [177], in which soft-like thresholding is incorporated in OA zones. Adaptive thresholding applied only to OA zone doesn't affect low-frequency components, and it also conserves the shape of electroencephalogram signal in non-artifact regimes, which is highly important in the clinical diagnosis. However, power spectral density as well as correlation results (matrics) are utilized. Authors [178], [179] have introduced a technique to adaptively recognize slow-variant OA regimes, and they have applied wavelet thresholding (adaptive) procedure only to identify OA regimes, which presents cancellation of background electroencephalogram signals. In [180], discrete-wavelet-transform (DWT) based thresholding method is used with adaptive noise cancellation technique. DWT method is used for creating a reference signal for adaptive method. According to reference signal, an adaptive filter activity changes weight-vector to minimize the error and removes the OA (eye blinking noise). In [181], Zhao *et al*. have proposed a hybrid denoising technique combining DWT and adaptive-predictor-filter (APF). A particular characteristic of this technique is usage of APF based on adaptive AR paradigm for the approximation of signalling waveforms in OA regimes. In [182], adaptive filtering scheme, that used RLS procedure and fast-RLS (FRLS), is proposed to suppress ocular artifacts from electroencephalography measurement through WT. Elapsed time may be reduced by utilizing the FRLS procedure. It is concluded that adaptive cancellation with the help of wavelet decomposition may be assumed as a pre-processed task, which is an apposite processing technique to enhance the quality of electroencephalogram waveforms in biomedical signal analysis. Romo-Vazquez *et al*. [183] have compared different combinations of wavelet-denoising (WD) and ICA procedures for artifacts suppression. Yoo *et al*. [184] have proposed a scheme for artifactual signal excision based on particular power

spectrum characteristics of independent constituents attained from electroencephalography by fusing ensemble average and cross-correlation parameters of electroencephalography, which involves artifactual signals corresponding to eye blinks.

The regression-based and component-based methods are compared in [185] to correct ocular artifacts. An automated PCA scheme efficiently alleviates OAs and results in very low spectral disturbances, however ICA correction appears as distortion power between $5Hz$ and $20Hz$. It is observed that adaptive filtering improves regression-based artifactual correction. The simulation results show that usage of short-epochs improves approximation of power for theta- alpha- and beta-bands, while worsening approximation of time-domain features because of the problem of re-attaching refined epochs. Ocular artifact removal approach proposed in [186] is based on ICA, which is evaluated in different operative scenarios, characterized by various SNR values and number of electrodes. Ocular activity generates enormous artifacts in electroencephalography. Epochs corrupted by OAs may be manually removed, but it is at the cost of clinical expertise, and significant information deficit. The correction algorithms may segregate brain electric activity from ocular potentials, by utilizing regression / PC-based paradigms [162], [164], [187]. The goal of research work in [185] is to utilize real-time and simulated electroencephalography datasets to compare multiple regression, PCA as well as ICA techniques for OA correction, with a certain focus on spectral analysis of electroencephalogram signals. To rectify or cancel OAs from EEG, different regression-based schemes have been suggested, which involve the time-domain regression [78], [161], [167] as well as frequency-domain regression [188], [189]. Nowadays, component-based schemes, like PCA [190] and ICA [77], [191], have been particularly incorporated in electroencephalography and electrooculogram segments, which are measured simultaneously. However, special care is required in re-attaching consecutive segments after correction [185]. Such schemes are not capable to perform in on-line, sample-by-sample cancellation of OAs, unless affixed set of correction parameters is pre-determined using

calibration experiments [164]. But, drawback of PCA-based techniques is a prior consideration that the decomposed constituents are algebraically orthogonal [192]. Moreover, PCA can't entirely segregate OAs from electroencephalogram signal, particularly when, these exhibit comparable amplitudes [170]. However in some ICA techniques, the visual examination of ICA constituents and manual classification of interference constituents are needed, which is undesirable in real-time artifactual signal excision.

The adaptive noise cancellation filter utilizing an ANN for actual suppression of EOG interference from electroencephalogram signals is presented in [193]. A recurrent NN is employed in [193] for modeling the interference signals to predict ocular interference from EEG signals, and its performance is also compared with that of a feedforward NN in removing eye blink. An effective metric has been proposed in [194] for quantitatively measuring the capability of OA suppression techniques, while minimizing distortion in EEG. Like most OA removal techniques, this $H\infty$ procedure needs a reference EOG signal. A linear combination of three EEG channels has been utilized as the reference signal instead of a recorded EOG signal needed by a number of OA reduction procedures, thus giving an alternative to directly recorded EOG.

In [195], an appropriate OA suppression method incorporates two famous adaptive filtering methods, (well-known as adaptive noise cancellation and adaptive signal enhancement), in one recurrent NN. Recurrent learning procedure is incorporated to train presented NN, which converges at fast rate to give low MSE. The NN may be realized with small number of nodes, for systematic eradication of OAs. Erfanian and Mahmoudi [196] have suggested an adaptive-noise-canceller (ANC) utilizing NN for actual suppression of eye blink artifacts present in electroencephalogram waveforms. Conventional ANC filter relies on linear model of interference. The results show that one electrode measurement gives adequate reference input correlated to noise in primary signal. Zhang and Li [197] have proposed a scheme with two references to suppress ECG and respiration artifacts from

electroencephalography recordings. The RLS procedure is utilized to simultaneously regulate the tap-coefficient vector for parallel filtering configuration. Chen *et al*. [198] have explored details about the adaptive noise cancellation, that relies on adaptive-neuro-fuzzy-interference for EOG artifactual signal eviction, that is relatively sensitive towards inputs and membership function under practical situations. Gaussian / generalized-bell-membership function is usually more authentic, which has appeared as a promising option for the excision of OAs.

A group of researchers [199] have proposed another measurement of ocular artifacts, which relies on video-based eye tracker instead of electrooculogram to cancel OAs, with minimum frame-rate. However, time-frequency investigation (e.g., spectrogram of STFT) is much efficient [200]. Noureddin *et al*. [199] have provided a time-frequency analysis of blinks and eye movements (especially high, frequent eye saccades) in EEG signal recorded at large sampling frequency. Moreover, lowest sampling-rate for the eye tracker-based alternative for OA suppression is also mentioned. In [185], a modified filtering technique for regression-based correction utilizing Bayesian adaptive splines [201], [202] is presented. This scheme utilizes nonlinear filtering to eliminate high-frequency event, in case amplitude fluctuations are low. It retains high-frequency events, in case amplitude variations are high. This adaptively filtered electrooculogram isolates events particularly associated with OAs, and also suppresses the cerebral events. The usage of this adaptive filtering prior to application of regression correction can significantly alleviate hazards arising due to bidirectional contamination. Authors have reported an adaptive procedure for the elimination of OAs from electroencephalograph recording in [203]. The outcomes depict that in case of shape mismatch or any misalignment between the reference electrooculogram and corresponding artifactual signal, the adaptive filtering technique may prove to be efficient to recover pure electroencephalogram signal by utilizing filter length more than one. An adaptive time-warped-polynomial-filter (TWPF) is presented in [204] for removing baseline wander. TWPF technique reacts quickly to the variations in signal's characteristics

independent of the amplitude of electroencephalogram along with its baseline. It doesn't need a reference signal, and it may be incorporated to deal with non-periodic waveforms also. This filter is capable to efficiently eliminate baseline wander, even when time-varying cut-off frequency of TWPF is specifically approximately 1 Hz.

A technique for suppression of OAs present in electroencephalogram signals has been proposed in [75]. This scheme has been applied by utilizing a LabView software for the actual excision of real-time electrooculogram artifactual signals. This technique is proved to be efficient in suppressing both vertical-electrooculogram (VEOG) and horizontal-electrooculogram (HEOG) artifactual signals [75]. An adaptive filtering scheme is presented in [205] to suppress these artifactual signals present in EEG signals. This technique has used VEOG, HEOG and electromyogram signals as three reference signals for filtering configuration. The artifact excision technique is applied by using a multichannel LMS algorithm. FIR filters with different lengths are used to provide the appropriate approximation of VEOG, HEOG and EMG. The outcomes of this practical artifact excision procedure satisfy expected protocols as well as design guidelines. In traditional adaptive filtering [193], the primary input is recorded electrooculogram and the reference inputs are VEOG as well as HEOG. In [206], Kavitha *et al*. have reported a filtering technique, which encompasses radial-EOG (REOG) signal as third reference input. It is found that this method provides much efficient results than existing two-reference technique. However, Shahabi *et al*. [207] have reported a novel technique to combat eye blink artifactual signals from EEG, without utilizing electrooculogram reference electrodes. Shahabi *et al*. [207] first model electroencephalogram event by an AR paradigm and eye blink by an output-error paradigm. Subsequently, the investigators utilize Kalman filtering procedure to approximate true EEG based on combination of these two models. The presented technique [207] relies on signal-modelling, time-variant covariance matrices and Kalman filtering approach.

1.5 Statement of Problem

The presented work includes a detailed study of electroencephalogram (EEG) signal analysis techniques for epileptic spike detection and artifact excision. Different artifacts, which may contaminate the true EEG signal, are epileptic spikes (ESs), electrooculogram (EOG) signals, residual electrocardiogram (ECG) signals, residual electromyogram (EMG) signal, baseline wander, powerline signal interference and inevitable additive-white-Gaussian-noise (AWGN) etc.

The presence of spikes is an indicator of epileptic seizures; and their detection as well as characterization are important for the diagnosis of various neurological disorders. However in the domain of signal processing, the presence of spikes means an increase in instantaneous energy associated with a nonstationary short-time broadband event. Moreover, different attributes of spikes, like amplitude, location of occurrence, polarity, spectrum and base-width change from patient-to-patient and time-to-time for a particular patient. These ESs emerge in electroencephalography as isolated spikes, sharp-waves and quasi-periodical oscillations of spike-and-waves. This is precisely why detection and pathological implications of spikes are tedious. More often, a spike identification method may be thought as a two-step procedure: enhancement and detection. The aim of enhancement-step is to make the epileptic spike samples stand out from rest of signal waveform (background activity), thereby simplifies the following process of detection. There is ample scope of improvement in such trendy approaches, by utilizing adaptive signal processing (based on Kalman, RLS and NLMS filtering algorithms) techniques for ES enhancement, and by using statistical adaptive approaches to design adaptive decision thresholding procedures in ES detection process.

But, when the eye movement takes place (saccade or blink), the electrical field around eye varies, generating an electric signal, usually called the electrooculogram. Such signal propagates over scalp, and it emerges in the measured electroencephalogram signalling waveform as artifactual signals (or noise) that presents severe hazards in

electroencephalography interpretation / analysis. When some applications need real-time excision/suppression of ocular artifactual signals, or when the calibration trials can't be performed owing to different limitations, the schemes like transform-based techniques and regression-based techniques become unsuitable. However, the noise suppression methods based on adaptive filters to eliminate ocular artifactual signals from electroencephalogram signal do not need calibration trials, and electrooculogram artifactual signals may be excluded on-line. Moreover, such linear adaptive signal processing approaches are fast and much more reliable than other conventional techniques. Therefore, our intended effort is to develop artifact excision techniques (adaptive approaches) in the presence of AWGN, to combat epileptic spikes and EOG signals present in the recorded EEG signal, to generate the refined electroencephalogram signal.

Based on abovementioned literature survey, the presented research work contains improved EEG signal analysis techniques for epileptic spike detection and artifact excision.

And the problem (P), as treated in this research effort, can be broken up into three foremost sections; which are as follows:

P1.) Analysis and design of nonstationary epileptic spike detection procedure for electroencephalogram signal utilizing smoothed nonlinear energy operator

It is based on "a time-domain windowing technique to generate SNEO output" and "an adaptive decision thresholding procedure for the detection of ESs", in the presence of AWGN.

P2.) Analysis and design of electroencephalogram epileptic spike detection scheme utilizing output correlation method: A Kalman filtering approach

It is based on "an adaptive filtering technique for ES enhancement" and "a decision thresholding procedure based on the output of same filter for the detection of ESs", in the presence of AWGN.

P3.) Analysis and design of ocular artifacts excision technique for EEG signals using numeric variable forgetting factor recursive least squares adaptive algorithm

It is based on "the application of adaptive signal processing algorithm for the removal of HEOG and VEOG signals (noise/artifacts) from recorded electroencephalogram signal", in the presence of AWGN.

1.6 Organisation of Thesis

Chapter 2:- "Nonstationary Epileptic Spike Detection Algorithm for EEG Signal Using SNEO"

In this chapter, we first give details about the synthetic electroencephalogram signal paradigm utilizing the underlying background process with superimposed triangular spikes. Subsequently, we describe SNEO along with the different window functions. The adaptive setting of threshold is also explored for the proficient epileptic spike detection. Further, simulation results are demonstrated for the randomly varying triangular spike base-width in the synthetic electroencephalogram signal. We also use the real-time EEG signals (WAG/Rij rat-data) for the performance evaluation of the presented adaptive ES detection technique. At last, summary of chapter is provided to illustrate the substantial contributions in this chapter.

Chapter 3:- "EEG Spike Detection Technique Using Output Correlation Method – A Kalman Filtering Approach"

In this chapter, we first describe the general Markov-model with time-varying parameters for the electroencephalogram signal. The raw EEG signal is defined as a composite signal consisting of the nonstationary Markovian background activity as well as the additive white Gaussian noise. We next give details about the basic Kalman filtering equations for the epileptic spike enhancement in the EEG signal, in which the measurement-noise variance and the process-noise variance are determined heuristically after long experimentation (for best results). It is based on a supposition that the recorded electroencephalogram signal encompasses an underlying nonstationary background activity (the aforementioned time-varying Markovian-parameters are generated by the first-order AR processes with constant AR coefficients), additive white Gaussian noise and superimposed transient nonstationarities i.e., ESs. In the presented output correlation method for the epileptic spike enhancement in the recorded EEG signal, aforementioned noise variances are determined using analytical

approach. Subsequently, these spikes are detected using the statistical threshold function based on the output of adaptive filtering configuration. The simulation outcomes are showcased by utilizing the synthetic EEG signal as well as the real-time WAG/Rij rat EEG signals to demonstrate the efficacy of proposed output correlation method. This unsupervised signal processing technique combats the noise as well as nonstationarities present in the recorded EEG signal for the efficient ES detection. In the end, summary of chapter is given to demonstrate the noteworthy contributions in proposed research work.

Chapter 4:- "Excision of Ocular Artifacts from EEG Using NVFF–RLS Adaptive Algorithm"

In this chapter, we first furnish details about the adaptive system paradigm used for the excision of ocular artifacts from the recorded electroencephalogram signal. We also provide attributes about the generation of synthetic EEG signal and synthetic EOG signals. Subsequently, the application of numeric variable forgetting factor in RLS algorithm based adaptive system is introduced. We next present the simulation outcomes to demonstrate the efficacy of the presented NVFF-RLS procedure in artifact removal. The performance of linear NVFF-RLS algorithm based ocular artifact and noise cancellation method is compared with the conventional linear FFF-RLS, linear FSS-NLMS and linear GVSS-NLMS algorithms, by using the synthetically generated EEG signals and the real-time recorded EEG signals corrupted by EOG and noise signals. Finally, summary of chapter is furnished to show the considerable contributions in this chapter.

Chapter 5:- "Concluding Remarks and Future Scope"

We conclude the dissertation with a summary of the imperative results/outcomes and suggestions for the future research work.

CHAPTER 2

NONSTATIONARY EPILEPTIC SPIKE DETECTION ALGORITHM FOR EEG SIGNAL USING SNEO

2.1 Introduction

Electroencephalogram (EEG) spikes are indicator of epileptic seizures [208], [209]. The epileptic seizure is engendered by the abnormal synchronization of neurons of the cerebral cortex of patients [210]. The Hilbert-transformation of intrinsic mode functions may be used to detect the focal temporal lobe epilepsy. However, the classification of normal, interictal and ictal EEGs may be accomplished, by calculating the quantitative values of relative wavelet-energy and wavelet-entropy from the different datasets, by using the wavelet-coefficients obtained through the discrete wavelet-transform [211], [212]. But, the associated computational complexity is significantly high.

Therefore, the focus of underlying research work is to explore computationally efficient adaptive epileptic-spike (ES) detection algorithm. In the domain of physiology, neurology and biomedical engineering, the most prominent example of interictal epileptiform activity is ES [213], which is akin to the increasing instantaneous energy at the localized high frequencies. However, the shape as well as the size of ESs differ among patients, which emerge in electroencephalogram signal as the isolated spikes, sharp-waves as well as the quasi-periodic oscillations of spikes/waves [214]. The energy concentration shifts towards the lower-frequency band, as the epileptic spike base-width increases. Due to the presence of energy corresponding to EEG signal in the same lower-frequency band, the detection as well as localization of ESs are found to be quite difficult.

In the field of signal processing, the spikes may be viewed as nonstationary short-time broadband activities with the high instantaneous energy. For the simulation of synthetic EEG

signal, Tzallas *et al*. consider 8 spikes characterized with randomly changing base-width / signal-duration $3T_s$ to $9T_s$ (with sampling time T_s of the discrete-time signal) in the presence of additive-white-Gaussian-noise (AWGN) in [213], since the base-width/signal-duration of real ESs ranges from 20 msec to 70 msec. The electroencephalogram signalling waveform is first modelled as an output of the time-varying autoregressive paradigm, which may be pre-emphasized by Kalman filtering approach. Subsequently, the output of filter is compared with a threshold [213]. The motive of the signal enhancement-step is to make the epileptic spike sample stand out from the rest of data prior to the detection process. The outputs of filtering configuration, which are higher than a predefined threshold, are judged as an indication of the existence of an epileptic spike at that position in the time-series. This threshold must be optimized to minimize the number of missing true peaks, while keeping the number of falsely detected peaks within a reasonable limit. However, the computational complexity and requirement of the knowledge of system model parameters may often preclude the above Kalman filtering-based approaches [215] in such biomedical engineering applications.

In time-domain signal processing techniques [144], [145], [216], the EEG signal is pre-processed to highlight the nonstationary epileptic spikes in a stationary background. The smoothed-nonlinear-energy-operator (SNEO) based approach presented in [96] is a two-step process, which involves spike accentuation and thresholding to detect epileptic spikes. For the simulation of synthetic EEG signal, Mukhopadhyay and Ray [96] consider 8 spikes represented with the fixed base-width/signal-duration yT_s in the presence of AWGN. In this scheme, the Bartlett window function is used to reduce interference and for the ES detection without loosing much of the time resolution. The value of thresholding is also a function of SNEO, which makes the ES detection algorithm robust. In this chapter, we propose the application of SNEO based approach using the different window functions for the ES detection, where the spike base-width/signal-duration varies randomly in time. Moreover, the

concept of adaptive thresholding is incorporated by exploiting the statistical characteristics of SNEO output for the improved ES detection.

This chapter is organized as follows. We first describe the synthetic EEG signal paradigm using the underlying background process with superimposed triangular spikes (transient nonstationarities) in section 2.2. We next provide details about SNEO along with the different window functions in section 2.3. Based on the statistical theory, the adaptive setting of threshold is also discussed for the efficient epileptic spike detection in section 2.4. Subsequently, the simulation results are presented in section 2.5 for the randomly varying triangular spike base-width in the synthetic EEG signal. Further, we use the real-time EEG signals (WAG/Rij rat-data) for the performance evaluation of the proposed adaptive ES detection scheme. Finally, the section 2.6 includes summary of chapter.

2.2. Synthetic EEG Signal Paradigm With ESs

The EEG signal can be approximately modelled as the slowly time-varying background signal $bs(n)$ in the synthetic environment [96], such that

$$\begin{aligned} eeg(n) &= bs(n) + \eta(n) \\ &= \left\{ sin(\omega n) - sin(2\omega n + \phi) + sin(4\omega n) \right\} + \eta(n) \end{aligned} \tag{2.1}$$

where, $\eta(n)$ is the net white Gaussian-noise (including all types of noises) with zero-mean and variance σ_η^2, $\omega = (2\pi/75)$ and $\phi = (\pi/2)$. In the presence of triangular spikes (akin to epileptic spikes) [213], the above synthetic EEG signal (nonstationary) can be expressed as

$$s(n) = eeg(n) + spi(n) = \left\{ bs(n) + \eta(n) \right\} + spi(n) \tag{2.2}$$

in which, the embedded spike train is defined as

$$spi(n) = \sum_{i=1}^{I} p(n - k_i) \tag{2.3}$$

with, $p(n-k_i) = A_i\delta(n-k_i) + \sum_{m=1}^{q} A_i \frac{(q-m)}{q}\left[\delta(n-k_i+m) + \delta(n-k_i-m)\right]$ (2.4)

where, I is the number of triangular spikes, the spike base-width is $2q = jT_s$ at the k_i^{th} instant, the magnitude of spike amplitude varies at random in the range $A_i \rightarrow U[2.5, 7.5]$ with randomly generated sign. It is noteworthy fact that the value of triangular spike base-width is considered to be randomly varying in the range $jT_s \rightarrow [2T_s, 10T_s]$, on contrary to the fixed spike base-width in [96].

2.3. SNEO Using Window Functions

Let $s(n)$ be a real discrete-time band-limited process with Kaiser's nonlinear-energy-operator Ψ (NEO) [217], [218], such that

$$E\left[\Psi\{s(n)\}\right] = E\left[s(n)s(n)\right] - E\left[s(n+1)s(n-1)\right] = R_s(l)\big|_{l=0} - R_s(l)\big|_{l=2} \quad (2.5)$$

where, $R_s(l)$ is an auto-correlation function exhibiting lag "l", and $E(\#)$ is the expectation operator. Since $bs(n)$, $\eta(n)$ and $spi(n)$ are assumed to be statistically uncorrelated signals, therefore the index of concentration of energy is derived by substituting Eq.(2.2) in Eq.(2.5), as

$$\begin{aligned} E\left[\Psi\{s(n)\}\right] &= E\left[\Psi\{eeg(n)\}\right] + E\left[\Psi\{spi(n)\}\right] \\ &= E\left[\Psi\{bs(n)\}\right] + E\left[\Psi\{\eta(n)\}\right] + E\left[\Psi\{spi(n)\}\right] \end{aligned} \quad (2.6)$$

If the factor $K_{HF}(n)$ is the ratio of energy in the high-frequency band to the total energy at an instant nT_s, then it can be demonstrated [96] that

$$\begin{aligned} E\left[\Psi\{s(n)\}\right] &= K_{eeg}(n)R_{eeg}(0) + K_{spi}(n)R_{spi}(0) \\ &= \left\{K_{bs}(n)R_{bs}(0) + K_{\eta}(n)\sigma_{\eta}^2\right\} + K_{spi}(n)R_{spi}(0) \end{aligned} \quad (2.7)$$

However, it is evident that the spike is associated with the higher level of instantaneous energy corresponding to the higher frequency range than the background signal (with small values of $K_{bs}(n)$ and $K_{\eta}(n)$). When the epileptic spike is present, the value of $K_{spi}(n)$ dominates in Eq.(2.7). On the contrary, the value of $K_{spi}(n)$ reduces to zero in the absence of spike at an instant nT_s. Therefore, the problem of detection of spike (nonstationary signal) is directly linked to the estimation of $E\left[\Psi\left\{s(n)\right\}\right]$. In this chapter, we consider the time-domain window-based modelling scheme [96] for the signal enhancement instead of any transform-domain scheme or signal-modelling approach [213]. Therefore instead of the time-domain averaging of $E\left[\Psi\left\{s(n)\right\}\right]$, the smoothed-nonlinear-energy-operator (SNEO) may be used to locate the epileptic spike, such that

$$\Psi_{SNEO}\left\{s(n)\right\} = \Psi\left\{s(n)\right\} * w_s(n) \tag{2.8}$$

where, the time-domain window function is denoted as $w_s(n)$ and " $*$ " represents the convolution operator. The performance indices of any ES detection algorithm are false-negative (FN) ratio and false-positive (FP) ratio, which are measured as

FN = (Number of spikes missed) / (Actual number of spikes) (2.9)

FP = (Number of false spikes detected) / (Actual number of spikes) (2.10)

After this ES accentuation process, the threshold is optimized to minimize the number of missing true peaks (i.e., FN), while keeping the number of false detection of peaks (i.e., FP) within a reasonable limit. The threshold value is determined by using the following

$$\Gamma_S(n) = (C/N)\sum_{\bar{n}=0}^{N-1}\Psi_{SNEO}\left\{s(n-\bar{n})\right\} \tag{2.11}$$

where, N is the number of samples and C is the scaling factor based on experimentation. For further analysis, we need to define the parameter β_C = (Maximum number of spikes in

the past N samples) / N. The SNEO output value $\Psi_{SNEO}(n)$ may be considered as ergodic in the wide sense, for the small values of β_C.

However, the aim of underlying research effort is to find out the exact location of ESs for the physiological and neurological disorder analysis. Therefore, the bias of spike detection in terms of the sampling points is incorporated for the best possible assessment of ES location, which is considered as

$$Bias = \frac{1}{\bar{M}} \sum_{m=1}^{\bar{M}} \left| n_m - \hat{n}_m \right| \tag{2.12}$$

where n_m *and* $\hat{n}_m$ are the actual and estimated locations of *ith* spike maxima respectively, and $\bar{M}$ is the number of correctly detected spikes. Finally, we focus on the different time-domain window functions $w_s(n)$ [219] to be considered for evaluation of $\Psi_{SNEO}\{s(n)\}$, which are

(i) Rectangular window is defined as

$$w_{\mathrm{Rec}}(n) = 1$$

(ii) Bartlett window is defined as

$$w_{Bar}(n) = \{1 - 2|n - 0.5(M-1)|\} / (M-1)$$

(iii) Hanning window is defined as

$$w_{Han}(n) = 0.5 - 0.5\cos\left(\frac{2\pi n}{M-1}\right)$$

(iv) Hamming window is defined as

$$w_{Ham}(n) = 0.54 - 0.46\cos\left(\frac{2\pi n}{M-1}\right)$$

(v) Kaiser window is defined as

$$w_{Kai}(n) = I_0\left[\alpha\sqrt{\left(0.5(M-1)\right)^2 - \left(n - 0.5(M-1)\right)^2}\right] \Big/ I_0\left[0.5\alpha(M-1)\right]$$

where, M is the finite impulse response filter length, $I_0(\#)$ is the zeroth-order modified Bessel function of the first-kind, and the factor α controls the way window function tapers at the edges in time-domain.

2.4. Adaptive Determination of Threshold for ES Detection

As the neural signal along with the ESs may be considered as the nonstationary process, the $E\left[\Psi\left\{s(n)\right\}\right]$ operator can be replaced by $\Psi_{SNEO}\left\{s(n)\right\}$ using Eq.(2.8) as

$$\Psi_{SNEO}\left\{s(n)\right\} = \sum_{m=0}^{M-1} w_s(m)\,\Psi\left\{s(n-m)\right\} \tag{2.13}$$

Since $\Psi_{SNEO}\left\{s(n)\right\}$ is found to be smoothly varying in time [220], therefore its mean μ_{SNEO} and variance σ^2_{SNEO} are determined as

$$\mu_{SNEO} = E\left[\Psi_{SNEO}\left\{s(n)\right\}\right] = \sum_{m=0}^{M-1} w_s(m)\,E\left[\Psi\left\{s(n-m)\right\}\right] \tag{2.14}$$

Substitution of Eq.(2.5) in Eq.(2.14) leads to

$$\mu_{SNEO} = \left[R_s(l)\big|_{l=0} - R_s(l)\big|_{l=2}\right]\sum_{m=0}^{M-1} w_s(m) \tag{2.15}$$

It can also be shown that

$$\sigma^2_{SNEO} = \mathrm{var}\left[\Psi_{SNEO}\left\{s(n)\right\}\right] = E\left[\Psi^2_{SNEO}\left\{s(n)\right\}\right] - \mu^2_{SNEO} \tag{2.16}$$

Here, the value of mean μ_{SNEO} and variance σ^2_{SNEO} depend on the auto-correlation function of the underlying neural signal. In the presented research work, we propose the following threshold function based on these statistical parameters as

$$\Gamma_A = C\mu_{SNEO} + \beta_{FA}\,\sigma_{SNEO} \tag{2.17}$$

The parameter Γ_A can serve as an adaptive detection threshold to detect the presence of epileptic spikes. The classical auto-correlation function is very sensitive to the occurrence of

ESs. Therefore, the value of parameter C needs to be adjusted with the increasing value of β_C obtained through experimentation. However, the parameter β_{FA} depends on the probability of false alarming in ES detection. The higher value β_{FA} induces a failure to detect the low magnitude spikes, while a low value of β_{FA} increases the false alarming rate. The value of parameter C may be adjusted for the initial coarse-tuning of detection threshold, whereas β_{FA} may be subsequently adjusted to achieve its final fine-tuning. However, if the process $\Psi_{SNEO}(n)$ exhibits mean-ergodicity and auto-covariance ergodicity, as its time-average tends to the ensemble average for $N \to \infty$ $(\beta_C \to 0)$ [221], then it is clear that the estimated value of mean is

$$\hat{\mu}_{SNEO} = \lim_{\beta_C \to 0} \frac{1}{N} \sum_{\bar{n}=0}^{N-1} \Psi_{SNEO}\left\{s(n-\bar{n})\right\} \to \mu_{SNEO} \tag{2.18}$$

For this estimated value of mean [221, sec. 5.3, pp. 108], the auto-covariance is determined as

$$\hat{\sigma}^2_{SNEO} \simeq \lim_{\beta_C \to 0} \frac{1}{N-1} \sum_{\bar{n}=0}^{N-1} \left[\Psi_{SNEO}\left\{s(n-\bar{n})\right\} - \hat{\mu}_{SNEO} \right]^2 \to \sigma^2_{SNEO} \tag{2.19}$$

Further, it can be demonstrated using Eq.(2.11) that

$$\Gamma_s = E\left[\Gamma_S(n)\right] = (C/N) \sum_{\bar{n}=0}^{N-1} E\left[\Psi_{SNEO}\left\{s(n-\bar{n})\right\}\right] \tag{2.20}$$

The above equation can be simplified by using Eq.(2.14) to give

$$\Gamma_s = C\mu_{SNEO} \tag{2.21}$$

It is noteworthy fact for the small values of β_C that

(i) $\Gamma_A \simeq \Gamma_s$ in Eq.(2.17), as $\beta_{FA} \to 0$ (2.22)

Equation (2.22) is found to be analogous to the threshold setting criterion reported in [96] by utilizing smoothed nonlinear energy operator.

(ii) $\Gamma_A \simeq \mu_{SNEO} + \beta_{FA}\, \sigma_{SNEO}$ in Eq.(2.17) , as $C \to 1$ (2.23)

The equation (2.23) is similar to the threshold setting criterion presented in [220] using the smoothed-Teager-energy-operator (STEO). In subsequent section, we shall utilize the following suggested adaptive threshold function for simulation.

$$\Gamma_A = C\hat{\mu}_{SNEO} + \beta_{FA}\,\hat{\sigma}_{SNEO} \tag{2.24}$$

Moreover for simulations, the rat EEG signals with spikes [222] may be used instead of the human EEG data.

2.5. Simulation Results

We shall investigate the behaviour of different aforementioned window functions in combination with SNEO for the variable base-width epileptic spike detection. The continuous-time composite signal (with duration $5sec$) is sampled at the interval $T_s = (1/128)sec$ to generate 640 discrete-time signal samples for the analysis [213] (as shown in Fig. 2.1 to Fig. 2.3 for a typical example). As the duration of real-time ES approximately ranges from $20m\sec$ *to* $70m\sec$, therefore we keep the base-width of each ES randomly varying between the range $2T_s$ to $10T_s$ in time-duration. For simulation at the threshold value $C = 2.5$, eight ESs (symmetric triangular pulses) are considered with amplitude A_i randomly varying between the range 2.5 *to* 7.5, and also with random location k_i as well as random sign. The FIR filter parameter $M = 5$ is fixed for all the simulations, while keeping the signal-to-noise-ratio equivalent to $+5dB$ due to the occurrence of white Gaussian-noise (including all types of noises).

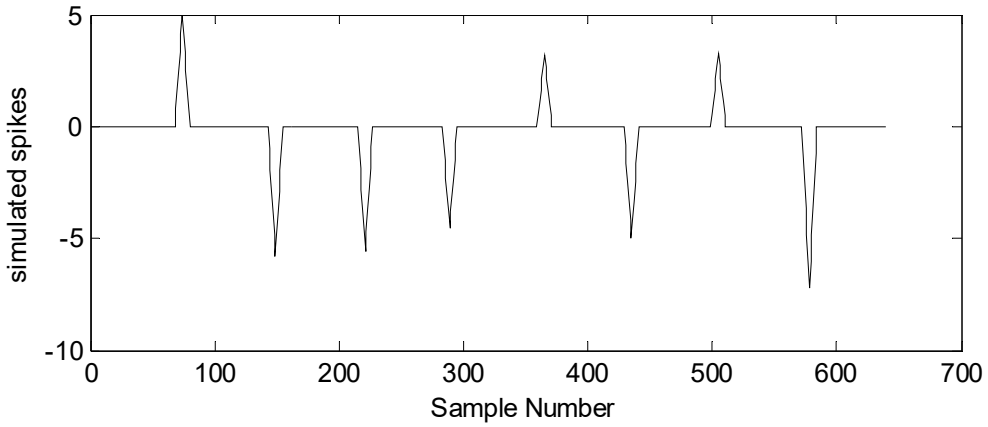

Fig. 2.1: Nonstationary spike train (randomly generated)

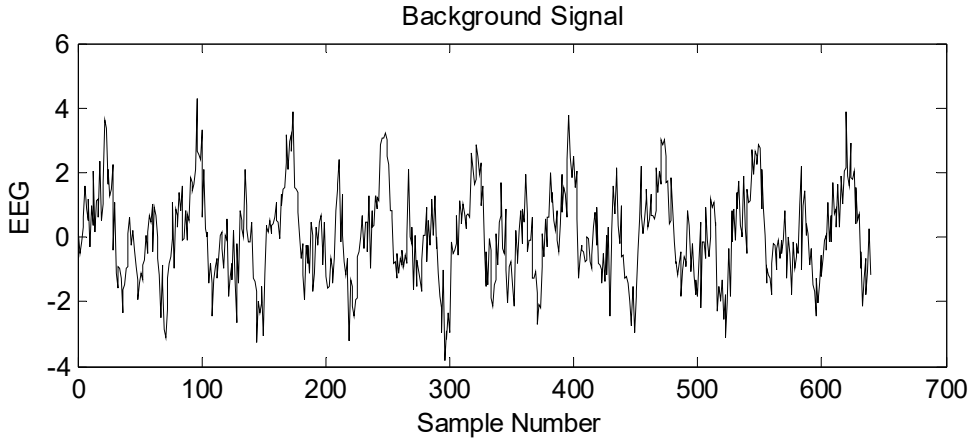

Fig. 2.2: Stationary background signal (randomly generated)

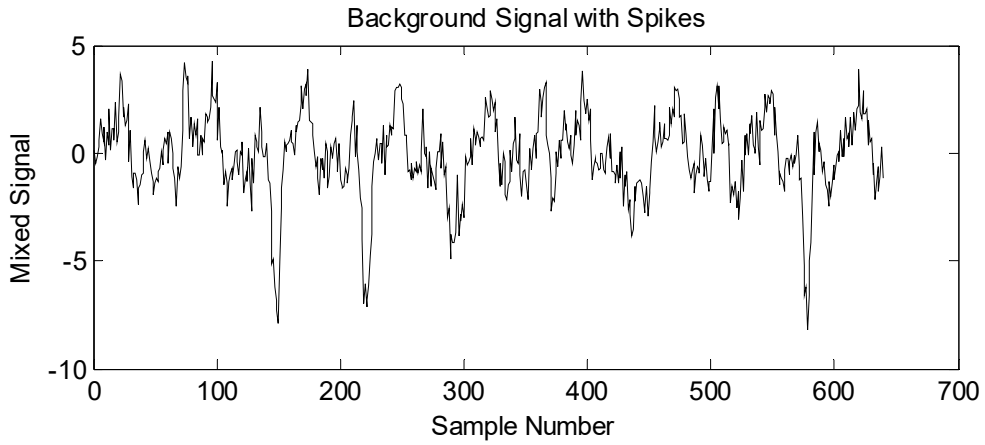

Fig. 2.3: Composite EEG signal along with nonstationary spikes

Case 1: The typical SNEO output for the Hamming window function is shown in Fig. 2.4, and the corresponding performance comparison of epileptic spike detection algorithm is depicted in Table 2.1 (depending on the ensemble average of 100 independent experiments). The approximate transition width of main-lobe is observed to be $(8\pi/M)$ for Bartlett, Hanning and Hamming window functions with peak side-lobes $-25dB$, $-31dB$ and $-41dB$ respectively. But in case of Rectangular window, the approximate transition-width of main-lobe is observed to be $(4\pi/M)$ with peak side-lobe $-13dB$. For Kaiser window, the ripple control parameter α allows the designer to trade-off the transition-width against ripples. However for different values of α, the resulting window functions are very similar to the Rectangular, Hanning and Hamming window functions, though they are not identical. It is apparent from the results presented in Table 2.1 that the Kaiser window-based SNEO outperforms other schemes. But, the Hamming window-based SNEO is computationally efficient in comparison to the Kaiser window-based SNEO.

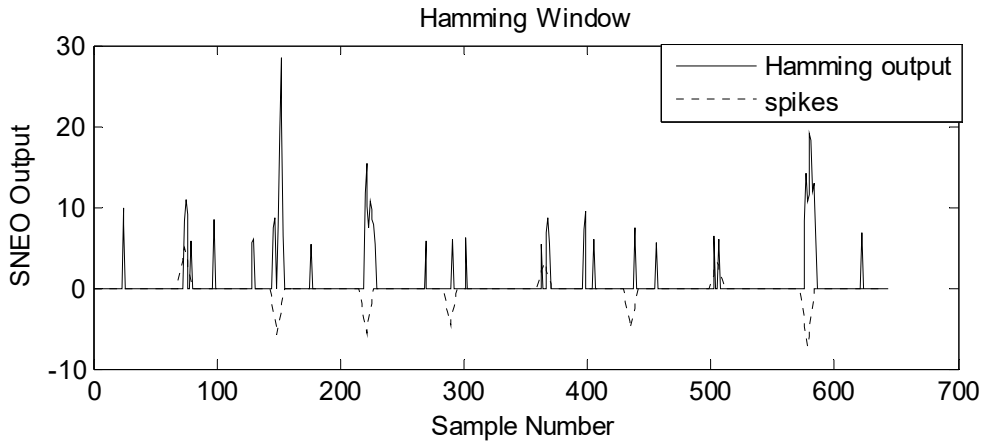

Fig. 2.4: SNEO output using Hamming window

Table 2.1: Performance evaluation of ES detection algorithm (SNEO) for different window functions

Window Function	Approx. False-Negative-Ratio (FNR)	Approx. False-Positive-Ratio (FPR)
Rectangular	0.5	1.95
Bartlett	0.125	1.79
Hanning	0.074	1.55
Hamming	0.05	1.25
Kaiser	0.055	0.88

Case 2: In the light of aforementioned discussion, we consider the Hamming window for the analysis of real-time ESs in the EEG signal, such that $w_s(m) = [0.08 \;\; 0.54 \;\; 1.0 \;\; 0.54 \;\; 0.08] = w_{Ham}(m)$. It is demonstrated by Semmaoui *et al*. in [220] that the mean and auto-covariance of EEG signal are

$$\mu_{SNEO} = 2.24\left[R_s(l)\big|_{l=0} - R_s(l)\big|_{l=2} \right] \tag{2.25}$$

$$\begin{aligned} \sigma^2_{SNEO} \approx\; & 4.8\, R_s^2(l)\big|_{l=0} + 0.7\, R_s^2(l)\big|_{l=1} + 4.4\, R_s^2(l)\big|_{l=2} \\ & + 0.6\, R_s^2(l)\big|_{l=3} - 9.3\, R_s(l)\big|_{l=0} R_s(l)\big|_{l=2} - 1.2\, R_s(l)\big|_{l=1} R_s(l)\big|_{l=3} \end{aligned} \tag{2.26}$$

The performance characteristics of three different epileptic spike detection algorithms are compared in Table 2.2 for the embedded triangular spikes with variable base-width/time-duration (as in case 1). The simulation results for 8-spikes as well as 16-spikes in Table 2.2 manifest that the significant reduction in FPR value is observed for the proposed adaptive scheme Eq.(2.24), though its FNR performance is slightly worse than STEO based approach Eq.(2.23). The value of FNR increases and FPR decreases for all the ES detection algorithms, when the number of spikes increases.

Table 2.2: Performance evaluation of ES detection algorithms for synthetic EEG signals with spikes

Method	Approx. False-Negative-Ratio (FNR)	Approx. False-Positive-Ratio (FPR)
SNEO [96], Eq.(2.11) with 8-spikes, $C = 2.5$, $\beta_C = 0.0125$	0.05	1.25
STEO [220], Eq.(2.23) with 8-spikes, $\beta_C = 0.0125$, $\beta_{FA} = 7.5$	0.024	0.85
Proposed, Eq.(2.24) with 8-spikes, $\beta_C = 0.0125$, $C = 2.5$, $\beta_{FA} = 7.5$	0.028	0.45
SNEO [96], Eq.(2.11) with 16-spikes, $C = 2.5$, $\beta_C = 0.025$	0.068	1.23
STEO [220], Eq.(2.23) with 16-spikes, $\beta_C = 0.025$, $\beta_{FA} = 7.5$	0.032	0.74
Proposed, Eq.(2.24) with 16-spikes, $\beta_C = 0.025$, $C = 2.5$, $\beta_{FA} = 7.5$	0.035	0.32

For the real-time ESs in EEG signal, the two-channel EEG recordings (of $5\,\text{sec}$ duration) at the left and right frontal cortex of adult WAG/Rij rats are used to test the proposed adaptive ESs detection scheme. These rats were born and received detailed care in the Laboratory of the Department of Comparative and Physiological Psychology in Nijmegen University, Holland, which were utilized for investigating the role of reticular thalamic nucleus in the inter-hemispheric synchronization of electroencephalogram signals [223], [224]. The frequency band of spike-wave discharges is found to be $8-10Hz$ [225], [226]. In this scenario, signals are referenced to an electrode positioned at cerebellum. These signals are subsequently filtered between $1-100Hz$ and sampled at $F_s = 200Hz$ to give 1000 sample points of the discrete-time neural signal. The normalized raw EEG signal with ESs and EEG signal without ESs are shown in Fig. 2.5 (only 640 sample points of rat-data, obtained from right cortical intracranial electrode). However, a typical sample of the normalized spike-wave discharges is shown in Fig. 2.6 (rat-data). The performance characteristics of three different epileptic spike detection algorithms are compared in Table 2.3 for the real-time EEG signal with ESs (publicly available rat-data).

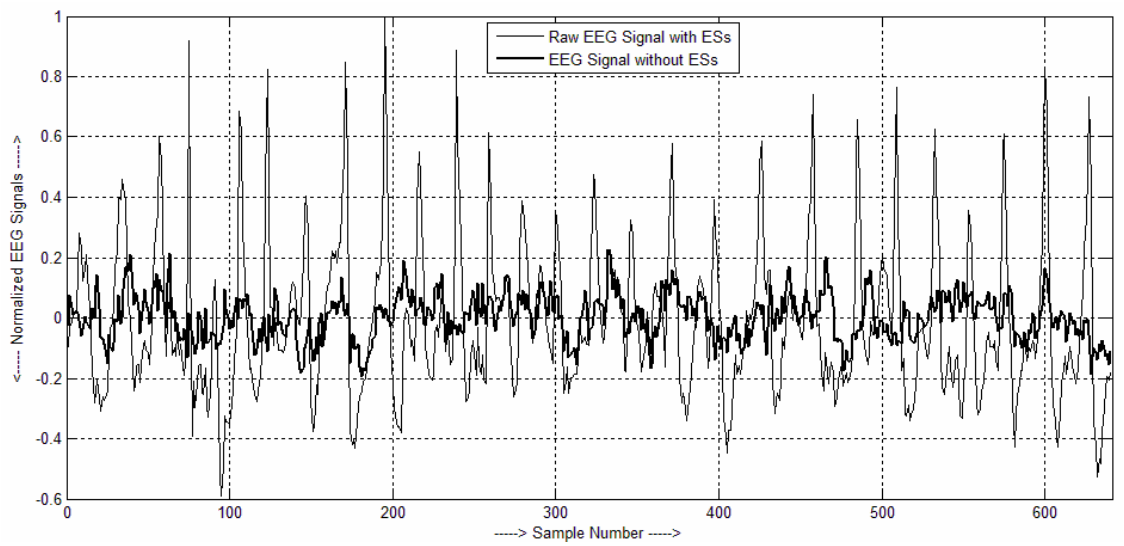

Fig. 2.5: EEG signal of rat vs. sample points

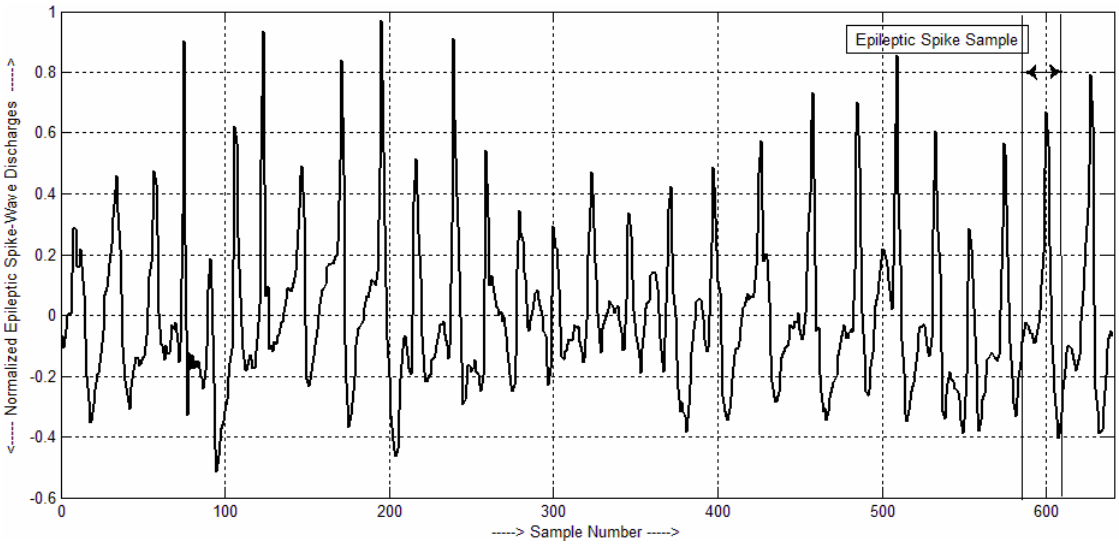
Epileptic Spike Sample
<----- Normalized Epileptic Spike-Wave Discharges ----->
1
0.8
0.6
0.4
0.2
0
-0.2
-0.4
-0.6
0
100
200
300
400
500
600
-----> Sample Number ----->

Table 2.3: Performance evaluation of ES detection algorithms for real-time EEG signals with epileptic spikes

Method	Approx. False-Negative-Ratio (FNR)	Approx. False-Positive-Ratio (FPR)
SNEO [96], Eq.(2.11) with $C = 1.75$	0.13	1.65
STEO [220], Eq.(2.23) with $\beta_{FA} = 6.5$	0.062	1.28
STEO [220], Eq.(2.23) with $\beta_{FA} = 7.5$	0.064	1.26
Presented, Eq.(2.24) with $C = 1.25$, $\beta_{FA} = 6.5$	0.067	1.05
Presented, Eq.(2.24) with $C = 1.75$, $\beta_{FA} = 6.5$	0.070	0.72

Simulation outcomes in Table 2.3 manifest that the substantial reduction in false-positive-ratio value is observed for the presented adaptive approach Eq.(2.24) with the increasing value of parameter C, though its false-negative-ratio performance is marginally worse than STEO based technique Eq.(2.23). However, the slight elevation in FNR value and alleviation in FPR value are also experienced with the increasing value of parameter β_{FA} Eq.(2.24). Therefore, the proposed adaptive threshold function results in the trade-off relationship between false-negative-ratio and false-positive-ratio values.

2.6. Summary of Chapter

In this chapter, the smoothed nonlinear energy operator based on time-domain window functions has been used to detect the nonstationary epileptic spikes encountered in electroencephalogram signal.

The incorporated window functions are Rectangular, Bartlett, Hanning, Hamming and Kaiser. The basic concept used in the presented research work is that the instantaneous epileptic spike induces high instantaneous energy content in the high-frequency range, which can be tackled using an appropriate window function.

In the presence of additive white Gaussian noise, simulation has been performed using triangular spikes (similar to ESs) in the synthetic EEG signal, in which triangular spikes exhibit stochastic amplitude, sign, base-width and arbitrary location of appearance in EEG signal. Subsequently, real-time EEG database related to the male adult WAG/Rij rats has been used to test the proposed adaptive scheme, in which modified (generalized) adaptive threshold function (generalized) has been used.

It is apparent from simulation results that time-domain window function has deep impact on the evaluation of nonstationary epileptic spike detection algorithm in the electroencephalogram signal using the smoothed linear energy operator.

Based on the computational burden, false-negative-ratio analysis and false-positive-ratio analysis, the smoothed nonlinear energy operator based on Hamming window is found to be optimal, under the appropriate adjustment of parameters C and β_{FA} in the proposed adaptive threshold setting. Under similar conditions, approximate value of false-negative-ratio, in case of Hamming window using SNEO method, is observed to be less in comparison to Kaiser window-based technique.

CHAPTER 3

EEG SPIKE DETECTION TECHNIQUE USING OUTPUT CORRELATION METHOD – A KALMAN FILTERING APPROACH

3.1 Introduction

The epileptiform activity in the electroencephalogram (EEG) signal is an indicator of epilepsy, which accounts for the abrupt recurrent and transient disturbances of mental functioning/response, due to the excessive abnormal discharge of a bunch of neurons in the brain [209], [244]. Usually high amplitude synchronized periodic waveforms appear in the EEG signal during seizures (ictal activity) [249]. The EEG signal sometimes contains epileptiform transient waveforms during the interictal activity, which can be detected using the conventional techniques by observing the short recordings for the diagnosis of epilepsy [96], [220], [233]. However, the detection of low amplitude EEG spikes is difficult in the presence of seizure-like activity due to other neurological disorders.

Out of the time-domain techniques [144], [240], the signal-modeling schemes [208], [229], [250] and the transform-domain strategies [222], [229], [230], we focus on the signal-modeling approach for the signal enhancement and detection. Tzallas *et al*. [213] have presented an epileptic spike (ES) detection scheme in [213], in which the spikes are accentuated prior to the usage of a spike detector for the enhanced sensitivity, to minimize the missed events while keeping the satisfactory selectivity level. Though several adaptive noise suppression/excision techniques have been proposed in the presence of noise and artifacts [238], [246], [247], but the nonstationary characteristics of the EEG signals have been ignored. However, Oikonomou *et al*. have proposed a new scheme for the electroencephalogram spike accentuation in [157] using the time-varying autoregressive (AR) paradigm to exploit the nonstationarity of EEG signal for the improved spike detection, in

which the AR coefficients [221] are estimated using the Kalman filtering (KF) approach. Under the wide variations of nonstationary characteristics of the epileptic spikes in addition to the presence of noise, such KF based epileptic spike enhancement and detection techniques [157], [213] outperform the smoothed nonlinear energy operator-based approach [96].

In this strategy, the epileptic spikes are pre-emphasized using the Kalman filter, which is followed by the epileptic detection procedure based on a threshold function [213]. Here, the absolute value of estimated EEG signal is used to determine the decision threshold by averaging its subsequent samples, which is scaled to minimize the missing true peaks and to keep the number of false event detection within the rational limit. But, it is exceptionally sensitive to the parameter ambiguities, and hence turns out to be unstable under the parameter mismatching situation. Therefore for the EEG signal processing and analysis, the variance of measurement-noise σ_R^2 and the variance of process-noise σ_Q^2 are to be chosen after the long experimentation [157], [213]. Moreover, the analytical procedure to determine the values of σ_R^2 and σ_Q^2 using the Kalman filtering approach is still an issue, for further research, in the domain of EEG signal analysis.

However, Mehra [243] has presented the different approaches to adaptive filtering by exploiting the Kalman-Bucy filtering equations, in which *a priori* statistics of measurement-noise and process-noise can be estimated on-line from the observed data using either the output correlation approach [242] and innovation correlation method [241] or the correlation matching technique [243]. In this chapter, we propose the usage of output correlation method for the EEG spike enhancement and detection using the Kalman filtering-based signal processing approach, in which the adopted strategy is motivated by the research work presented in [157], [213], [243].

This chapter is arranged as follows. In section 3.2, we first describe a general Markov-model with time-varying parameters for the EEG signal. The raw EEG signal is defined as

the composite signal consisting of the nonstationary Markovian background activity as well as the white Gaussian-noise. We next give details about the basic Kalman filtering equations for the epileptic spike enhancement in the EEG signal, in which the measurement-noise variance (σ_R^2) and the process-noise variance (σ_Q^2) are determined heuristically after long experimentation (for best results) as in [157], [213]. It is based on the supposition that the recorded electroencephalogram signal encompasses an underlying nonstationary background event (the aforementioned time-varying Markovian-parameters are generated by the first-order AR processes with constant AR coefficients), white Gaussian-noise and superimposed transient nonstationarities, i.e., ESs. Section 3.3 introduces the proposed output correlation method for the epileptic spike enhancement in the recorded EEG signal, in which σ_R^2 and σ_Q^2 are determined using analytical approach. Subsequently in section 3.4, these spikes are detected using the statistical threshold function based on the output of adaptive filter. In section 3.5, the simulation results are presented using the synthetic EEG signal as well as the real-time WAG/Rij rat EEG signals to demonstrate the efficacy of proposed output correlation method. This unsupervised signal processing technique combats the noise as well as nonstationarities present in the recorded EEG signal for the efficient ES detection. Finally, summary of chapter is given in section 3.6.

3.2 Basic Kalman Filtering Approach for Epileptic Spike Enhancement in EEG Signal

The EEG signal corresponds to the summed postsynaptic potentials of neurons in the brain, in which the presence of spikes indicates the epileptic disorder. In the field of signal processing, the spikes are considered to be nonstationary short-time processes with high level instantaneous energy spread over a large band of frequencies, which create problems not only in the EEG signal analysis but also in many biomedical engineering applications [232]. However, the enhancement of patient's recorded EEG signal prior to the detection procedure

leads to the spike samples stand out from the rest of data. Therefore, the main aim of research work reported in the field of EEG biosignal processing is to clearly distinguish the transient waveforms, isolated spikes, sharp-waves and spike-wave composite signals from the background activity [157], [213], [214]. For mathematical modeling of EEG signal, let $\vec{Y}(t+P)$ be the $N\times 1$ observation vector for the single channel raw EEG signal at time $t+P$, in which we consider that the raw EEG signal can be described by using a Markov paradigm [157], [213], [215], [228] consisting of the time-varying state parameters, such that

$$\vec{Y}(t+P)=\vec{C}(t+P)\vec{S}(t+P)+\vec{V}(t+P) \tag{3.1}$$

where, $\vec{Y}(t+P)=\left[\, y1(t+P)\;\; y2(t+P)\;\; .....\;\; yn(t+P)\;\; .....\;\; yN(t+P)\right]^T$ (3.2)

$$\vec{C}(t+P)=\begin{bmatrix} \vec{C}1(t+P) \\ \vec{C}2(t+P) \\ ..... \\ \vec{C}n(t+P) \\ ..... \\ \vec{C}N(t+P) \end{bmatrix} \tag{3.3}$$

which is the $N\times P$ dimensional known measurement-matrix, and

$$\vec{S}(t+P)=\left[\, s_1(t+P)\;\; s_2(t+P)\;\; .....\;\; s_P(t+P)\right]^T \tag{3.4}$$

which is the $P\times 1$ dimensional state vector with time-varying Markovian-state parameters as elements in the state-space form of EEG signal Eq.(3.1), and

$$\vec{V}(t+P)=\left[\, v1(t+P)\;\; v2(t+P)\;\; .....\;\; vN(t+P)\right]^T \tag{3.5}$$

which is the $N\times 1$ dimensional measurement or observation white Gaussian-noise vector, with zero-mean and $N\times N$ dimensional covariance-matrix $\vec{R}$. The off-diagonal elements of the observation noise covariance-matrix are zero, which results in $\vec{R}=diag\left[\,\sigma_R^2\;,\;\sigma_R^2\;,\;.....\;,\;\sigma_R^2\right]$. However, *nth* scalar observation in the above model can be represented as

$$yn(t+P) = \vec{C}n(t+P)\,\vec{S}(t+P) + vn(t+P) \tag{3.6}$$

where,

$$\vec{C}n(t+P) = \left[\, yn(t+P-1) \;\; yn(t+P-2) \;\; ..... \;\; yn(t) \,\right] \tag{3.7}$$

which is the $1 \times P$ dimensional known measurement vector, and

$$\vec{S}(t+P) = \vec{A}\vec{S}(t+P-1) + \vec{W}(t+P) \tag{3.8}$$

It is the $P \times 1$ dimensional state vector, in which the time-varying state parameters $s_i(t+P)$ are governed by the first-order AR process. However, these are responsible for the nonstationarity of EEG signal because of the dynamically linear model Eq.(3.8), in which the $P \times P$ dimensional constant AR coefficient-matrix is given as

$$\vec{A} = diag\{a_1,\; a_2,\; ..... \;, a_P\} \tag{3.9}$$

However, $\vec{W}(t+P) = \left[\, w_1(t+P) \;\; w_2(t+P) \;\; ..... \;\; w_P(t+P) \,\right]^T$ (3.10)

which is the $P \times 1$ dimensional state/process white Gaussian-noise vector, with zero-mean and $P \times P$ dimensional covariance-matrix $\vec{Q}$. The off-diagonal elements of the state/process-noise covariance-matrix are zero, which results in $\vec{Q} = diag\left[\, \sigma_Q^2 \;,\; \sigma_Q^2 \;,\; ..... \;,\; \sigma_Q^2 \,\right]$. Further, the Eq.(3.6) can be simplified as

$$yn(t+P) = \sum_{p=1}^{P} yn(t+P-p)\, s_p(t+P) + vn(t+P) \tag{3.11}$$

where, $s_i(t+P) = a_i s_i(t+P-1) + w_i(t+P)$ (3.12)

which is *ith* time-varying Markovian-parameter with the constant AR coefficient a_i. Moreover in the aforementioned equations, P is the order of proposed EEG model.

We further focus on the determination of estimate $\hat{S}^{+}(t+P)$ of the time-varying state vector $\vec{S}(t+P)$ based on the measurements $\vec{Y}(t+P)$ Eq.(3.2). As the primary state follows

a Gaussian distribution with the linear evolution, therefore the state at later stage also pursues a Gaussian distribution [157], [213]. In this conventional Kalman filtering approach, we consider $\hat{S}^{-}(t+P)$ as the *a priori* estimate of state vector $\vec{S}(t+P)$ conditioned on all the prior measurements except the one at time $t+P$ and denote $\hat{S}^{+}(t+P)$ as the *a posteriori* estimate of the same state vector $\vec{S}(t+P)$ conditioned on all the available measurements at time $t+P$. Both estimates can be related to each other by using the following relation

$$\hat{S}^{-}(t+P)=\vec{A}\hat{S}^{+}(t+P-1) \tag{3.13}$$

The objective is to find an equation that compute $\hat{S}^{+}(t+P)$ as a linear combination of $\hat{S}^{-}(t+P)$ and a weighted difference between the actual EEG measurement $\vec{Y}(t+P)$ and a measurement prediction $\hat{Y}^{-}(t+P)$; where

$$\hat{Y}^{-}(t+P)=\vec{C}(t+P)\hat{S}^{-}(t+P) \tag{3.14}$$

It follows that

$$\hat{S}^{+}(t+P)=\hat{S}^{-}(t+P)+\vec{K}(t+P)\left[\vec{Y}(t+P)-\hat{Y}^{-}(t+P)\right] \tag{3.15}$$

where $\vec{Y}(t+P)-\hat{Y}^{-}(t+P)$ is identified as the measurement innovation or the residual, which reflects the discrepancy between the actual and predicted measurements. The zero residual indicates that both are in absolute agreement. The $P\times N$ dimensional matrix $\vec{K}(t+P)$ is known as the gain or blending factor. The *a priori* estimation error is

$$\hat{e}^{-}(t+P)=\vec{S}(t+P)-\hat{S}^{-}(t+P) \tag{3.16}$$

Using Eqs. (3.8) and (3.13), the above equation can be simplified as

$$\hat{e}^{-}(t+P)=\vec{A}\vec{S}(t+P-1)+\vec{W}(t+P)-\vec{A}\hat{S}^{+}(t+P-1) \tag{3.17}$$

$$\hat{e}^{-}(t+P)=\vec{A}\hat{e}^{+}(t+P-1)+\vec{W}(t+P) \tag{3.18}$$

The corresponding *a priori* estimation error $P\times P$ dimensional covariance-matrix is

represented as

$$\hat{P}_e^{-}\left(t+P\right)=E\left[\hat{e}^{-}\left(t+P\right)\hat{e}^{-}\left(t+P\right)^{T}\right]=\vec{A}\hat{P}_e^{+}\left(t+P\right)\vec{A}^{T}+\vec{Q} \tag{3.19}$$

where, $E\left[.\right]$ is the expectation operator or ensemble average operator. Similarly, the *a posteriori* estimation error is given as

$$\hat{e}^{+}\left(t+P\right)=\vec{S}\left(t+P\right)-\hat{S}^{+}\left(t+P\right) \tag{3.20}$$

Using Eqs.(3.1), (3.14) and (3.15), the above equation can be simplified as

$$\hat{e}^{+}\left(t+P\right)=\left[I_P-\vec{K}\left(t+P\right)\vec{C}\left(t+P\right)\right]\hat{e}^{-}\left(t+P\right)-\vec{K}\left(t+P\right)\vec{V}\left(t+P\right) \tag{3.21}$$

where, I_P is the $P\times P$ dimensional identity-matrix. The corresponding *a posteriori* estimation error $P\times P$ dimensional covariance-matrix is represented as

$$\hat{P}_e^{+}\left(t+P\right)=E\left[\hat{e}^{+}\left(t+P\right)\hat{e}^{+}\left(t+P\right)^{T}\right] \tag{3.22}$$

The optimum choice of gain factor minimizes the *a posteriori* error covariance, which leads to

$$\hat{P}_e^{+}\left(t+P\right)\Big|_{Optimum}=\left[I_P-\vec{K}\left(t+P\right)\vec{C}\left(t+P\right)\right]\hat{P}_e^{-}\left(t+P\right) \tag{3.23}$$

under optimum conditions with

$$\vec{K}\left(t+P\right)\Big|_{Optimum}=\hat{P}_e^{-}\left(t+P\right)\vec{C}^{T}\left(t+P\right)\left[\vec{C}\left(t+P\right)\hat{P}_e^{-}\left(t+P\right)\vec{C}^{T}\left(t+P\right)+\vec{R}\right]^{-1} \tag{3.24}$$

As the *a priori* estimation error covariance tends to zero, the gain factor $\vec{K}\left(t+P\right)$ weights the residual less heavily. However as the measurement-noise covariance $\vec{R}$ approaches zero, the actually measured EEG signal $\vec{Y}\left(t+P\right)$ is trusted more and more because $\vec{K}\left(t+P\right)$ weights residual more heavily [236], [239].

Though the Kalman filter is known as best-linear-unbiased-estimator (BLUE) [234], [235], but it requires the system model parameters to solve the system identification problem under the nonstationary environment [9]. The effectiveness of abovementioned methodology

depends on the choice of system/model parameters i.e., the variance of observation/measurement-noise σ_R^2, the variance of state/process-noise σ_Q^2, the order P of time-variant Markov-model and the constant AR coefficient-matrix A. The values of constant AR coefficients are kept very low to maintain a low degree of correlation between time-varying Markovian-parameters i.e., $a_1 = a_2 = ... = a_P = 0.1$. However, the value of σ_Q^2 is fixed at 0.1 with $P = 15$ [248] and σ_R^2 = 1.5 × (average absolute value of the raw electroencephalogram signal without ESs) [157].

For the raw electroencephalogram signal containing epileptic spikes, which are close to each other, the motive of above spike enhancer is to maximize the selectivity to decrease the false detections. It is noteworthy that the autoregressive processing produces the noisy EEG signal [157], [213] using the aforementioned equations, which undoubtedly makes the spike detection process difficult. However on the contrary, the Kalman filter [236], [239] is capable to distinguish the low-amplitude spikes from the background activity using the estimated time-varying Markovian-parameters Eq.(3.15). This KF proficiently cancels the background activity and noise to generate the perceptible epileptic spikes by exploiting/using the temporal information and time-variant nature of the electroencephalogram signal. Hence using the above formulation, we are able to accentuate existing spikes and other events, which are akin to spikes; but at the cost of tedious heuristic parameter setting procedure. However at this stage, we can explore different approaches to adaptive filtering as presented in [243]; which are correlation methods and covariance-matching techniques. When $\vec{Q}$ is assumed to be known and $\vec{R}$ is unknown in the covariance-matching method, then in the present scenario

$$\zeta^{-}(t+P) = \vec{Y}(t+P) - \hat{Y}^{-}(t+P) \tag{3.25}$$

Using Eqs.(3.1), (3.14) and (3.16), the above zero-mean $N \times 1$ measurement/observation innovation vector can be simplified to give

$$\zeta^{-}(t+P)=\vec{C}(t+P)\hat{e}^{-}(t+P)+\vec{V}(t+P) \tag{3.26}$$

The $N\times N$ dimensional observation innovation covariance-matrix is

$$\vec{\beta}(t+P)=E\left[\zeta^{-}(t+P)\zeta^{-}(t+P)^{T}\right]=\vec{C}(t+P)\hat{P}_{e}^{-}(t+P)\vec{C}^{T}(t+P)+\vec{R} \tag{3.27}$$

Here, the measurement-noise covariance-matrix can be represented as

$$\vec{R}=E\left[\zeta^{-}(t+P)\zeta^{-}(t+P)^{T}\right]-\vec{C}(t+P)\hat{P}_{e}^{-}(t+P)\vec{C}^{T}(t+P) \tag{3.28}$$

which may be calculated using the simple statistical approach as

$$\vec{R}(t+P)=\sum_{m=0}^{M-1}\frac{\zeta^{-}(t+P-m)\zeta^{-}(t+P-m)^{T}}{M}-\left[\vec{C}(t+P)\hat{P}_{e}^{-}(t+P)\vec{C}^{T}(t+P)\right] \tag{3.29}$$

But, the lack of ability to estimate $\vec{Q}$ matrix is quite motivational for the inception of new adaptive approaches. However, the innovation correlation approach is found to be unviable in the case of proposed nonstationary EEG signal paradigm (Appendix-A). As the innovation correlation method exhibits high computational complexity [241], which stringently requires the approximate value of initial Kalman gain for the solution of Riccati equations. Subsequently, the convergence of covariance matching technique is reported to be doubtful [243], as the value of process-noise can't be determined uniquely. On the contrary, the output correlation method is found to be an appropriate start-up procedure using the Kalman filtering approach, as it doesn't require *a priori* values of the noise statistics and initial Kalman gain. The next section presents the efficacy of output correlation technique in the current scenario.

3.3 Output Correlation Method for Epileptic Spike Enhancement in EEG Signal

In the output correlation method, we first determine the auto-correlation of time-varying Markovian-parameters as

$$\vec{R}_{S}(l)=E\left[\vec{S}(t+P)\vec{S}^{T}(t+P-l)\right]=\vec{R}_{S}(l;t+P) \tag{3.30}$$

By invoking the stationarity property, it is can be depicted that

$$\vec{R}_S(l) = \vec{R}_S(l;t+P) = \vec{R}_S(l;t+P-p)$$

Incorporation of Eqs.(3.8) and (3.9) in Eq.(3.30) for the zero lag/delay results in

$$\vec{R}_S(l) = \left[\vec{A}\vec{R}_S(0)\vec{A}^T + \vec{Q} \qquad for\ l=0 \right. \tag{3.31}$$

Further, the substitution of Eqs.(3.8) and (3.9) in Eq.(3.30) for the non-zero lag/delay leads to

$$\vec{R}_S(l) = E\left[\left\{ \vec{A}\vec{S}(t+P-1) + \vec{W}(t+P-1) \right\} \vec{S}^T(t+P-l) \right] \qquad for\ l>0$$

$$\vec{R}_S(l) = E\left[\vec{A}\vec{S}(t+P-1)\vec{S}^T(t+P-l) \right] \qquad for\ l>0$$

$$\vec{R}_S(l) = \left[\vec{A}^l\vec{R}_S(0) \qquad for\ l>0 \right. \tag{3.32}$$

However, the auto-correlation of measurement/observation signal can be denoted as

$$\vec{R}_Y(l) = E\left[\vec{Y}(t+P)\vec{Y}^T(t+P-l) \right] = \vec{R}_Y(l;t+P) \tag{3.33}$$

Under the stationary conditions,

$$\vec{R}_Y(l) = \vec{R}_Y(l;t+P) = \vec{R}_Y(l;t+P-p)$$

By substituting Eqs.(3.1) and (3.30) in Eq.(3.33), it can be shown that

$$\vec{R}_Y(l) = \left[\vec{C}(t+P)\vec{R}_S(0)\vec{C}^T(t+P) + \vec{R} \qquad for\ l=0 \right. \tag{3.34}$$

$$\vec{R}_Y(l) = \begin{cases} \vec{C}(t+P)\vec{A}^l\vec{R}_S(0)\vec{C}^T(t+P-l) & for\ l>0 \\ = \vec{C}(t+P)\vec{R}_S(0)\vec{A}^l\vec{C}^T(t+P-l) \end{cases} \tag{3.35}$$

The simple mathematical rearrangement gives

$$\vec{R}_Y^T(l) = \left[\vec{C}(t+P-l)\vec{R}_S^T(0)\vec{A}^{lT}\vec{C}^T(t+P) \qquad for\ l>0 \right. \tag{3.36}$$

$$\vec{R}_Y^T(l) = \left[\vec{C}(t+P-l)\vec{A}^{lT}\vec{R}_S^T(0)\vec{C}^T(t+P) \qquad for\ l>0 \right. \tag{3.37}$$

The Eq.(3.37) may be rewritten in the matrix form as

$$\begin{bmatrix} \vec{R}_Y^T(1) \\ \vec{R}_Y^T(2) \\ ..... \\ ..... \\ ..... \\ \vec{R}_Y^T(L) \end{bmatrix} = \begin{bmatrix} \vec{C}(t+P-1)\vec{A}^{1T}\vec{R}_S^T(0)\vec{C}^T(t+P) \\ \vec{C}(t+P-2)\vec{A}^{2T}\vec{R}_S^T(0)\vec{C}^T(t+P) \\ ..... \\ ..... \\ ..... \\ \vec{C}(t+P-L)\vec{A}^{LT}\vec{R}_S^T(0)\vec{C}^T(t+P) \end{bmatrix} \tag{3.38}$$

$$\begin{bmatrix} \vec{R}_Y^T(1) \\ \vec{R}_Y^T(2) \\ ..... \\ ..... \\ ..... \\ \vec{R}_Y^T(L) \end{bmatrix} = \begin{bmatrix} \vec{C}(t+P-1)\vec{A}^{1T} \\ \vec{C}(t+P-2)\vec{A}^{2T} \\ ..... \\ ..... \\ ..... \\ \vec{C}(t+P-L)\vec{A}^{LT} \end{bmatrix} \vec{R}_S^T(0)\vec{C}^T(t+P) \tag{3.39}$$

$$\text{If } \left[\vec{C}(t+P-1)\vec{A}^{1T} \;\; \vec{C}(t+P-2)\vec{A}^{2T} \;\; ..... \;\; \vec{C}(t+P-L)\vec{A}^{LT}\right]^T = \vec{Z}(t+P), \tag{3.40}$$

then Eq.(3.39) can be represented as

$$\left[\vec{R}_Y^T(1) \;\; \vec{R}_Y^T(2) \;\; ..... \;\; \vec{R}_Y^T(L)\right]^T = \vec{Z}(t+P)\vec{R}_S^T(0)\vec{C}^T(t+P) \tag{3.41}$$

Taking the Moore-Penrose pseudo – inverse [252] of matrix in Eq.(3.41) to get

$$\left[\vec{Z}^T(t+P)\vec{Z}(t+P)\right]^{-1}\vec{Z}^T(t+P)\begin{bmatrix} \vec{R}_Y^T(1) \\ \vec{R}_Y^T(2) \\ ..... \\ ..... \\ ..... \\ \vec{R}_Y^T(L) \end{bmatrix} = \vec{R}_S^T(0)\vec{C}^T(t+P) = \vec{R}_S(0)\vec{C}^T(t+P) \tag{3.42}$$

However $\vec{R}_S^T(0) = \vec{R}_S(0)$, because the off-diagonal elements of this correlation-matrix are small enough to be neglected. Let us consider that

$$\vec{G}(t+P) = \vec{R}_S(0)\vec{C}^T(t+P) \tag{3.43}$$

which can be calculated by using Eq.(3.42) based on all the known parameters and measurements. Now, $\vec{R}_S(0)$ can be calculated by taking the pseudo-inverse of Eq.(3.43) as

$$\vec{G}(t+P)\vec{C}(t+P)\left[\vec{C}^{T}(t+P)\vec{C}(t+P)\right]^{-1}=\vec{R}_{S}(0) \tag{3.44}$$

From Eq.(3.34), it is obvious that

$$\vec{R}=\vec{R}_{Y}(0)-\vec{C}(t+P)\left[\vec{R}_{S}(0)\vec{C}^{T}(t+P)\right] \tag{3.45}$$

Therefore by incorporating Eq.(3.42) into Eq.(3.45), we can easily calculate $\vec{R}$, and by using the Eq.(3.31) and Eq.(3.44), it can be demonstrated that

$$\vec{Q}=\vec{R}_{S}(0)-\vec{A}\vec{R}_{S}(0)\vec{A}^{T} \tag{3.46}$$

Moreover, we can approximately compute $\vec{R}_{Y}(0)$, $\vec{R}_{Y}(1)$, $\vec{R}_{Y}(2)$, ... $\vec{R}_{Y}(L)$ by using the procedure presented in Appendix-B, which facilitates the calculation of vital Kalman filtering parameters $\vec{R}$ and $\vec{Q}$. Further, the procedure for the estimation of optimal Kalman gain or blending factor matrix $\vec{K}$ is discussed, which requires

$$\vec{J}(t+P)=E\left[\hat{S}^{-}(t+P)\hat{S}^{-}(t+P)^{T}\right] \tag{3.47}$$

The equation (3.15) can be rearranged using Eq.(3.25) as

$$\hat{S}^{+}(t+P-1)=\hat{S}^{-}(t+P-1)+\vec{K}(t+P-1)\zeta^{-}(t+P-1) \tag{3.48}$$

Incorporating Eq.(3.48) in Eq.(3.13) leads to

$$\hat{S}^{-}(t+P)=\vec{A}\left[\hat{S}^{-}(t+P-1)+\vec{K}(t+P-1)\zeta^{-}(t+P-1)\right] \tag{3.49}$$

From Eq.(3.47) and Eq.(3.49),

$$\vec{J}(t+P)=\vec{A}\left[\vec{J}(t+P-1)+\vec{K}(t+P-1)\vec{\beta}(t+P-1)\vec{K}^{T}(t+P-1)\right]\vec{A}^{T} \tag{3.50}$$

However using Eq.(3.16), the time-varying AR parameter vector can be expressed as

$$\vec{S}(t+P)=\hat{S}^{-}(t+P)+\hat{e}^{-}(t+P) \tag{3.51}$$

Substitution of Eq.(3.51) in Eq.(3.30) for $l=0$ results in

$$\vec{R}_{S}(0)=E\left[\hat{S}^{-}(t+P)\hat{S}^{-}(t+P)^{T}\right]+\hat{P}_{e}^{-}(t+P) \tag{3.52}$$

$$\vec{R}_S(0) = \vec{J}(t+P) + \hat{P}_e^-(t+P) \tag{3.53}$$

Subsequently from Eq.(3.24) and Eq.(3.27), the Kalman gain factor matrix is

$$\vec{K}(t+P) = \hat{P}_e^-(t+P)\vec{C}^T(t+P)\vec{\beta}(t+P)^{-1} \tag{3.54}$$

Its further simplification using the Eq.(3.53) results in

$$\vec{K}(t+P) = \left[\vec{R}_S(0) - \vec{J}(t+P)\right]\vec{C}^T(t+P)\left[\vec{C}(t+P)\hat{P}_e^-(t+P)\vec{C}^T(t+P) + \vec{R}\right]^{-1} \tag{3.55}$$

Applying Eq.(3.45) in the above equation generates

$$\begin{aligned}\vec{K}(t+P) = &\left[\vec{R}_S(0) - \vec{J}(t+P)\right]\vec{C}^T(t+P) \\ &\times\left[\vec{C}(t+P)\left\{\hat{P}_e^-(t+P) - \vec{R}_S(0)\right\}\vec{C}^T(t+P) + \vec{R}_Y(0)\right]^{-1}\end{aligned} \tag{3.56}$$

It can also be represented as

$$\vec{K}(t+P) = \left[\vec{R}_S(0) - \vec{J}(t+P)\right]\vec{C}^T(t+P)\left[\vec{R}_Y(0) - \vec{C}(t+P)\vec{J}(t+P)\vec{C}^T(t+P)\right]^{-1} \tag{3.57}$$

However the incorporation of Eq.(3.54) in Eq.(3.50) provides

$$\vec{J}(t+P) = \vec{A}\left[\vec{J}(t+P-1) + \hat{P}_e^-(t+P-1)\vec{C}^T(t+P-1)\vec{K}^T(t+P-1)\right]\vec{A}^T \tag{3.58}$$

Moreover using Eq.(3.53), the above equation can also be formulated as

$$\vec{J}(t+P) = \vec{A}\left[\vec{J}(t+P-1) + \left\{\vec{R}_S(0) - \vec{J}(t+P-1)\right\}\vec{C}^T(t+P-1)\vec{K}^T(t+P-1)\right]\vec{A}^T \tag{3.59}$$

Now, the Kalman blending factor matrix $\vec{K}(t+P)$ can be calculated using the Eq.(3.57) and Eq.(3.59), which only requires known $\vec{A}$, $\vec{C}$ and the already computed $\vec{R}_Y(0)$ *and* $\vec{R}_S(0)$. The computational complexity of proposed method is approximately $O(N^3)$, where N is filter length [235].

→ The proposed output correlation scheme is summarized as

Step 1: For each observation vector $\vec{Y}(t+P)$, repeat step 2 to 7.

Step 2: Generate the auto-correlation $\vec{R}_Y(l)$ of observation vector $\vec{Y}(t+P)$ for $l = 1, 2, 3, \ \ldots \ , L$ as in Eq.(3.33) by using Eq.(B5) of Appendix-B.

Step 3: Compute the auto-correlation $\vec{R}_S(0)$ of the state vector for $l = 0$ as given in Eq.(3.44) by using Eqs.(3.40) – (3.43).

Step 4: Calculate the measurement-noise covariance-matrix $\vec{R}$ and the process-noise covariance-matrix $\vec{Q}$ using $\vec{R}_S(0)$, as given in Eq.(3.45) and Eq.(3.46) respectively.

Step 5: Compute the Kalman gain/Blending factor $\vec{K}$ using Eq.(3.57) and Eq.(3.59).

Step 6: Calculate *a posteriori* estimate $\hat{S}^+(t+P)$ of state vector as in Eq.(3.15) using $\vec{K}$.

Step 7: Determine the measurement estimate $\hat{Y}^+(t+P)$ as in Eq.(3.61), which is further used for the statistical threshold selection in the spike detection, as given in section 3.4.

3.4 Epileptic Spike Detection Based on Statistical Threshold

The exclusive features of an excellent EEG spike detection algorithm/system include high sensitivity and selectivity. However, the conventional systems with high detection threshold level exhibit the low false detection rate, but at the cost of significant number of missed events. As the identification of epilepsy comprises visual scanning of electroencephalogram signal recording for the epileptic spikes (ESs), therefore the false detections may be further checked afterwards during analysis. For the detection of enhanced ESs in the presented research work, the threshold is considered to be scaled replica of the average of absolute value of the approximated EEG signal in recorded signal segment, which is motivated by the Kalman filtering approach presented in [213]. Here, the threshold value for the proposed adaptive spike detection scheme is selected as

$$\Gamma_{KF}\left(t+P\right)=\left(C_{KF}/N_{KF}\right)\sum_{\bar{n}=0}^{N_{KF}-1}\left|\hat{Y}^{+}\left(t+P-\bar{n}\right)\right| \tag{3.60}$$

in which, $\hat{Y}^{+}(t+P)=\vec{C}\left(t+P\right)\hat{S}^{+}\left(t+P\right)$ (3.61)

where, N_{KF} is the number of samples, C_{KF} is the scaling factor based on the experimentation and $\left|\hat{Y}^{+}(t+P)\right|$ is the absolute value of estimated electroencephalogram signal. Further, the average value of decision threshold $\Gamma_{KF}\left(t+P\right)$ is denoted as $\Gamma_{Avg}=E\left[\Gamma_{KF}\right]$.

3.5 Simulation Results

3.5.1 Simulation Results Based on Synthetic EEG Signal

In this section, the synthetic EEG signal paradigm with epileptic spikes (ESs) is considered. The raw EEG signal can be approximately modeled as the slowly time-varying background signal $bs\left(n\right)$ (stationary) in the synthetic environment [96], which follows that

$$\begin{aligned} eeg\left(n\right) &= bs\left(n\right)+\eta s\left(n\right) \\ &= \left\{sin\left(\bar{\omega}n\right)-sin\left(2\bar{\omega}n+\phi\right)+sin\left(4\bar{\omega}n\right)\right\}+\eta s\left(n\right) \end{aligned} \tag{3.62}$$

where, $\eta s\left(n\right)$ is the total white Gaussian-noise (including all types of noises) with zero-mean and variance $\sigma_{\eta s}^{2}$, $\bar{\omega}=\left(2\pi/75\right)$ and $\bar{\phi}=\left(\pi/2\right)$. However, the triangular spikes may be assumed akin to the epileptic spikes [96], [213], [233] in the signal processing approach, by which the nonstationarity is introduced in the above synthetic EEG signal. It can be articulated as

$$\bar{s}\left(n\right)=eeg\left(n\right)+spi\left(n\right)=\left\{bs\left(n\right)+\eta s\left(n\right)\right\}+spi\left(n\right) \tag{3.63}$$

in which, the embedded spike train is denoted as

$$spi\left(n\right)=\sum_{i=1}^{\bar{I}}\bar{p}\left(n-k_{i}\right) \tag{3.64}$$

with, $\overline{p}\left(n-k_i\right)=As_i\delta\left(n-k_i\right)+\sum_{m=1}^{\overline{q}}As_i\frac{\left(\overline{q}-m\right)}{\overline{q}}\left[\delta\left(n-k_i+m\right)+\delta\left(n-k_i-m\right)\right]$ (3.65)

where, $\overline{I}$ is the number of triangular spikes, the spike base-width is $2\overline{q}=jT_s$ at the k_i^{th} instant, the magnitude of spike amplitude varies at random in the range $As_i \rightarrow U\left[2.5,7.5\right]$ with randomly generated sign [96], [213], [233] and T_s is the sampling duration. The value of triangular spike base-width is assumed to be randomly varying in the range $jT_s \rightarrow \left[2T_s,10T_s\right]$. The continuous-time raw EEG signal with or without epileptic spikes is sampled at the interval $T_s=1/128$ sec for the generation of discrete-time samples for the analysis. The duration of real-time epileptic spike is about $20m$sec to $70m$sec [227], [245], therefore the base-width of each ES is randomly varying between $2T_s$ to $10T_s$ in duration. From the continuous-time composite EEG signal of 5sec duration, the 640 discrete-time signal samples are obtained for simulations, which also consists of 8 ESs (symmetric triangular with random sign) with amplitude As_i randomly varying between 2.5 to 7.5 at the random locations k_i. In addition, the signal-to-noise-ratio (SNR) in dB is determined by using the signal level (background activity) and the zero-mean total white Gaussian-noise level [231]. However, the composite EEG signal is normalized in the range [-1, +1]. The performance indices of any epileptic spike detection algorithm are false-negative-ratio (FNR) as well as false-positive-ratio (FPR), which are calculated as

FNR = (Number of spikes missed) / (Actual number of spikes)

FPR = (Number of false spikes detected) / (Actual number of spikes)

The enhanced triangular spikes in the EEG signal are shown in Fig. 3.1 and Fig. 3.3 by using the conventional KF approach and the proposed output correlation approach, respectively, in which the parameter C_{KF} is adjusted in Eq.(3.60) to keep the average threshold value approximately same in both cases (i.e., $\Gamma_{Avg}=+0.15$) at $+10dB$ SNR. In Fig. 3.2 and Fig.

3.4, the upper red line and lower red line indicate the maximum value of threshold (Γ_{Max}) and the minimum value of threshold (Γ_{Min}), respectively. Based on the average threshold value (blue line), it may be inferred from Fig. 3.2 and Fig. 3.4 that the number of missed spikes as well as the number of falsely detected spikes are less in case of the proposed scheme. However, it is apparent from outcomes demonstrated in Fig. 3.1 to Fig. 3.4 that the output correlation method boosts the eight triangular spikes (ES1 – ES8) relatively more as compared to the KF method, which in turn controls FNs and FPs.

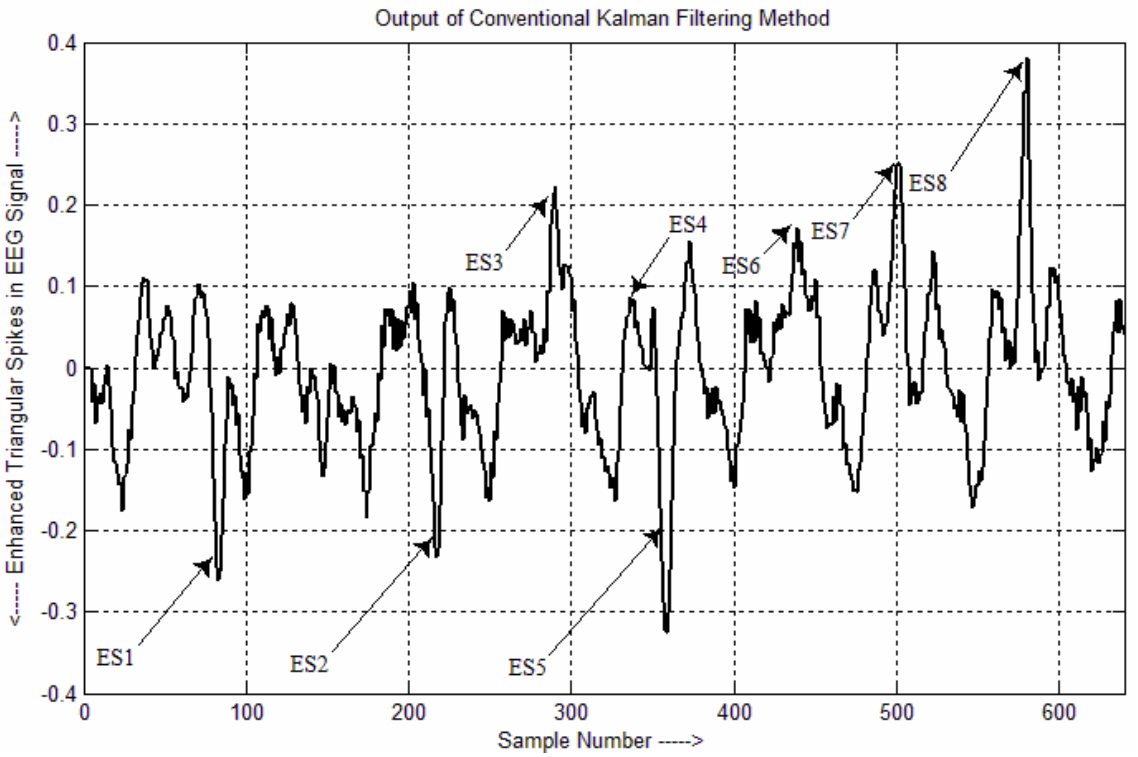

Fig. 3.1: Enhanced triangular spikes in EEG signal by using conventional Kalman filtering approach (a typical simulated example)

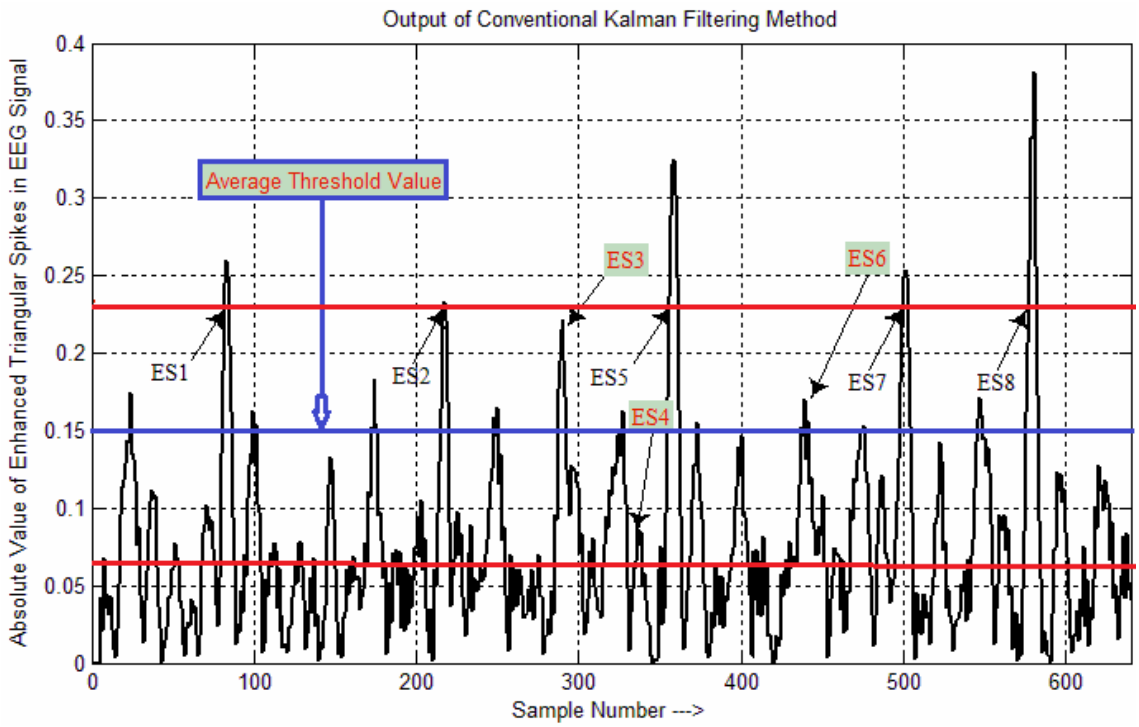

Fig. 3.2: Absolute value of enhanced triangular spikes in EEG signal in case of Kalman filtering approach

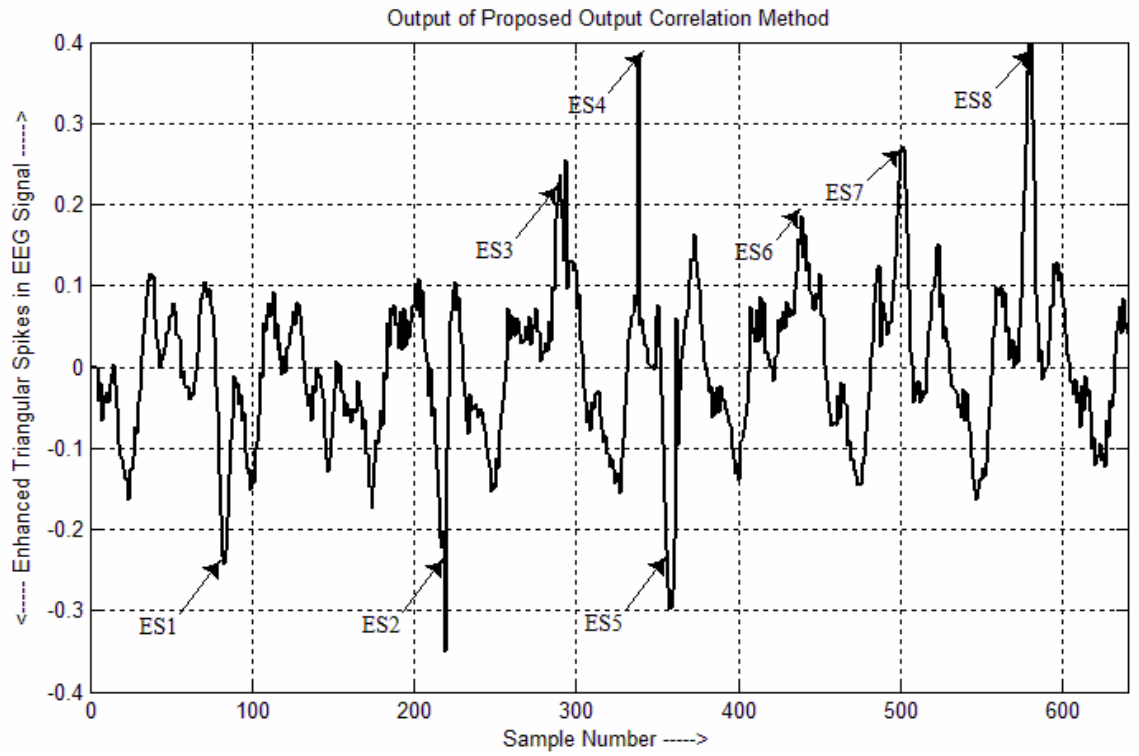

Fig. 3.3: Enhanced triangular spikes in EEG signal by using proposed output correlation approach (a typical simulated example)

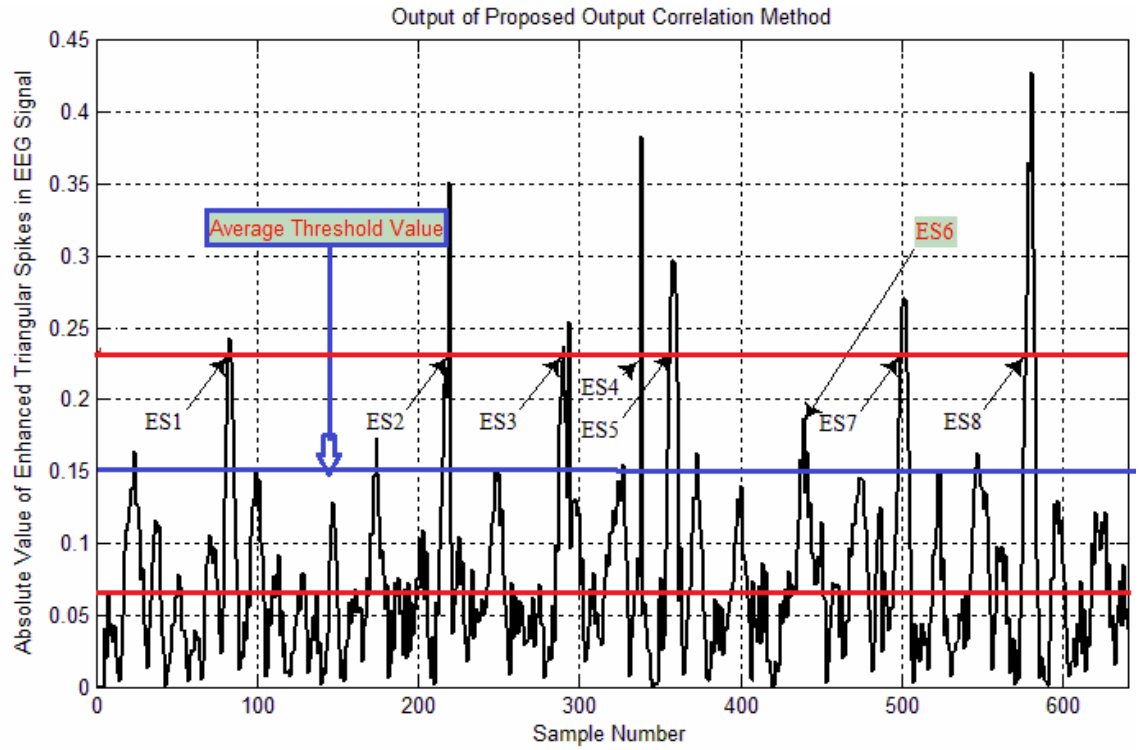

Fig. 3.4: Absolute value of enhanced triangular spikes in EEG signal in case of output correlation approach

3.5.2 Simulation Results Based on Real-time EEG Signal

For the real-time epileptic spikes in the composite EEG signal, the two-channel EEG recordings (of $5\,\text{sec}$ duration) at the left and right frontal cortex of adult WAG/Rij rats are used to test the presented spike enhancement and detection technique. The recording of this raw EEG signal with epileptic spikes has been investigated by an expert neurologist, who could rate spikes based on the spatial as well as temporal contextual dataset. These rats were born and received detailed care in the Laboratory of Department of Comparative and Physiological Psychology in the Nijmegen University, Holland, which were utilized for investigating the role of reticular thalamic nucleus in the inter-hemispheric synchronization of the real-time electroencephalography [223], [224], which is a genetic animal paradigm of human epilepsy. The frequency band of spike-wave discharges is observed to be $8-10Hz$ [225], [226]. The EEG signals are referenced to an electrode positioned at the cerebellum, which are filtered between $1-100Hz$ and sampled at $F_s = 200Hz$ to obtain 1000 sample points of the discrete-time neural signal. A typical sample of the normalized raw EEG signal with ESs and EEG signal without ESs is presented in Fig. 3.5 (250 sample points of rat data, obtained from right cortical intracranial electrode).

The performance characteristics of the proposed epileptic spike enhancement and detection scheme based on the output correlation method are compared with the conventional KF techniques for the real-time EEG signal with ESs (publicly available rat data). The five pairs of electroencephalogram signals acquired from electrodes positioned on the left and right frontal cortex of male adult WAG/Rij rats are utilized for the testing of presented adaptive approach in the real-time environment.

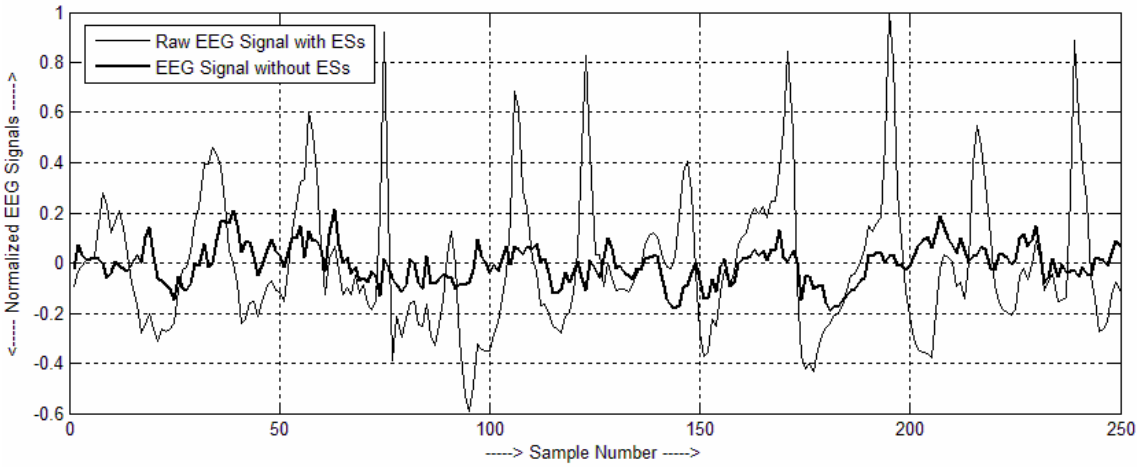

Fig. 3.5: EEG signal of rat vs. sample points

The results presented in Fig. 3.6 and Fig. 3.7 depict that the output correlation method outperforms the conventional KF technique in case of ES enhancement, in which the parameter C_{KF} is adjusted in Eq.(3.60) to keep the average threshold value approximately same in both cases (i.e., $\Gamma_{Avg} = +0.055$) at $+20dB$ SNR. The FNR and FPR observations based on Fig. 3.6 and Fig. 3.7 confirm the efficacy of the proposed spike enhancement technique. The output correlation method exhibits relatively lower FPR and higher FNR in comparison to the conventional KF scheme.

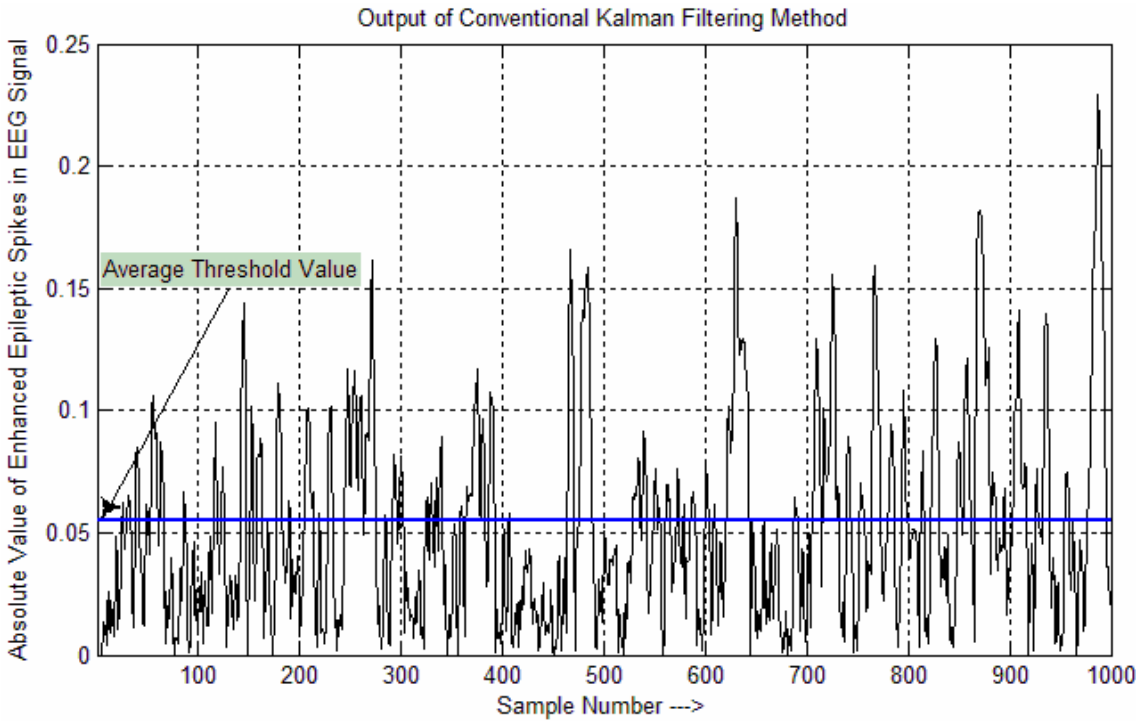

Fig. 3.6: Absolute value of enhanced epileptic spikes in EEG signal in case of conventional Kalman filtering approach (a typical real-time dataset)

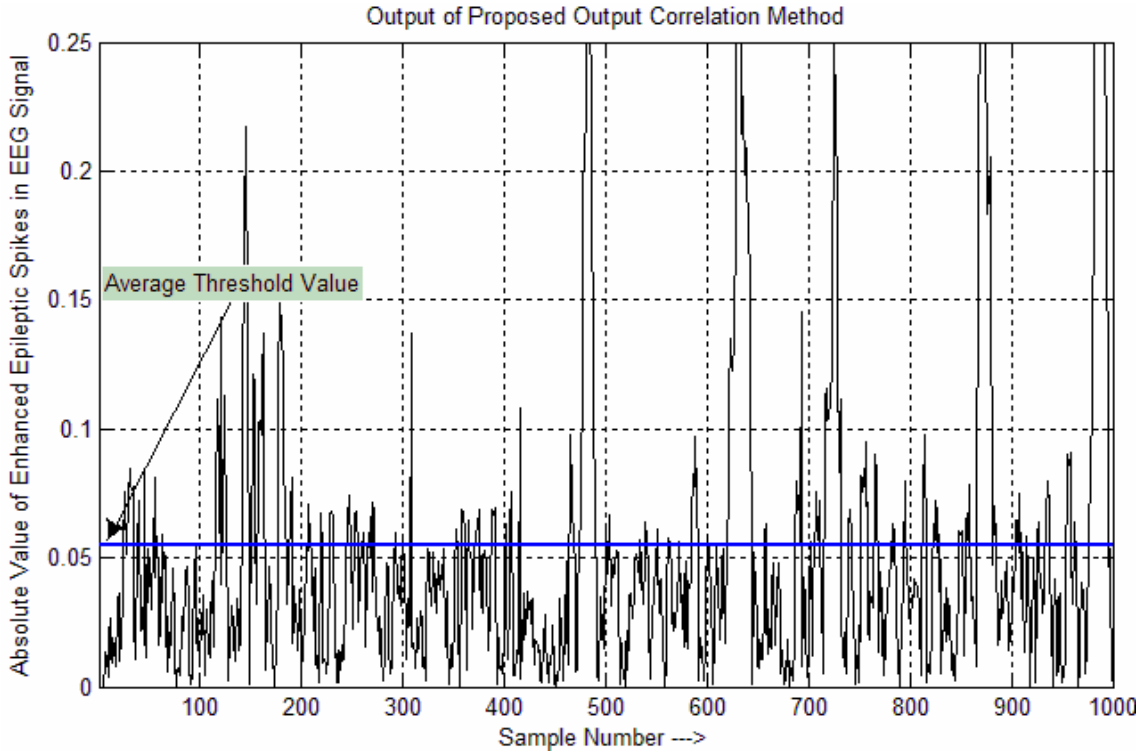

Fig. 3.7: Absolute value of enhanced epileptic spikes in EEG signal in case of proposed output correlation approach (a typical real-time dataset)

Table 3.1: Performance evaluation of spike enhancement and detection methods for synthetic and real-time EEG signals, using FPR (Mean ± Standard Deviation)

Approximate Value of ⇩ False-Positive-Ratio	**SNR = 25dB**	**SNR = 20dB**	**SNR = 15dB**	**SNR = 10dB**	**SNR = 5dB**	**SNR = 1dB**
Kalman filtering algorithm in case of trinagular spikes	0.1 ± 0.055	0.95 ± 0.35	1.6 ± 0.65	2.0 ± 0.7	3.5 ± 0.95	4.4 ± 1.25
Output Correlation Method in case of trinagular spikes	0.04 ± 0.007	0.45 ± 0.1	0.9 ± 0.4	1.2 ± 0.55	2.9 ± 0.85	3.6 ± 1.15
Kalman filtering algorithm in case of of epileptic spikes	0.275 ± 0.08	1.2 ± 0.55	2.7 ± 0.74	3.6 ± 0.9	6.5 ± 1.55	7.2 ± 2.5
Output Correlation Method in case of epileptic spikes	0.2 ± 0.045	0.76 ± 0.15	1.4 ± 0.625	2.6 ± 0.725	4.25 ± 1.25	5.2 ± 2.0

Table 3.2: Performance evaluation of spike enhancement and detection methods for synthetic and real-time EEG signals, using FNR (Mean ± Standard Deviation)

Approximate Value of False-Negative-Ratio ⇩	**SNR = 25dB**	**SNR = 20dB**	**SNR = 15dB**	**SNR = 10dB**	**SNR = 5dB**	**SNR = 1dB**
Kalman filtering algorithm in case of trinagular spikes	0.01 ± 0.001	0.05 ± 0.003	0.1 ± 0.025	0.125 ± 0.04	0.25 ± 0.06	0.12 ± 0.08
Output Correlation Method in case of trinagular spikes	0.02 ± 0.003	0.09 ± 0.01	0.125 ± 0.03	0.15 ± 0.055	0.28 ± 0.075	0.15 ± 0.09
Kalman filtering algorithm in case of of epileptic spikes	0.05 ± 0.002	0.1 ± 0.012	0.4 ± 0.05	0.9 ± 0.07	1.25 ± 0.085	1.15 ± 0.1
Output Correlation Method in case of epileptic spikes	0.07 ± 0.005	0.25 ± 0.035	0.55 ± 0.075	1.05 ± 0.08	1.50 ± 0.15	1.25 ± 0.25

For detailed analysis, the threshold value Γ_{KF} for the proposed adaptive spike detection scheme is selected by using Eq.(3.60). Here, C_{KF} is kept fixed at 1.75 in the case of triangular spikes and 2.5 in the case of real-time EEG with ESs, based on the experimentation. Subsequently, the epileptic spikes are detected by comparing the absolute value of estimated EEG signal $\left|\hat{Y}^{+}(t+P)\right|$ with the computed threshold Γ_{KF}. The simulation results in Table 3.1 manifest that the substantial reduction in FPR value is observed for the proposed output correlation method with the increasing value of SNR, which is substantially lower than the conventional KF approach. The output correlation method suppresses the background activity (low-amplitude EEG signal) and noise, but it enhances the ESs efficiently. At 10dB SNR, the output correlation method provides approximately 40 % reduction in FPs for the triangular spikes in synthetic EEG signal and approximately 27.5 % reduction in FPs for ESs in the WAG/Rij rat EEG data as compared to the KF scheme. However in Table 3.2, the value of FNR is found to be high at small values of SNR because high-amplitude peaks in background activity and noise signals are also enhanced along with ESs. But, the value of FNR reduces with the increasing value of SNR, which is moderately higher in case of the presented output correlation method than the KF technique. At 10dB SNR, the output correlation method provides approximately 16.5 % enhancement in FNs for the triangular spikes in synthetic EEG signal and approximately 14.25 % enhancement in FNs for ESs in the rat EEG data as compared to the KF method. Therefore, it is noteworthy that the value of FPR is substantially alleviated at the cost of moderately elevated FNR value in the proposed adaptive approach, as the spike enhancer maximizes the selectivity to decrease the false detections.

3.6. Summary of Chapter

In this chapter, the output correlation technique for the epileptic spike enhancement and detection has been proposed to refine electroencephalogram signal. This technique has been developed by exploiting adaptive Kalman filtering paradigm for the nonstationary time-varying signal boosting. By using this method, the pre-emphasized epileptic spikes can be detected using the appropriate decision threshold. The basic concept used in the presented research work is that the electroencephalogram signal can be expressed in terms of general Markov-model equation, in which time-varying Markov-model coefficients/parameters are also considered to be following the first-order autoregressive process. However, the proposed output correlation scheme doesn't require process-noise variance, measurement-noise variance and initial Kalman gain for implementation. Simulation has been conducted using the synthetic EEG signal as well as real-time EEG signal (WAG/Rij rat-data). The simulation results connote that the proposed output correlation technique leads to substantial reduction in false-positive-ratio in comparison to the traditional Kalman filtering approach.

Therefore, the neurophysiological disorders pertaining to epilepsy can be investigated efficiently by using the proposed adaptive output correlation technique, at the cost of marginal increase in computational complexity.

Appendix – A

In the innovation correlation approach [243], it is apparent that

$$\vec{\beta}\left(l;t+P\right)=E\left[\zeta^{-}\left(t+P\right)\zeta^{-}\left(t+P-l\right)^{T}\right] \tag{A1}$$

Substitution of Eq.(3.26) in the above equation results in

$$\begin{aligned}\vec{\beta}\left(l\neq 0;t+P\right)=\vec{C}\left(t+P\right)E\left[\hat{e}^{-}\left(t+P\right)\hat{e}^{-}\left(t+P-l\right)^{T}\right]\vec{C}^{T}\left(t+P\right)\\ +\ \vec{C}\left(t+P\right)E\left[\hat{e}^{-}\left(t+P\right)\vec{V}^{T}\left(t+P-l\right)\right]\end{aligned} \tag{A2}$$

$$\vec{\beta}\left(l=0;t+P\right)=\vec{C}\left(t+P\right)\hat{P}_{e}^{-}\left(t+P\right)\vec{C}^{T}\left(t+P\right)+\vec{R}=\vec{\beta}\left(t+P\right) \tag{A3}$$

However, the solution of Eq.(A2) requires $\hat{e}^{-}\left(t+P\right)$ and $\hat{e}^{-}\left(t+P-l\right)$. Therefore, by using Eq.(3.18) and Eq.(3.21), it can be shown that

$$\begin{aligned}\hat{e}^{-}\left(t+P\right)=\vec{A}\left[I_{P}-\vec{K}\left(t+P-1\right)\vec{C}\left(t+P-1\right)\right]\hat{e}^{-}\left(t+P-1\right)\\ -\vec{A}\left[\vec{K}\left(t+P-1\right)\vec{V}\left(t+P-1\right)\right]+\vec{W}\left(t+P\right)\end{aligned} \tag{A4}$$

Further simplification of Eq.(A4) is only possible under the static conditions i.e., $\vec{K}\left(t+P-1\right)=\vec{K}\left(t+P\right)=\vec{K}_{0}$ (*a priori* sub-optimal Kalman gain) and $\vec{C}\left(t+P-1\right)=\vec{C}\left(t+P\right)=\vec{C}$, which leads to

$$\begin{aligned}\hat{e}^{-}\left(t+P\right)=\left[\vec{A}\left\{I_{P}-\vec{K}_{0}\vec{C}\right\}\right]^{l}\hat{e}^{-}\left(t+P-l\right)+\sum_{j=1}^{l}\left[\vec{A}\left\{I_{P}-\vec{K}_{0}\vec{C}\right\}\right]^{j-1}\vec{W}\left(t+P-j+1\right)\\ -\sum_{j=1}^{l}\left[\vec{A}\left\{I_{P}-\vec{K}_{0}\vec{C}\right\}\right]^{j-1}\vec{A}\vec{K}_{0}\vec{V}\left(t+P-j\right)\end{aligned} \tag{A5}$$

This method is not supporting the dynamic conditions arising in the nonstationary EEG signal. Moreover, this approach is extremely cumbersome.

Appendix – B

In the mathematical analysis of EEG signals, we need to calculate $\vec{R}_Y(l;t+P)$, such that

$$\vec{R}_Y(l;t+P) = E\left[\vec{Y}(t+P)\vec{Y}^T(t+P-l)\right] \tag{B1}$$

It can be calculated using the simple statistical approach [221] as

$$\hat{R}_Y(l;t+P) = \left(1/(M+1)\right)\sum_{m=l}^{M}\vec{Y}(t+P-m+l)\vec{Y}^T(t+P-m) \tag{B2}$$

where, the value of M is kept high to give

$$\hat{R}_Y(l;t+P) = \left(1/(M+1)\right)\left[\begin{array}{l}\vec{Y}(t+P)\vec{Y}^T(t+P-l)+\\ \quad\sum_{\bar{m}=l}^{M-1}\vec{Y}(t+P-\bar{m}+l-1)\vec{Y}^T(t+P-\bar{m}-1)\end{array}\right] \tag{B3}$$

However, it can be approximated as

$$\hat{R}_Y(l;t+P) \approx \left[\frac{\vec{Y}(t+P)\vec{Y}^T(t+P-l)}{M+1}\right] + \left[\hat{R}_Y(l;t+P-1) - \frac{\hat{R}_Y(l;t+P-1)}{M+1}\right] \tag{B4}$$

$$\hat{R}_Y(l;t+P) \approx \hat{R}_Y(l;t+P-1) + \left[\frac{\vec{Y}(t+P)\vec{Y}^T(t+P-l) - \hat{R}_Y(l;t+P-1)}{M+1}\right] \tag{B5}$$

CHAPTER 4

EXCISION OF OCULAR ARTIRACTS FROM EEG USING NVFF-RLS ADAPTIVE ALGORITHM

4.1 Introduction

The electroencephalography (EEG) is beneficial for clinical diagnosis and in biomedical engineering applications for the biosignal processing and analysis. However, the recorded EEG signal from the frontal channels is often corrupted due to the presence of artifacts produced by eye movements (saccade, blink / unusual sudden movements). The eye can be viewed as an electric dipole, in which the cornea and retina are considered to be positive and negative respectively. An electric field is produced due to the significant movement of eye, which changes the electric field around the eye. This superfluous signal is called an electrooculogram (EOG) signal, which propagates over the scalp and it is also noticeable in measured electroencephalogram signal as an unavoidable artifact. It may also be called a type of noise/artifact, which causes serious problems in the EEG interpretation as well as investigations.

The traditional technique of eye blink artifact cancellation is elimination of the segment of electroencephalogram signal data, in which eye blinks appear. The eye blinks are generally identified by means of the information measured from the electrodes positioned above and beneath the patient's left eye. An eye blink is considered to have occurred, if signal amplitude crosses a predetermined threshold level. The amplitude of EOG signal is generally six times more than the artifact-free EEG signal. All electroencephalogram signal segments, in which eye blinks appear are then abolished, which leads to significant EEG data loss.

In the past few decades, many regression-based schemes have been reported to suppress the ocular artifactual signals present in the recorded EEG signal, which include the time-

domain regression [253] and the frequency-domain regression [188], [189]. However, the calibration trials are performed to obtain the transfer coefficients between the electrooculogram signalling channels and each of the electroencephalogram signalling channels [164], which are then used to estimate the electrooculogram constituent (in recorded electroencephalogram signal) in the correction phase to remove it by using the subtraction procedure. A group of researchers [77] have mentioned independent component analysis to segregate the electrooculogram signal from the recorded electroencephalogram signals. The efficacy of this technique relies on the accurate recognition of the artifact constituents, which are utilized for the off-line analysis and processing of information gathered from a substantial number of channels. The principal component analysis has also been suggested as a technique for eliminating the eye artifactual signals from multichannel electroencephalogram signals [170]. But, it can't completely segregate eye artifacts from the measured electroencephalogram signals, particularly when they possess proportionate amplitude level. In real-time scenario, these methods are found to be unsuitable, as the calibration trials can't be conducted subject to different constraints.

Owing to the inherently nonlinear nature of the biological systems, the development of a nonlinear adaptive filtering configuration would be desirable for the adaptive processing of biomedical signals. Therefore, Connor [254] *et al*. make use of the benefits of the artificial neural networks in the development of an adaptive noise canceller for the real-time ocular artifactual signal eradication. The recurrent networks exhibit benefits over the feedforward neural networks in much the similar way that the autoregressive-moving-average-paradigms have benefits over the autoregressive-paradigms [254]. But, the computation complexity and stability related issues restrict the usage of nonlinear adaptive techniques. Moreover, the disadvantages also include "black box" nature, proneness to overfitting and the empirical nature of neural network-based paradigm evolution [18]. Unlike the linear adaptive filtering,

the neural networks sometimes switch to the local mean squared error based decisions instead of the global minimum mean square error criterion-based decisions.

The linear adaptive filtering configurations proffer a paramount tool for the modeling and prediction of stochastic/random signals. Moreover, its low computational complexity and stability make it an appropriate technique for the adaptive noise cancellation, which considers EOG artifact as a type of noise. Therefore, He *et al*. [75] have reported an artifact elimination technique based on adaptive filtering, which is appropriate for the on-line elimination of electrooculogram artifactual signals. There are at least two types of EOG artifactual signals to be removed: 1) those engendered by the vertical eye movement (the related electrooculogram signal is known as VEOG) and 2) those engendered by the horizontal eye movement (the corresponding electrooculogram signal is called HEOG). This scheme utilizes separately measured vertical electrooculogram and horizontal electrooculogram signals as two reference inputs. To measure the eye blink or saccade, one pair of electrodes are positioned above (on forehead) and beneath (on temple), and another pair of electrodes are positioned at the right and left temple on the patient's left eye. Every reference input is first processed by a finite impulse response filtering configuration, and then it is subtracted from the measured EEG signal. This technique is implemented using the recursive least squares procedure based FIR filters, which track the nonstationary portion of the EOG signals. This adaptive procedure converges at a fast rate and it exhibits stability in the case of on-line elimination of EOG artifactual signals. However, its computational complexity is higher than the LMS procedure based techniques.

A new metric is suggested in [194], [253] that captures both the amount of artifactual signal removed and the likelihood that a given method would distort the underlying EEG signal. It utilizes three frontal EEG channels as the reference signals instead of EOG signal. In [165], [188], a cascade of three adaptive filtering configurations based on LMS procedure

is presented, in which the first one removes interference artifact, the second adaptive filter cancels ECG artifacts and the third one suppresses electrooculogram artifactual signals. However, the proposed scheme in [189], [205] utilizes HEOG, VEOG and EMG signals as three reference digital filter inputs, in which the real-time artifactual signal elimination procedure is incorporated by using the multichannel LMS algorithm. But under nonstationary environment, the tracking performance of LMS procedure suffers due to lag-misadjustment in the filter coefficient updating [255]. In such scenario, the RLS algorithm based EOG excision technique is an appropriate choice, due to the lower lag-noise in the tracking-mode, in spite of the computational burden. In this chapter, we propose the usage of numerical variable forgetting factor [14], [15] in combination with the RLS procedure to track and estimate the nonstationary EOG (artifact) signal, which can be subtracted from the measured EEG signal to get the artifact-free EEG signal. In [75], authors consider only HEOG and VEOG artifact signals for suppression. However in this work, the main focus is not only on the ocular artifact suppression akin to [75], but also on the noise excision.

This chapter is organized as follows. In section 4.2, we first furnish details about the adaptive system model used for the excision of ocular artifacts from the recorded EEG signal. We also provide attributes about the generation of synthetic EEG signal [256] and synthetic EOG signals [193]. Subsequently, section 4.3 introduces the application of numeric variable forgetting factor in aforementioned RLS algorithm based adaptive system (as shown in Fig. 4.1). We next present simulation outcomes to demonstrate the efficacy of presented NVFF-RLS procedure in artifact removal, in section 4.4. The performance of linear NVFF-RLS algorithm based ocular artifact/noise cancellation method is compared with the conventional linear FFF-RLS, linear FSS-NLMS and linear GVSS-NLMS algorithms [17], [257], by using the synthetically generated EEG signals and the real-time recorded EEG signals corrupted by EOG and noise signals. Finally, summary of chapter is presented in section 4.5.

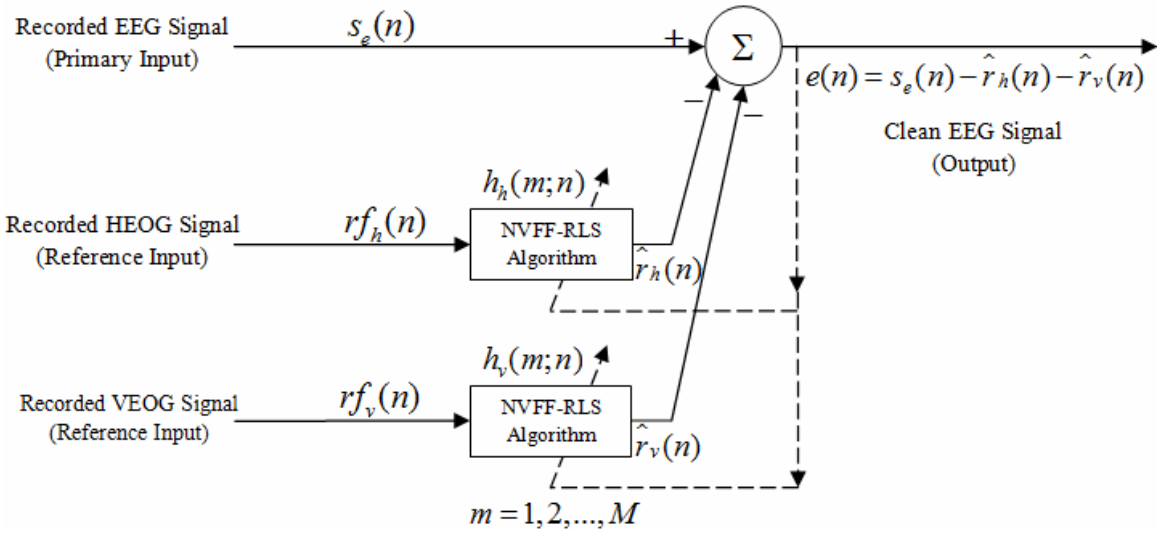

Fig. 4.1: EOG artifact/noise canceller using NVFF-RLS filtering algorithm with two reference inputs

4.2 Adaptive System Model for Excision of EOG signals from Recorded EEG

4.2.1 Basic System Model

Let the primary input to the system be the recorded electroencephalogram signal $s_e(n)$ at the n^{th} time instant, which is picked up by a particular electrode, such that

$$s_e(n) = s_{eeg}(n) + \eta_w(n) + r_v(n) + r_h(n) \tag{4.1}$$

where, $s_{eeg}(n)$ is the true EEG signal with zero-mean and variance σ_{eeg}^2, $\eta_w(n)$ is the zero-mean additive white Gaussian-noise with variance σ_w^2; $r_h(n)$ and $r_v(n)$ are the true HEOG and true VEOG signals respectively, which contaminates the true EEG signal $s_{eeg}(n)$ at the n^{th} time instant (sample). In the presented system, $rf_h(n) = r_h(n) + \eta_{wh}(n)$ and $rf_v(n) = r_v(n) + \eta_{wv}(n)$ are two reference inputs, which are independently measured HEOG and VEOG signals respectively. The reference signals are also corrupted by interference and noise, therefore these signals need to be processed and refined first. The additive white Gaussian-noise components $\eta_{wh}(n)$ and $\eta_{wv}(n)$ exhibit zero-mean and variance $\sigma_w^2 = \sigma_{wh}^2 = \sigma_{wv}^2$. These reference inputs are processed through the adaptive filtering procedure to generate the estimated replica of true HEOG and true VEOG signals i.e., $\hat{r}_h(n)$ and $\hat{r}_v(n)$ respectively, which results in

$$\hat{r}_h(n) = h_h(n) * rf_h(n) = \sum_{m=1}^{M} h_h(m;n)\, rf_h(n+1-m) \tag{4.2}$$

$$\hat{r}_v(n) = h_v(n) * rf_v(n) = \sum_{m=1}^{M} h_v(m;n)\, rf_v(n+1-m) \tag{4.3}$$

where, $*$ is the linear convolution operator, M is the length of FIR filter, and h_x is the filter coefficients. In the present scenario, two filters (as shown in Fig. 4.1) can have different lengths M_h and M_v respectively. The performance of adaptive filtering configuration is not

very sensitive towards the selection of M, which is supported by the research work presented by Kenemans *et al*. in [78]. Therefore, we have kept the filter length fixed at $M_h = M_v = M$. It follows that

$$r_h(n) = \hat{r}_h(n) + \eta_h(n) \tag{4.4}$$

$$r_v(n) = \hat{r}_v(n) + \eta_v(n) \tag{4.5}$$

where, estimation errors $\eta_h(n)$ and $\eta_v(n)$ exhibit variances σ^2_{heog} and σ^2_{veog} (usually small) respectively with zero-mean. Estimated replica of true HEOG ($\hat{r}_h(n)$ in Eq.(4.2)) and VEOG ($\hat{r}_v(n)$ in Eq.(4.3)) are subtracted from recorded EEG signal ($s_e(n)$ in Eq.(4.1)) to give

$$e(n) = s_e(n) - \hat{r}_v(n) - \hat{r}_h(n) \tag{4.6}$$

Incorporating Eqs.(4.4) – (4.5) in Eq.(4.6) yields

$$e(n) = s_{eeg}(n) + \eta_w(n) + \eta_v(n) + \eta_h(n) \tag{4.7}$$

The corresponding mean squared value is

$$\sigma_e^2 = E\left[e^2(n)\right] \tag{4.8}$$

Its further simplification results in

$$\sigma_e^2 = E\left[s_{eeg}^2(n)\right] + \sigma_w^2 + \sigma_{veog}^2 + \sigma_{heog}^2 = \sigma_{eeg}^2 + \sigma_w^2 + \sigma_{veog}^2 + \sigma_{heog}^2 \tag{4.9}$$

where, $E[\bullet]$ is the ensemble average operator. The signal-to-"noise-plus-artifact"- ratio (SNAR) is defined as $SNAR = \sigma_{eeg}^2 \times \left(\sigma_w^2 + \sigma_{veog}^2 + \sigma_{heog}^2\right)^{-1}$ and the signal-to-noise-ratio (SNR) is defined as $SNR = \sigma_{eeg}^2 / \sigma_w^2$. The synthetic true EEG signal [256] is considered to be

$$s_{eeg}(n) = 1.5084 s_{eeg}(n-1) - 0.1587 s_{eeg}(n-2) - 0.3109 s_{eeg}(n-3) - 0.0510 s_{eeg}(n-4) + v(n) \tag{4.10}$$

In the above autoregressive equation, $v(n)$ is a driven zero-mean white-noise process satisfying a Gaussian distribution with small variance σ_v^2. It has been observed in [256] that

the spectrum of simulated EEG Eq.(4.10) is similar to that of a typical true EEG signal [258]. The synthetic true HEOG and true VEOG signals are generated by using the exponentially damped sinusoidal signals with stochastically varied amplitudes and shapes satisfying the uniform distribution. The j^{th} artifact is simulated as per the procedure given in [193] i.e.,

$$Art_j(k) = Ka_j e^{-k/\tau_j} sin(2\pi k/N_a) \text{ for } k = 0,1,2,.....,N_a - 1 \quad (4.11)$$

where, N_a is the length of artifact waveform. The parameter a_j is the amplitude of j^{th} artifact, τ_j is a parameter determining the shape, and K is an amplitude scaling factor. At the onset of each artifact, the values of a_j and τ_j are stochastically selected from a Gaussian distributed dataset, which introduces variations in the artifact signals.

4.2.2 Variable Forgetting Factor RLS Algorithm

Under the aforementioned system, the aim of adaptive artifact and noise canceller is to generate an output signal $e(n)$, which should be comparable to the true EEG signal $s_{eeg}(n)$ as much as possible. To develop the paradigm based variable forgetting factor RLS algorithm equations, we first define the cost function as

$$J(n) = \sum_{i=M}^{n} \left[\lambda(n)\right]^{n-i} e^2(i) \quad (4.12)$$

$$J(n) = e^2(i) + \lambda(n)e^2(n-1) + ... + \left[\lambda(n)\right]^{n-M} e^2(M) \quad (4.13)$$

where, $e(i) = s_e(i) - \sum_{m=1}^{M} h_v(m;n)\, rf_v(n+1-m) - \sum_{m=1}^{M} h_h(m;n)\, rf_h(n+1-m)$ (4.14)

and $\lambda(n)$ is the variable forgetting factor. The filter length M and forgetting factor $\lambda(n)$ are two main factors, which influence the performance of RLS algorithm. The forgetting factor in the range $0 < \lambda(n) < 1$ provides more weight to the more recent sample values. The actual selection of $\lambda(n)$ is dependent on the stationarity of the underlying process, and it also

depends on the stability of the relationship between the reference inputs and the actual electrooculogram constituents contaminating a true EEG signal. However, the possible sources that could alter aforementioned relationship involve changes in the features of the skin-electrode interface and/or a drift of the electrical properties of amplifier [75]. In the presented work, we consider EOG-to-EEG transfer to be linear, which facilitates the application of linear adaptive signal processing algorithms in the present scenario.

The cost function $J(n)$ is a type of sample mean, which is an approximation of $E\left[e^2(n)\right]$. Therefore, we deal with the minimization of $J(n)$ instead of the expected value of $e^2(n)$. The filter coefficients $h_v(m;n)$ and $h_h(m;n)$, at the n^{th} instant of time for $m = 1, 2, ..., M$, are obtained to minimize the cost function by solving $2 \times M$ equations. It follows that

$$\frac{dJ(n)}{dh_v(m)} = 0 \tag{4.15}$$

Substitution of Eqs.(4.12) - (4.14) in Eq.(4.15) results in

$$\frac{dJ(n)}{dh_v(m)} = 2\sum_{i=M}^{n}\left[\lambda(n)\right]^{n-i} e(i)\frac{de(i)}{dh_v(m)} \tag{4.16}$$

$$\frac{dJ(n)}{dh_v(m)} = -2\sum_{i=M}^{n}\left[\lambda(n)\right]^{n-i} e(i)\, rf_v(i+1-m) \tag{4.17}$$

Similarly, $\frac{dJ(n)}{dh_h(m)} = -2\sum_{i=M}^{n}\left[\lambda(n)\right]^{n-i} e(i)\, rf_h(i+1-m)$ (4.18)

Further, we define the cross-correlation terms / elements of $M \times 1$ dimension vectors $\vec{P}_v(n)$ and $\vec{P}_h(n)$ as

$$P_v(j;n) = \sum_{i=M}^{n}\left[\lambda(n)\right]^{n-i} s_e(i)\; rf_v(i+1-j) \tag{4.19}$$

$$P_h(j;n) = \sum_{i=M}^{n} \left[\lambda(n)\right]^{n-i} s_e(i)\ rf_h(i+1-j) \tag{4.20}$$

for $j = 1,2...,M$

The cross-correlation terms / elements of $M \times M$ dimension square matrices $\vec{R}_{vh}(n)$ and $\vec{R}_{hv}(n)$ are defined as

$$R_{vh}(j,k;n) = \sum_{i=M}^{n} \left[\lambda(n)\right]^{n-i} rf_v(i+1-j) rf_h(i+1-k) \tag{4.21}$$

$$R_{hv}(j,k;n) = \sum_{i=M}^{n} \left[\lambda(n)\right]^{n-i} rf_h(i+1-j) rf_v(i+1-k) \tag{4.22}$$

The auto-correlation terms / elements of $M \times M$ dimension square matrices $\vec{R}_{vv}(n)$ and $\vec{R}_{hh}(n)$ are defined as

$$R_{vv}(j,k;n) = \sum_{i=M}^{n} \left[\lambda(n)\right]^{n-i} rf_v(i+1-j) rf_v(i+1-k) \tag{4.23}$$

$$R_{hh}(j,k;n) = \sum_{i=M}^{n} \left[\lambda(n)\right]^{n-i} rf_h(i+1-j) rf_h(i+1-k) \tag{4.24}$$

for $j = 1,2...,M$ and for $k = 1,2...,M$

In the matrix form, the two sets of Eqs.(4.17) – (4.18) are rearranged as

$$\vec{R}_{vv}(n)\vec{H}_v(n) + \vec{R}_{vh}(n)\vec{H}_h(n) = \vec{P}_v(n) \tag{4.25}$$

$$\vec{R}_{hv}(n)\vec{H}_v(n) + \vec{R}_{hh}(n)\vec{H}_h(n) = \vec{P}_h(n) \tag{4.26}$$

where,

$$\vec{H}_v(n) = \left[h_v(1;n) \quad h_v(2;n) \quad . \quad . \quad . \quad h_v(\mathrm{M};n)\right]^T \tag{4.27}$$

$$\vec{H}_h(n) = \left[h_h(1;n) \quad h_h(2;n) \quad . \quad . \quad . \quad h_h(\mathrm{M};n)\right]^T \tag{4.28}$$

$$\vec{P}_v(n) = \left[P_v(1;n) \quad P_v(2;n) \quad . \quad . \quad . \quad P_v(\mathrm{M};n)\right]^T \tag{4.29}$$

$$\vec{P}_h(n) = \left[P_h(1;n) \quad P_h(2;n) \quad . \quad . \quad . \quad P_h(\mathrm{M};n) \right]^T \tag{4.30}$$

Here, $(\bullet)^T$ is the matrix transpose operator. In more compact form, above equations can be further rearranged as

$$\vec{\mathbf{R}}(n)\vec{\mathbf{H}}(n) = \vec{\mathbf{P}}(n) \tag{4.31}$$

$$\vec{\mathbf{H}}(n) = \left[\vec{\mathbf{R}}(n) \right]^{-1} \vec{\mathbf{P}}(n) \tag{4.32}$$

where, $\vec{\mathbf{R}}(n) = \begin{bmatrix} \vec{R}_{vv}(n) & \vec{R}_{vh}(n) \\ \vec{R}_{hv}(n) & \vec{R}_{hh}(n) \end{bmatrix}$ (4.33)

$$\vec{\mathbf{H}}(n) = \begin{bmatrix} \vec{H}_v(n) \\ \vec{H}_h(n) \end{bmatrix} \tag{4.34}$$

$$\vec{\mathbf{P}}(n) = \begin{bmatrix} \vec{P}_v(n) \\ \vec{P}_h(n) \end{bmatrix} \tag{4.35}$$

Using Eq.(4.32), optimum set of filter coefficients can be calculated for the presented adaptive system, which minimizes the cost function $J(n)$ under the nonstationary environment. To obtain the variable forgetting factor RLS algorithm equations, the reference input signals are expressed in the vector form as

$$\vec{rf}_v(n) = \left[rf_v(n) \quad rf_v(n-1) \quad . \quad . \quad . \quad rf_v(n+1-M) \right]^T \tag{4.36}$$

$$\vec{rf}_h(n) = \left[rf_h(n) \quad rf_h(n-1) \quad . \quad . \quad . \quad rf_h(n+1-M) \right]^T \tag{4.37}$$

And in matrix form as

$$\vec{\mathbf{rf}}(n) = \begin{bmatrix} \vec{rf}_v(n) \\ \vec{rf}_h(n) \end{bmatrix} \tag{4.38}$$

Using the concepts and theory of RLS algorithm [18], the required VFF-RLS algorithmic equations can be written as

$$\vec{\mathbf{R}}(n) = \lambda(n)\vec{\mathbf{R}}(n-1) + \vec{\mathbf{rf}}(n)\vec{\mathbf{rf}}^T(n) \tag{4.39}$$

$$\left[\vec{\mathbf{R}}(n)\right]^{-1} = \left[\lambda(n)\right]^{-1}\left[\vec{\mathbf{R}}(n-1)\right]^{-1} - \left[\lambda(n)\right]^{-1}\vec{\mathbf{K}}(n)\vec{\mathbf{rf}}^{T}(n)\left[\vec{\mathbf{R}}(n-1)\right]^{-1} \tag{4.40}$$

The inverse of the correlation-matrix of the input signal vector conceives the effect of whitening the tap-inputs.

$$\vec{\mathbf{K}}(n) = \frac{\left[\vec{\mathbf{R}}(n-1)\right]^{-1}\vec{\mathbf{rf}}(n)}{\lambda(n) + \vec{\mathbf{rf}}^{T}(n)\left[\vec{\mathbf{R}}(n-1)\right]^{-1}\vec{\mathbf{rf}}(n)} \tag{4.41}$$

The weights / coefficients updating equation is

$$\vec{\mathbf{H}}(n) = \vec{\mathbf{H}}(n-1) + \vec{\mathbf{K}}(n)e(n/n-1) \tag{4.42}$$

where,

$$e(n/n-1) = s_e(n) - \vec{\mathbf{rf}}^{T}(n)\vec{\mathbf{H}}(n-1) \tag{4.43}$$

$$e(n) = s_e(n) - \vec{\mathbf{rf}}^{\mathbf{T}}(n)\vec{\mathbf{H}}(n) \tag{4.44}$$

To initialize the algorithm, it is appropriate to use

$$\vec{\mathbf{H}}(n-1) = Null \text{ at the starting point} \tag{4.45}$$

(*i.e.*, $h_v(m;n) = h_h(m;n)$ = zero at initial point for $m = 1, 2..., M$)

$$\left[\vec{\mathbf{R}}(n-1)\right]^{-1} = \zeta^{-1}\mathbf{I} \text{ at the starting point} \tag{4.46}$$

where, $\mathbf{I}$ is $2M \times 2M$ dimensional identity-matrix, the parameter ζ is a small positive value for the high SNR and it is a large positive value for the low SNR. Moreover, the rate of convergence of RLS procedure is invariant to the eigenvalue spread of the ensemble averaged correlation-matrix of the input signal vector. It is apparent from the above equations that the matrix inversion procedure to procure the optimum filter coefficients in Eq.(4.32) can be avoided by using the matrix inversion lemma in VFF-RLS algorithm. The presented adaptive filter uses the recursive system to update the weights or coefficient-vector in Eq.(4.42), which substantially reduces the computational burden.

4.3 Numeric Variable Forgetting Factor Updating Procedure

In the conventional RLS adaptive algorithm, the fixed value of forgetting factor is suitable for the stationary environment with an elevated degree of precision. The estimation error is large for the low values of forgetting factor, but it is low for the high values of λ. As the value of forgetting factor decreases, the rate of convergence increases. The usage of lower forgetting factor is intended to ensure that data values in the distant past are forgotten in order to afford the possibility of following the statistical variations of the observable data, when RLS algorithm based filter operates in the nonstationary environment. However, NVFF-RLS algorithm is incorporated for the estimation of noise-free HEOG and VEOG signals, in which the variable forgetting factor $\lambda(n)$ is required to be updated at each sample point. On the basis of extended estimation error criterion, an extended estimation of output signal is determined as

$$Z(n)=\frac{1}{Q}\sum_{q=0}^{Q-1}\left|e(n-q)\right|^2 \tag{4.47}$$

The value of Q is kept small to minimize the asymptotic memory length. The adaptation speed is dependent upon the asymptotic memory length as

$$N(n)=\frac{1}{1-\lambda(n)} \tag{4.48}$$

Consequently, the extended estimation error criterion-based theory [259] results in

$$N(n)=\frac{\sigma_e^2 N_{\max}}{Z(n)} \tag{4.49}$$

However, the memory lengths corresponding to λ_{Max} and λ_{Min} are depicted as N_{Max} and N_{Min} respectively. It follows that

$$0<\lambda_{\min}<\lambda(n)=1-\left[N(n)\right]^{-1}<\lambda_{\max}<1 \tag{4.50}$$

From Eq.(4.9), it is clear that

$$\sigma_e^2 = \left[\sigma_{eeg}^2 + \sigma_w^2\right]\left[1 + \frac{\sigma_{veog}^2 + \sigma_{heog}^2}{\sigma_{eeg}^2 + \sigma_w^2}\right] \tag{4.51}$$

For $\sigma_{eeg}^2 + \sigma_w^2 \gg \sigma_{veog}^2 + \sigma_{heog}^2$, the above equation is approximated as

$$\sigma_e^2 \simeq \sigma_{eeg}^2 + \sigma_w^2 \tag{4.52}$$

On contrary to the stationary case, a smaller value of the forgetting factor in the nonstationary environments appears to be more efficient. When the underlying signal experiences nonstationarity, the value of NVFF decreases to modify the tracking performance of the presented adaptive procedure. Therefore, it is compatible with both linear as well as nonlinear parameter estimation and noise cancellation adaptive algorithms.

4.4 Simulation Results

In this section, we shall investigate the behavior of presented linear NVFF-RLS algorithm based artifact and noise removal scheme, in which the separately recorded noisy HEOG and VEOG reference signals are first refined by using two FIR filters, and subsequently subtracted from the recorded EEG signal for the EOG artifact removal. Its performance will be compared with the linear FFF-RLS, linear FSS-NLMS, and linear GVSS-NLMS algorithm based approaches. The artifacts $Art_{h,j}$ and $Art_{v,j}$ are generated using Eq.(4.11), in which the length of artifact waveform N_a is kept 128 samples, the values of a_j and τ_j are randomly chosen from a Gaussian distributed dataset with mean (μ_a) = 1, variance (σ_a^2) = 0.1 and mean (μ_τ) = 250, variance (σ_τ^2) = 50 respectively [193]. Theses generated artifactual signals are exponentially distributed over time, with the occurrence rate of 0.5 per unit time, in which one unit time corresponds to 1024 samples of discrete-time series [193].

For the generation of true EEG signal, the value of σ_v^2 is set to 0.001 in Eq.(4.10). The

SNR is fixed at $+30dB$. The true EEG signal, noisy EOG artifact signals and the simulated corrupted EEG signal are shown in Fig. 4.2, which are normalized in the range $[-1,+1]$. The low values of K are affecting the amplitude of EOG signals, which are found to be lower than the predetermined threshold value. This threshold value is considered to be six times more than the artifact-free EEG signal [193]. Therefore, such simulated artifact signals are not suitable for analysis.

However, the high values of K lead to the higher amplitude of EOG signals, which are found to be more than the threshold value as well as the true EEG signal, and such EOG signals can be used for further analysis (as shown in Fig. 4.3). The values of K for the generation of HEOG and VEOG signals are kept at 0.99 and 0.98 respectively, in Eq.(4.11). The length of both FIR filters is considered to be $M = 35$, the value of Q is 5 in Eq.(4.47), the maximum and minimum values of the forgetting factor are fixed at $\lambda_{Max} = 0.97$ and $\lambda_{Min} = 0.95$ respectively. The fixed forgetting factor value in the conventional RLS algorithm is kept $\lambda_{FFF} = 0.97$. For the appropriate performance of NVFF-RLS algorithm, we fix $\zeta = 0.01$ for the stable initialization. As the synthetic signals are used to simulate EEG, EOG and additive noise signals, the value of $\left(\sigma_{eeg}^2 + \sigma_w^2\right)$ can be easily calculated from the available data statistics, in which the value of $\sigma_{eeg}^2(dB)$ is $10\log_{10}\left(15\times10^{-6}\right)^2 = -222.15dB$. The performance of FFF-RLS and NVFF-RLS based EOG artifact and noise excision techniques are compared in Fig. 4.4 and Fig. 4.5.

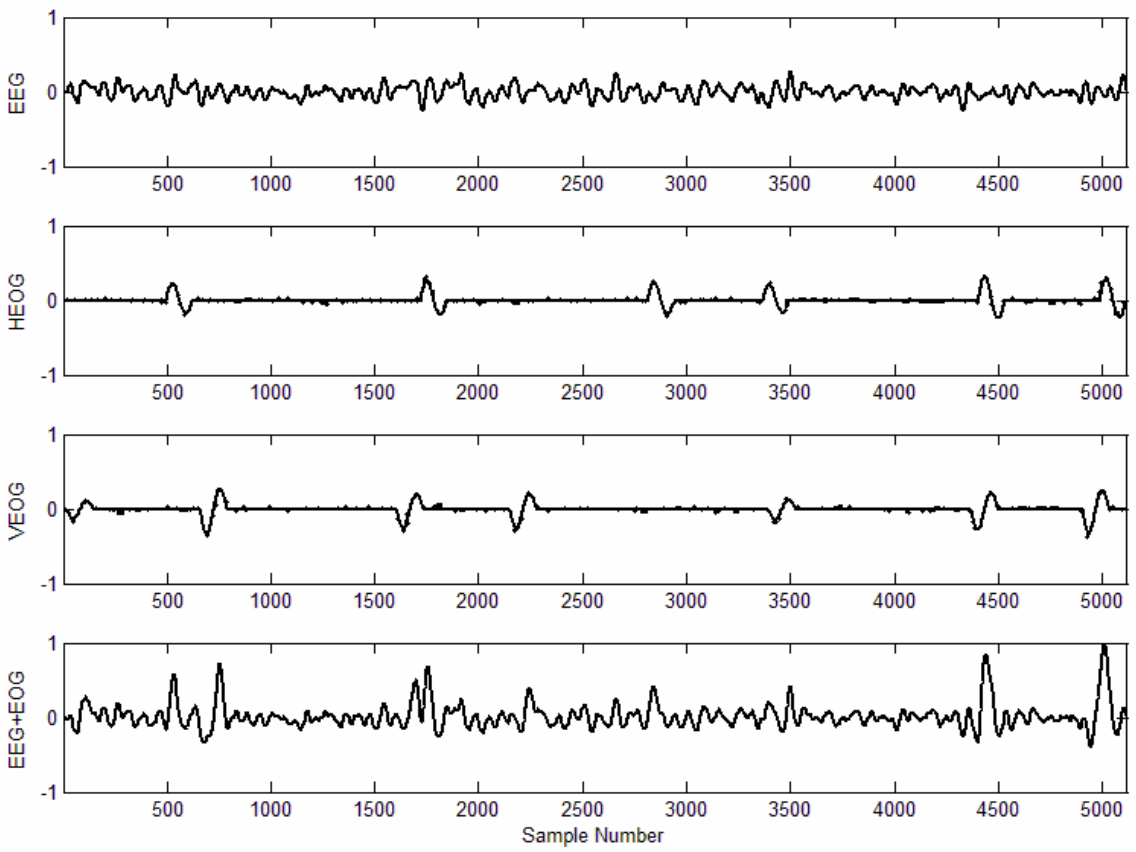

Fig. 4.2: True EEG, HEOG, VEOG and corrupted EEG signal for low values of K (a typical case)

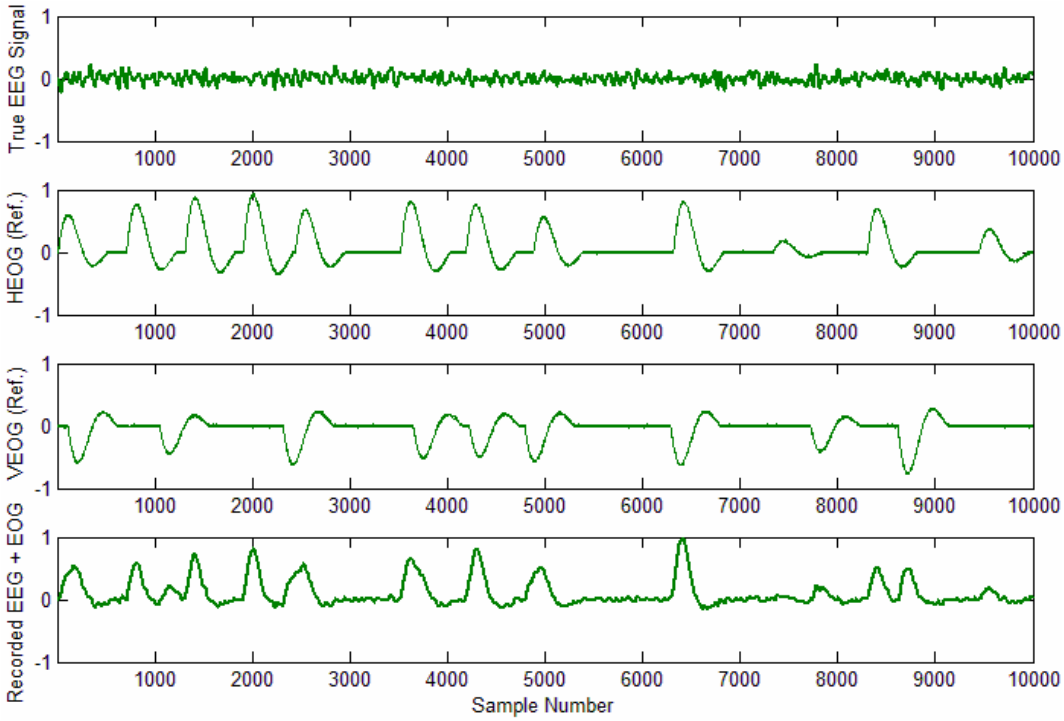

Fig. 4.3: True EEG, HEOG, VEOG and corrupted EEG signal for high values of K (a typical case)

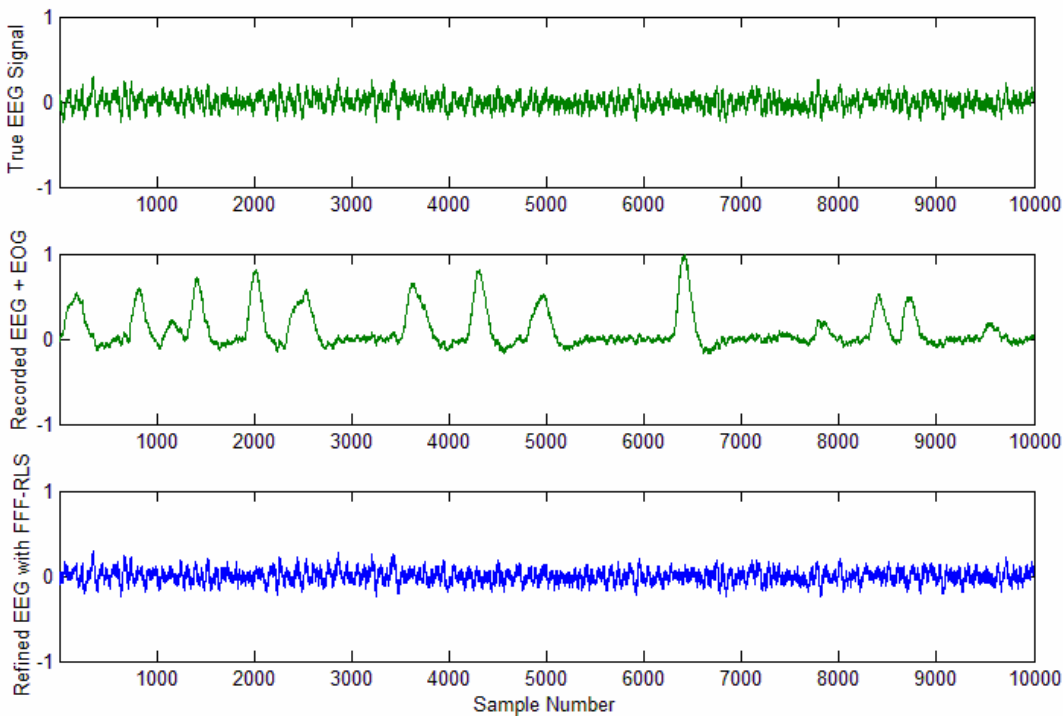

Fig. 4.4: Refined EEG signal (blue colored) at the output of FFF-RLS based adaptive system (a typical case)

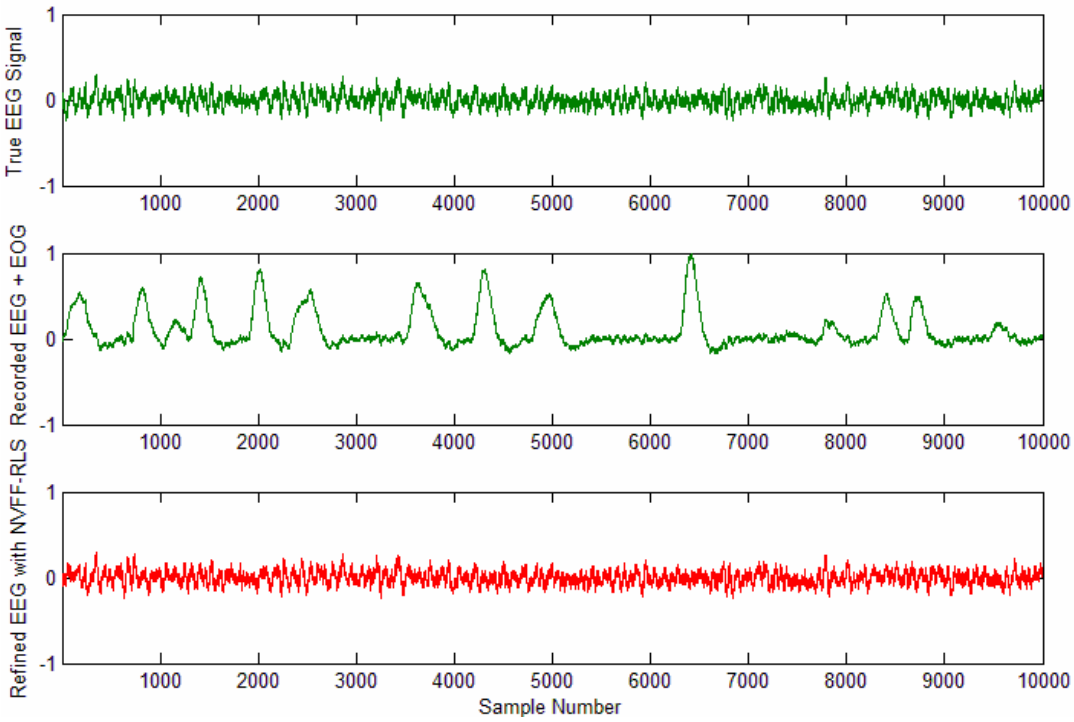

Fig. 4.5: Refined EEG signal (red colored) at the output of NVFF-RLS based adaptive system (a typical case)

As we are dealing with synthetic EEG and EOG signals, therefore it is possible to use the mean-squared-error (MSE) criterion for the appraisal of FSS-NLMS, GVSS-NLMS, FFF-RLS and NVFF-RLS procedures. In the present scenario, linear GVSS-NLMS algorithm is given as

$$\vec{\mathbf{H}}(n)_{GVSS-NLMS} = \vec{\mathbf{H}}(n-1)_{GVSS-NLMS} + \mu'(n)e(n)\frac{\vec{\mathbf{rf}}(\mathbf{n})}{\left\|\vec{\mathbf{rf}}(\mathbf{n})\right\|_2^2} \tag{4.53}$$

where, $\|\bullet\|_2$ is the L_2 norm [17] and $\mu'(n)$ is the generalized variable step-size, which follows that

$$\mu'(n) = \bar{\alpha}\mu'(n-1) + \bar{\gamma}J_1(n-1) + \bar{\beta}J_2(n) \tag{4.54}$$

where, $J_1(n) = \sum_{\bar{p}=0}^{\bar{P}} \lambda_1^{\bar{p}} e(n)e(n-\bar{p})$ with $0 \le \lambda_1 < 1$ (4.55)

$$J_2(n) = \left[\sum_{\bar{q}=1}^{\bar{Q}} \lambda_2^{\bar{q}} e(n-\bar{q})\,\vec{\mathbf{rf}}^T(\mathbf{n})\right]\vec{\mathbf{rf}}(\mathbf{n})e(n) \quad \text{with } 0 \le \lambda_2 < 1 \tag{4.56}$$

where, $0 < \bar{\alpha} \le 1$, $0 \le \bar{\gamma} < 1$, and $0 \le \bar{\beta} < 1$. The parameter $\bar{\alpha}$ induces the global exponential forgetting in the variable step-size, $\bar{\gamma}$ controls the convergence rate as well as the level of misadjustment [257], $\bar{\beta}$ adjusts the adaptive behavior of step-size sequence $\mu'(n)$. However, λ_1 *and* λ_2 are the local exponential forgetting factors in Eq.(4.55) and Eq.(4.56) respectively. For appropriate convergence, VSS should be bounded in the range $\mu'_{Min} \le \mu'(n) \le \mu'_{Max}$. The initial step-size is usually taken as μ'_{Max}, which ensures that MSE of algorithm is remaining bounded. However, μ'_{Min} is chosen to achieve the minimum level of tracking ability, which is kept close to the step-size of FSS-NLMS algorithm [17]. The values of parameters are kept at $\lambda_1 = 0.66$, $\lambda_2 = 0.66$, $\bar{\alpha} = 0.97$, and $\bar{\beta} = \bar{\gamma} = 0.8\times10^{-4}$. The value of the minimum step-size is $\mu'_{Min} = 5\times10^{-8}$, and the maximum bounded value of step-size is $\mu'_{Max} = 5\times10^{-7}$. The number of samples is considered to be 10000 in each experiment at a

particular SNR. In t^{th} experiment, let us assume the residual error in the artifact-free EEG signal to be $e_s(t,n) = s_{eeg}(t,n) - e(t,n)$.

The corresponding MSE be $J_{eeg}(t) = E\left[e_s^2(t,n)\right] = \sum_{n=1}^{10000} \frac{e_s^2(t,n)}{10000}$. The presented results in Fig. 4.6 are based on the ensemble average of 2500 independent simulation runs/experiments for the different parameter values *i.e.*, MSE at a particular SNR is

$$\bar{\mathbf{J}}_{\mathbf{EEG\_SNR}} = E\left[J_{eeg}(t)\right] = \sum_{t=1}^{2500} \frac{J_{eeg}(t)}{2500} \tag{4.57}$$

For further analysis, we determine $MSE_{Threshold} = 1\%\ of\ \sigma_{eeg}^2 = -268.2dB$ (as illustrated in Fig. 4.4). If MSE value is lower than $-268.2dB$, then the adaptive procedure based ocular artifact / noise cancellation method is appraised to be competent.

It is inferred from the outcomes presented in Fig. 4.6 that NVFF-RLS procedure proffers $-268.2dB$ average mean squared error at $12.3dB$ SNR. Whereas, $MSE_{Threshold}$ is achieved by FFF-RLS, GVSS-NLMS and FSS-NLMS algorithms at SNR values $13.5dB$, $15.75dB$ and $19.5dB$ respectively. However, NVFF-RLS outperforms FFF-RLS, GVSS-NLMS and FSS-NLMS procedure based artifact / noise suppression method for entire range of SNR values. At $20dB$ SNR, the performance benefits of NVFF-RLS procedure over FFF-RLS and GVSS-NLMS procedures are approximately $14dB$ and $34dB$ respectively. These performance benefits in terms of average mean squared error get enhanced with the increasing value of signal-to-noise-ratio. At $30dB$ SNR, average mean squared error values for NVFF-RLS and GVSS-NLMS procedures are approximately $-430dB$ and $-367dB$ respectively, which are significantly lower than $MSE_{Threshold} = -268.2dB$.

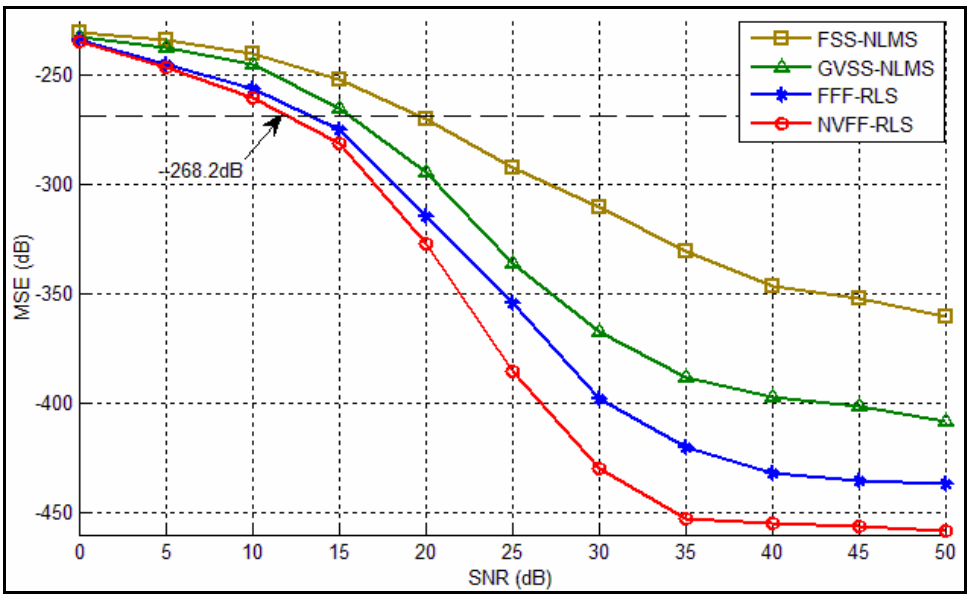

Fig. 4.6: MSE (dB) vs. SNR (dB) to illustrate comparison of FSS-NLMS, GVSS-NLMS, FFF-RLS and NVFF-RLS adaptive algorithm based artifact and noise suppression systems

Though algorithm providing lowest MSE is preferable, but its computational complexity is another major concern from implementation point of view. Wagner *et al*. [260] have demonstrated that FSS-NLMS algorithm exhibits quite lower computational complexity in terms of the number of additions, multiplications and divisions per iteration, in comparison to conventional FFF-RLS algorithm. It is noteworthy that number of computations required per iterations for NVFF [15] and GVSS [17] calculation is small. Therefore at higher SNR values, GVSS-NLMS is also a lucrative option because its computational complexity is quite lower than NVFF-RLS and FFF-RLS algorithms.

In the real-time recorded EEG signals corrupted by EOG artifacts (data obtained from [261], as shown in Fig. 4.7), we add $-20dB$ zero-mean additive white Gaussian-noise. The approximate value of variance $\left(\sigma_{eeg}^2 + \sigma_w^2\right)$ is determined by using the recorded EEG data segments identified by an expert neurologist, in which artifacts are not present. In this case, the length of single FIR filter is considered to be $2M$, in which the measured EOG-reference signal (right) is provided as input. It is observed that the FSS-NLMS and GVSS-NLMS algorithms fail to perform well due to time-variations in the measured real-time EEG signal in the presence of rapidly varying high amplitude EOG and additive noise signals. This problem usually arises due to the high lag-misadjustment [18] in the adaptive weight-vector under the nonstationary environment. The simulation results are shown in Fig. 4.8 – Fig. 4.9 to demonstrate the performance of NVFF-RLS and FFF-RLS algorithms, in which NVFF-RLS algorithm supersedes FFF-RLS algorithm under appropriate parameter setting.

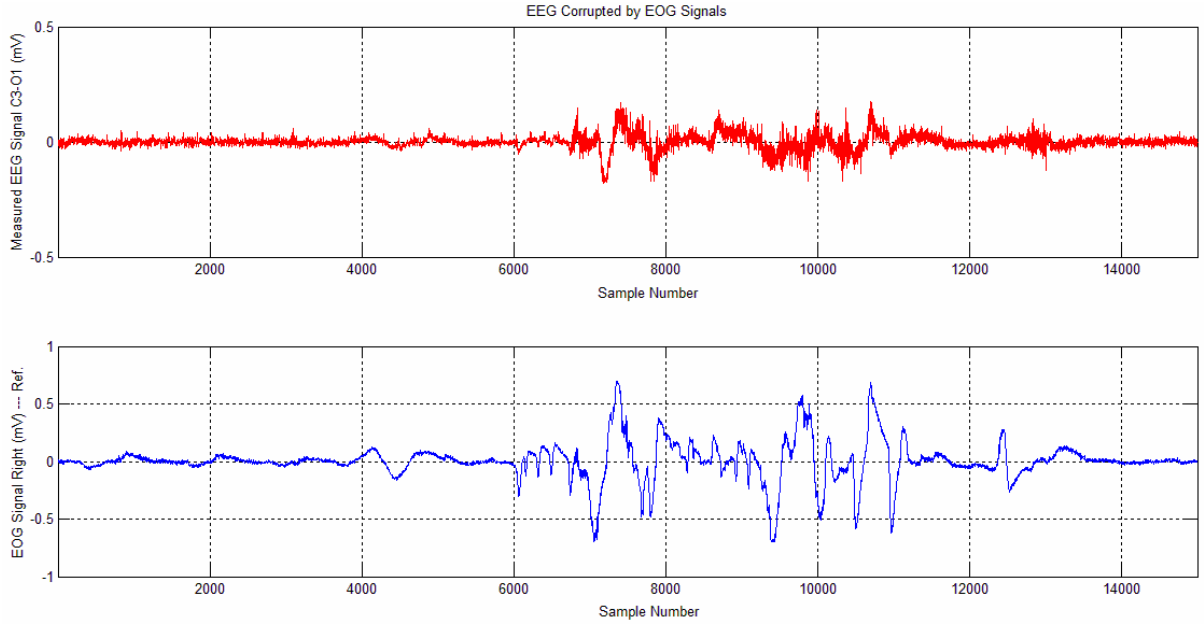

Fig. 4.7: Measured EEG signal (corrupted by EOG and noise) at C3-O1 and measured EOG-reference signal (right)

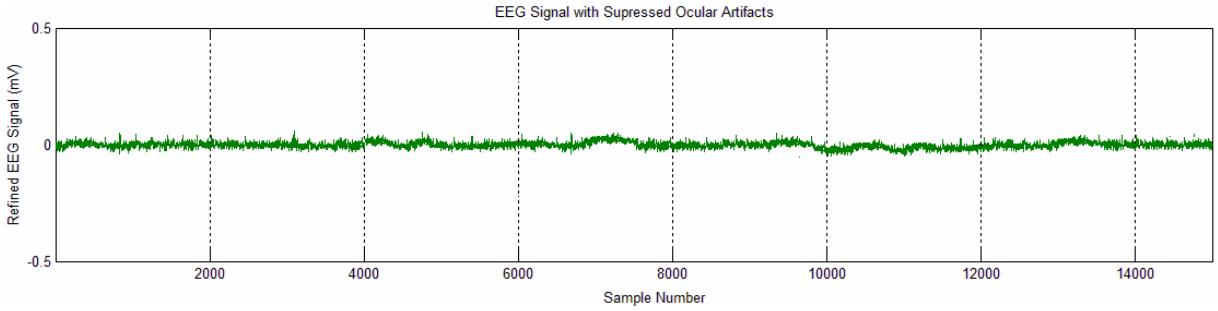

Fig. 4.8: Refined EEG signal with suppressed artifacts and noise using FFF-RLS algorithm

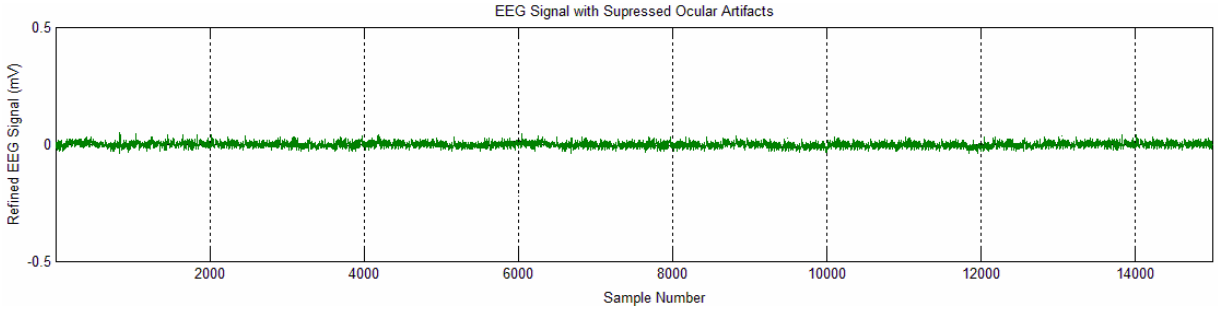

Fig. 4.9: Refined EEG signal with suppressed artifacts and noise using NVFF-RLS algorithm

4.5 Summary of Chapter

In this chapter, ocular artifacts present in electroencephalogram signal are suppressed using the adaptive filtering scheme. The major focus is on the performance of numeric variable forgetting factor recursive least squares procedure, when used for the ocular horizontal electrooculogram and vertical electrooculogram artifact suppression. The basic concept used in the presented research work is that the separately recorded HEOG and VEOG signals are processed using the adaptive filter to generate two reference signals, which can be subtracted from the recorded EEG signal to obtain an artifact-free EEG signal, in the presence of additive white Gaussian-noise. Simulation has been preformed using synthetic EEG as well as real-time EEG signals, which are corrupted by EOG signals and noise. The simulation results manifest that GVSS-NLMS algorithm performs well only under high signal-to-noise-ratio conditions for the ocular artifact removal. Under similar conditions, NVFF-RLS algorithm based technique is found to be much more affective in EOG suppression, in comparison to FFF-RLS, FSS-NLMS and GVSS-NLMS algorithm at low as well high values of SNR.

Therefore, NVFF-RLS algorithm based ocular artifact mitigation scheme can be applied efficiently to refine real-time recorded EEG signals in the presence of additive white Gaussian noise.

CHAPTER 5

CONCLUDING REMARKS AND FUTURE SCOPE

Epilepsy leads to a reduction in productivity of human beings, which is classified as a neurological disorder that affects the functioning of brain. Electroencephalography is one of the dominant technologies for noninvasive measurements of the dynamic whole-brain electrical activity. The classical signal processing methods for EEG analysis have mostly included discrete-time filtering, spectral analysis, or source separation. But, we have mainly focused on the discrete-time filtering techniques to process the electroencephalogram signals. In this research work, we have studied various electroencephalogram signal analysis techniques for the epileptic spike detection and artifact excision. In the following, we summarize important results of our study and also give suggestions for further investigations.

5.1 Concluding Remarks

We have first proposed the performance evaluation of epileptic spike detection algorithm in electroencephalogram signal using smoothed nonlinear energy operator, which is based on the usage of different window functions. The detection of epileptic spikes in the biomedical signal (i.e., EEG) is difficult because of the wide variations in nonstationary characteristics of these embedded spikes. However, this intricacy is compounded in the presence of white Gaussian-noise. For simulations, we have considered all the attributes of ES including the amplitude, sign, base-width and the location of occurrence, which are stochastic in nature. However, it can be inferred from the presented simulation outcomes that the high computational complexity of Kaiser window function often precludes its usage in SNEO model, though it outperforms Hamming window-based scheme. Therefore, the SNEO based on Hamming window is apposite for the ES detection in the real-time EEG signals for the analysis of physiological and neurological disorders.

The main focus of the presented work is on the determination of adaptive threshold for ES detection Eq.(2.24), which encompasses the previously reported results Eq.(2.22) and Eq.(2.23). This proposed ES detection algorithm is tested using the real-time WAG/Rij-rat EEG data, which outperforms the conventional schemes. The adaptive characteristics of the presented scheme can be controlled by adjusting the parameters C and β_{FA} to optimize the trade-off between FNR and FPR values.

Further, the neurophysiological disorders related to the epilepsy can also be investigated (by utilizing the adaptive signal processing based techniques) as well as analyzed using the patient's electroencephalogram signals. Subsequently, we have proposed a technique for the epileptic spike enhancement and detection in EEG signals using the output correlation method, which is a Kalman filtering approach. Here, the enhancement of ESs is a sort of pre-processing to increase the sensitivity of detection process. The raw EEG signal has been expressed as the general Markov-model with time-varying Markovian-parameters, which vary as per the first-order autoregressive process. On contrary to the conventional Kalman filtering techniques [157], [213], [251], the exclusive feature of the presented output correlation method is that it also computes the process-noise variance as well as measurement-noise variance, which in turn improves the performance of proposed system. By more careful investigation of the synthetic EEG and the real-time WAG/Rij-rat EEG signals after pre-processing, we may monitor that the false detections have been significantly alleviated because the presented scheme utilizes the temporal information and time-variant nature of electroencephalogram signal constituents to identify epileptic spikes. But, this method exhibits relatively higher computational complexity.

We have next presented an NVFF-RLS algorithm based adaptive system, which processes the independently recorded reference HEOG and VEOG signals using the FIR filtering. These processed EOG signals are then subtracted from the recorded contaminated EEG

signals for the ocular artifact removal. This artifact and noise canceller encompasses two FIR filtering configurations exhibiting the same length, and it can be simply demonstrated that the algorithm development will be exactly same when the two filtering configurations have different lengths. It is also straight forward to extend this technique to cases having three or more reference signals. In the adaptive artifact and noise cancellation procedure, the quality of reference signal is typically sensitive factor. It must appear uncorrelated with the desired signalling waveforms. As the level of crosstalk between the reference signalling waveform and desired signalling waveform increases, the performance of adaptive artifact canceller commences to degrade.

Under appropriate parameter setting, the presented NVFF-RLS algorithm outperforms FFF-RLS, GVSS-NLMS and FSS-NLMS algorithms, as far as the ocular artifact and noise excision is concerned. It is apparent from simulation results using the synthetic EEG, EOG and noise signals that the GVSS-NLMS can also be incorporated for the artifact removal only at the high SNR values, which incur low computational complexity in comparison to conventional RLS algorithms. However for the real-time recorded EEG signals corrupted by the rapidly varying EOG and noise signals, the NVFF-RLS algorithm appears to be the most appropriate choice under the low as well as high SNR conditions, where the GVSS-NLMS algorithm fails to perform well due to the filter weight-vector lag-misadjustment.

5.2 Suggestions for Further Work

Future scope includes the development of efficient Kalman filtering-based adaptive epileptic spike detection schemes [213], which is an extension of proposed output correlation method based on the Kalman filtering to the multichannel EEG recordings. Moreover, the method to differentiate between the enhanced noisy transients and epileptic spikes in the presence of artifacts is yet to be proposed. However, the information about the epileptic spikes obtained from the different channels can be combined using the smart techniques, which can be used

for the classification/diagnosis of neurophysiological disorders. Even single-channel source separation technique [262] can be used to retrieve the true EEG signal from the mixture of noise/artifacts. Segmentation of template pattern and extraction of features can also be used to refine EEG using different classifiers [263] and machine learning techniques [264]. However, fuzzy-logic, DWT and SVM are also useful in epileptic seizure detection [265] in the presence of noise/artifacts. Moreover, various artifacts like power line interference and baseline wander problem etc. can be handled amicably by incorporating interference/noise/artifact suppression techniques based on GVSS-LMP [257] and two-step RK-LMS algorithms [255], [266]. Future work also includes the performance evaluation of presented NVFF-RLS algorithm based noise, EOG [267], ECG [268] and EMG artifact removal technique using the real-time clinical data, and the application of linear NVFF-RLS adaptive algorithm in the EEG epileptic spike detection and excision scheme [269].

However, the performance of EEG refining technique also depends on the quality of measurement electrode [270], which may be explored subsequently. The electroencephalogram signal analysis for different sex, awake/sleep-state [271] and age-groups for healthy or unhealthy subjects needs to be investigated further.

REFERENCES

[1] W. Wu, S. Nagarajan, and Z. Chen, "Bayesian machine learning: EEG/EMG signal processing measurements," *IEEE Signal Process. Mag.*, vol. 1. no. 33, pp. 14 – 36, January 2016.

[2] C.T. Lombroso, E. Niedermeyer, and F.H.L.D. Silva, *Neonatal EEG Polygraphy in Normal and Abnormal Newborns – Electroencephalography, Basic Principles, Clinical Applications and Related Fields,* pp. 802 – 875, 3rd Edition, Baltimore: Williams and Wilkins, 1993.

[3] B. Boashash, H. Carson, and M. Mesbah, "Detection of seizures in newborns using time-frequency analysis of EEG signals," *Proc. IEEE 10th Workshop on Statistical Signal and Array Process*., Pocono Manor, PA, pp. 564 – 568, August 2000.

[4] K. Lehnertz, J. Arnhold, P. Grassberger, and C.E. Elger, "Chaos in Brain?," *Proc. of Workshop World Scientific*, Germany, March 1999.

[5] P.J. Franaszczuk, G.K. Bergey, P.J. Durka, and H.M. Eisenberg, "Time-frequency analysis using matching pursuit algorithm applied to seizures originating from mesial temporal lobe," *Electro. Clin. Neutophys.*, vol. 106, no. 6, pp. 513 – 521, June 1998.

[6] H.P. Zaveri, W.J. Williams, L.D. Iasemidis, and J.C. Sackellares, "Time-frequency representation of electrocorticograms in temporal lobe epilepsy," *IEEE Trans. Biomed. Eng*., vol. 39, no. 5, pp. 502 – 509, May 1992.

[7] P. Celka, B. Boashash, and P. Colditz, "Preprocessing and time-frequency analysis of newborn EEG seizures," *Proc. IEEE Eng. in Medicine and Biology*, vol. 20, no. 5, pp. 30 – 39, September/October 2001.

[8] L.M. Davis, I.B. Collings, and R.J. Evans, "Coupled estimators for equalization of fast-fading mobile channels," *IEEE Trans. Commun*., vol. 46, no. 10, pp. 1262 – 1265, October 1998.

[9] A.H. Sayed and T. Kailath, "A state-space approach to adaptive RLS filtering," *IEEE Signal Process. Mag.*, vol. 11, no. 3, pp. 18 – 60, July 1994.

[10] L. Lindbom, M. Sternad, and A. Ahlen, "Tracking of time-varying mobile radio channels – Part I: The Wiener LMS algorithm," *IEEE Trans. Commun*., vol. 49, no. 12, pp. 2207 – 2217, December 2001.

[11] L. Lindbom, A. Ahlen, M. Sternad, and M. Falkenstrom, "Tracking of time-varying mobile radio channels – Part II: A case study," *IEEE Trans. Commun*., vol. 50, no. 1, pp. 156 – 167, January 2002.

[12] C.F. So and S.H. Leung, "Variable forgetting factor RLS algorithm based on dynamic equation of gradient of mean square error," *Electro. Lett.*, vol. 37, no. 3, pp. 202 – 203, February 2001.

[13] S.H. Leung and C.F. So, "Gradient-based variable forgetting factor RLS algorithm in time-varying environments," *IEEE Trans. Signal Process*., vol. 53, no. 8, pp. 3141 – 3150, September 2005.

[14] A.K. Kohli, A. Rai, and M.K. Patel, "Variable forgetting factor LS algorithm for polynomial channel model," *ISRN Signal Process.*, pp. 1 – 4, vol. 2011, January 2011.

[15] A.K. Kohli and A. Rai, "Numeric variable forgetting factor RLS algorithm for second-order Volterra filtering," *Springer, Circuits Sys. Signal Process.*, vol. 32, no. 1, pp. 223 – 232, February 2013.

[16] A. Rai, "Analysis and design of adaptive Volterra filters for system identification in time-varying environment," Ph.D Thesis, Thapar University, ECE Dept., India, October 2015.

[17] A. Rai and A.K. Kohli, "Volterra filtering scheme using generalized variable step-size NLMS algorithm for nonlinear acoustic echo cancellation," *Acta Acustica United with Acustica*, vol. 101, no. 4, pp. 821 – 828, July/August 2015.

[18] S. Haykin, *Adaptive Filter Theory*. 4th Edition, New Jersey: Prentice Hall, 2002.

[19] W.O. Tatum, B.A. Dworetzky, W.D. Freeman, and D.L. Schomer, "Artifact: Recording EEG in special care units," *J. Clinical Neurophysiology*, vol. 28, no. 3, pp. 264 – 277, June 2011.

[20] J. Ma, P. Tao, S. Bayram, and V. Svetnik, "Muscle artifacts in multichannel EEG: Characteristics and reduction," *J. Clinical Neurophysiology*, vol. 123, no. 8, pp. 1676 – 1686, August 2012.

[21] C. Carl, A. Acik, P. Konig, A.K. Engel, and J.F. Hipp, "The saccadic spike artifact in MEG," *J. NeuroImage*, vol. 59, no. 2, pp. 1657 – 1667, January 2012.

[22] I. Daly, N. Nicolaou, S.J. Nasuto, and K. Warwick, "Automated artifact removal from the electroencephalogram: A comparative study," *Clinical EEG and Neuroscience Society (ECNS)*, vol. 44, no. 4, pp. 291 – 306, October 2013.

[23] R.J.M. Somsen and B. Beek, "Ocular artifacts in children's EEG: selection is better than correction," *Biological Psychology*, vol. 48, no. 3, pp. 281 – 300, April 1998.

[24] D. Hagemann and E. Naumann, "The effects of ocular artifacts on (lateralized) broadband power in the EEG," *J. Clinical Neurophysiology*, vol. 112, no. 2, pp. 215 – 231, February 2001.

[25] N.T. Haumann, L. Parkkonen, M. Kliuchko, and E. Brattico, "Comparing the performance of popular MEG/EEG artifact correction methods in an evoked-resonance study," *Comput. Intellig. and Neurosc.*, vol. 2016, pp. 1 – 10, June 2016.

[26] M. Hamalainen, R. Hari, R.J. Ilmoniemi, J. Knuutila, and O.V. Lounasmaa, "Magnetoencephalography-theory, instrumentation, and applications to noninvasive studies of the working human brain," *Reviews of Modern Physics*, vol. 65, no. 2, pp. 413 – 497, April 1993.

[27] A.A. Dingle, R.D. Jones, G.J. Carroll, and W.R. Fright, "A multistage system to detect epileptiform activity in the EEG," *IEEE Trans. on Biomedical Eng.*, vol. 40, no. 12, pp. 1260 – 1268, December 1993.

[28] H.J. Park, D.U. Jeong, and K.S. Park, "Automated detection and elimination of periodic ECG artifacts in EEG using the energy interval histogram method," *IEEE Trans. Biomedical Eng.*, vol. 49, no. 12, pp. 1526 – 1533, December 2002.

[29] D. Dimitriadis, A. Potamianos, and P. Maragos, "A comparison of the squared energy and Teager-Kaiser operators for short-term energy estimation in additive noise," *IEEE Trans. on Signal Process.*, vol. 57, no. 7, pp. 2569 – 2581, July 2009.

[30] E.L. Masherov, P.E. Volynsky, and G.A. Shekut'ev, "An approach to removing spatially uncorrelated artifacts from EEG recordings," *Human Physiology*, vol. 35, no. 4, pp. 502 – 512, July 2009.

[31] J. Gao, Y. Yang, P. Lin, and P. Wang, "Online EMG artifacts removal from EEG based on blind source separation," *Proc. IEEE 2nd Int. Asia Conf. Informatics in Control, Automation and Robotics (CAR)*, Wuhan, vol. 1, pp. 28 – 31, March 2010.

[32] W.D. Clercq, B. Vanrumste, J-M. Papy, W.V. Paesschen, and S.V. Huffel, "Modeling common dynamics in multichannel signals with applications to artifact and background removal in EEG recordings," *IEEE Trans. Biomedical Eng.*, vol. 52, no. 12, pp. 2006 – 2015, December 2005.

[33] T.P. Jung, C. Humphries, T.W. Lee, S. Makeig, M.J. McKeown, V. Iragui, and T.J. Sejnowski, "Removing electroencephalographic artifacts: Comparison between ICA and PCA," *Proc. IEEE Neural Networks Signal Processing Society Workshop*, Cambridge, pp. 63 – 72, August/September 1998.

[34] W. Zhou, J. Zhou, H. Zhao, and L. Ju, "Removing eye movement and power line artifacts from the EEG based on ICA," *Proc. IEEE 27th Annual Int. Conf. Eng. Medicine and Biology Society (EMBS)*, Shanghai, China, vol. 6, pp. 6017 – 6020, September 2005.

[35] S. Boudet, L. Peyrodie, P. Gallois, and C. Vasseur, "A global approach for automatic artifact removal for standard EEG record," *Proc. IEEE 28th Annual Int. Conf. in Eng.*

Medicine and Biology Society (EMBS), New York, USA, pp. 5719 – 5722, August/September 2006.

[36] S. Devuyst, T. Dutoit, P. Stenuit, M. Kerkhofs, and E. Stanus, "Removal of ECG artifacts from EEG using a modified independent component analysis approach," *Proc. IEEE 30th Annual Int. Conf. Eng. in Medicine and Biology Society*, Vancouver, BC, Canada, pp. 5204 – 5207, August 2008.

[37] N. Milijkovic, V. Matic, S.V. Huffel, and M.B. Popovic, "Independent component analysis (ICA) methods for neonatal EEG artifact extraction: Sensitivity to variation of artifact properties," *Proc. IEEE 10th Symp. Neural Network Applications in Electrical Eng. (NEUREL)*, Belgrade, pp. 19 – 21, September 2010.

[38] A. Zachariah, J. Jai, and G. Titus, "Automatic EEG artifact removal by independent component analysis using critical EEG rhythms," *Proc. IEEE Int. Conf. Control Commun. and Comput. (ICCC)*, Thiruvananthapuram, pp. 364 – 367, December 2013.

[39] N.N. Kumar and A.G. Reddy, "Removal of ECG artifact from EEG data using independent component analysis and S-transform," *Int. J. of Science, Eng. and Tech. Research (IJSETR)*, vol. 5, no. 3, pp. 712 – 716, March 2016.

[40] A. Turnip, "Automatic artifacts removal of EEG signals using robust principal component analysis," *Proc. IEEE 2nd Int. conf. Tech., Informatics, Management, Eng. and Environment (TIME-E)*, Bandung, Indonasia, pp. 331 – 334, August 2014.

[41] S. Hu, M. Stead, and G.A. Worrell, "Removal of scalp reference signal and line noise for intracranial EEGs," *Proc. IEEE Conf on Networking, Sensing and Control (ICNSC)*, Sanya, pp. 1486 – 1491, April 2008.

[42] A.Qayoom and W. Abdul, "Artifact processing of epileptic EEG signals: An overview of different types of artifacts," *Proc. of IEEE Int. Conf. Adv. Comp. Sc. Applications and Tech. (ACSAT)*, Kuching, pp. 358 – 361, December 2013.

[43] S. Jirayucharoensak, P. Israsena, S. Pan-ngum, and S. Hemrungrojn, "Online EEG

artifact suppression for neurofeedback training systems," *Proc. IEEE 6th Int. conf. Biomedical Eng., (BMEiCON)*, Amphur Muang, pp. 1 – 5, October 2013.

[44] V. Patil and C. Srinivas, "Fully automated artifact removal for BCI," *Int. J. Advanced Research in Computer and Comm. Eng. (IJARCCE)*, vol. 5, no. 4, pp. 691 – 696, April 2016.

[45] R. Vigano, V. Jousmaki, M. Hamalaninen, R. Hari, and E. Oja, "Independent component analysis for identification of artifacts in magnetoencephalographic recordings," *Advances in Neur. Inform. process. Sys.*, vol.10, pp. 229–235, July 1998.

[46] R. Ferdousy, A.I. Choudhory, M.S. Islam, M.A. Rab, and M.E.H. Chowdhory, "Electrooculographic and electromyographic artifacts removal from EEG," *Proc. IEEE 2nd Int. Cong. Chemical, Biological and Environment Eng. (ICBEE)*, Cairo, pp 163 – 167, November 2010.

[47] A.R. Teixeira, A.M. Tome, and I.M. Santos, "Automatic elimination of high amplitude artifacts in EEG signals," *1st Int. Conf. Advances in Signal, Image and Video Process. (IARIA)*, France, pp. 21 – 26, March 2016.

[48] N.T. Anh-Dao, T. Duc-Nghia, N. Thi-Hao, T. Duc-Tan, and N. Linh-Trung, "An effective procedure for reducing EOG and EMG artifacts from EEG signals," *Proc. IEEE Int. Conf. Advanced Technologies for Commun. (ATC)*, Hochi Minh City, pp. 328 – 332, October 2013.

[49] R. Dhiman, J.S. Saini, Priyanka, and A.P. Mittal, "Artifact removal from EEG recordings – An overview," *National Conf. on Computational Instrumentation (NCCI)*, CSIO Chandigarh, India, pp. 62 – 66, March 2010.

[50] N.A. Chadwick, D.A. McMeekin, and T. Tan, "Classifying eye and head movement artifacts in EEG signals," *Proc. IEEE 5th Int. Digital Ecosystems and Technologies (DEST)*, Daejeon Korea, pp. 285 – 291, May/June 2011.

[51] W. Ma, D. Tran, T. Le, H. Lin, and S.M. Zhou, "Using EEG artifacts for BCI

applications," *Proc. IEEE Int. Joint Conf. Neural networks (IJCNN)*, Beijing, China, pp. 3628 – 3635, July 2014.

[52] E.C. Ifeachor, M.T. Hellyar, D.J. Mapps, and E.M. Allen, "Knowledge-based enhancement of human EEG signals," *Proc. IEE Artificial Intelligence in Signal Processing*, vol. 137, no. 5, pp. 302 – 310, October 1990.

[53] C.J. James, M.T. Hagan, R.D. Jones, P.J. Bones, and G.J. Carroll, "Spatio-temporal filtering of the EEG via neural network based multireference adaptive noise canceling," *Proc. IEEE 18th Annual Int. Conf. Eng. in Medicine and Biology Society*, vol. 3, pp. 911 – 912, October/November 1996.

[54] T.P. Exarchos, A.T. Tzallas, D.I. Fotiadis, S. Konitsiotis, and S. Giannopoulos, "A data mining based approach for the EEG transient event detection and classification," *Proc. IEEE 18th Symp. Computer-Based Med. Sys. (CBMS)*, pp. 35 – 40, June 2005.

[55] C. Gope, N. Kehtarnavaz, and D. Nair, "Neural network classification of EEG signals using time-frequency representation," *Proc. IEEE Int. Joint Conf. Neural Networks*, Montreal, Canada, vol. 4, pp. 2502 – 2507, July/August 2005.

[56] L.F. Araghi, "A new method for artifact removing in EEG signals," *Proc. Int. Multi-Conf. Engineers and Computer Scientists (IMECS)*, Hong Kong, vol. 1, March 2010.

[57] Y. Chen, M. Akutagawa, T. Emoto, and Y. Kinouchi, "The removal of EMG in EEG by neural networks," *Physiological Measurement*, vol. 31, pp. 1567 – 1584, October 2010.

[58] S. Shigemura, T. Nishimura, M. Tsubai, and H. Yokoi, "An investigation of EEG artifacts elimination using a neural network with non-recursive 2nd order volterra filters," *Proc. IEEE 26th Annual Int. Conf. Eng. Medicine and Biology Society (IEMBS)*, San Francisco, USA, vol. 1, pp. 612 – 615, September 2004.

[59] V. Schetinin and J. Schult, "The combined technique for detection of artifacts in clinical electroencephalograms of sleeping newborns," *IEEE Trans. Inf. Tech. in*

Biomedicine, vol. 8, no. 1, pp. 28 – 35, March 2004.

[60] W. Philips, "Adaptive noise removal from biomedical signals using warped polynomials," *IEEE Trans. Biomed. Eng.*, vol. 43, no. 5, pp. 480 – 492, May 1996.

[61] J. Mateo, A. Torres, M.A. Garcia, C. Sanchez, and R. Carvigon, "Robust volterra filter design for enhancement of electroencephalogram signal processing," *Circuit Syst. Signal Process.*, vol. 32, no.1, pp. 233 – 253, February 2013.

[62] A. Turnip and I.R. Setiawan, "Artifacts removal of EEG signals using nonlinear adaptive autoregressive," *Int. J. Inf. and Electronics Eng.*, vol. 5, no. 3, pp. 180 – 183, May 2015.

[63] M. Shao, K.E. Barner, and M.H. Goodman, "An interference cancellation algorithm for noninvasive extraction of transabdominal fetal electroencephalogram (TaFEEG)," *Proc. IEEE Trans. Biomed. Eng.*, vol. 51, no. 3, pp. 471 – 483, March 2004.

[64] D. Schachinger, K. Schindler, and T. Kluge, "Automatic reduction of artifacts in EEG-Signals," *Proc. IEEE 15th Int. Conf. Digital Signal Processing*, Cardif, pp. 143 – 146, July 2007.

[65] M.A.A. Dewan, M.J. Hossain, M.M. Hoque, and O. Chae, "Contaminated ECG artifact detection and elimination from EEG using energy function based transformation," *Proc. IEEE Int. Conf. Information and Comm. Tech. (ICICT)*, Dhaka, Bangladesh, pp. 52 – 56, March 2007.

[66] S. Boudet, L. Peyrodie, P. Gallois, and C. Vasseur, "A robust method to filter various types of artifacts on long duration EEG recordings," *Proc. IEEE 2nd Int. Conf. Bioinformatics and Biomedical Eng.*, Shanghai, pp. 2357 – 2360, May 2008.

[67] F. Morbidi, A. Garulli, D. Prattichizzo, C. Rizzo, and S. Rossi, "Application of Kalman filter to remove TMS-induced artifacts from EEG recordings," *IEEE Trans. Control Systems Tech.*, vol. 16, no. 6, pp. 1360 – 1366, November 2008.

[68] R. Princy, P. Thamarai, and B. Karthik, "Denoising EEG signal using wavelet

transform," *Int. J. of Advanced Research in Computer Eng. & Tech.*, vol. 4, no. 3, pp. 1070 – 1074, March 2015.

[69] A. GuruvaReddy and S. Narava, "Artifact removal from EEG signals," *Int. J. of Computer App.*, vol. 77, no.13, pp. 17 – 19, September 2013.

[70] N. Saito and T. Sone, "Influence of modeling error on noise reduction performance of active noise control systems using filtered-X LMS algorithm," *J. Acoust. Soc.,* Japan. (E), vol. 17, no. 4, pp. 195 – 202, 1996.

[71] H.W. Sorenson, "Least-squares estimation: From Gauss to Kalman," *IEEE Spectrum*, vol. 7, no. 7, pp. 63 – 68, July 1970.

[72] S.C. Douglas and T. H-Y. Meng, "Normalized data nonlinearities for LMS adaptation," *IEEE Trans. Signal Process.*, vol. 42, no. 6, pp. 1352 – 1365, June 1994.

[73] J. Arenas-Garcia, A.R. Figueiras-Vidal, and A.H. Sayed, "Mean-square performance of a convex combination of two adaptive filters," *IEEE Trans. Signal Process.*, vol. 54, no. 3, pp. 1078 – 1090, March 2006.

[74] J. Dhiman, S. Ahmad, and K. Gulia, "Comparison between adaptive filter algorithms (LMS, NLMS and RLS)," *Int. J. Science Eng. and Tech. Research (IJSETR)*, vol. 2, no. 5, pp. 1100 – 1103, May 2013.

[75] P. He, G. Wilson, and C. Russell, "Removal of ocular artifacts from electro-encephalogram by adaptive filtering," *Medical, Biological Eng. & Computing*, vol. 42, no. 3, pp. 407 – 412, May 2004.

[76] T. Gasser, L. Sroka, and J. Mocks, "The transfer of EOG activity into the EEG for eyes open and closed," *Electroencephalography and Clinical Neurophysiology*, vol. 61, no. 2, pp. 181 – 193, August 1985.

[77] T.P. Jung, S Makeig, M. Westerfield, J. Townsend, E. Courchesne, and T.J. Sejnowski, "Removal of eye activity artifacts from visual event-related potential in normal and clinical subjects," *Clin. Neurophysiol.*, vol. 111, no. 10, pp. 1745 – 1758,

October 2000.

[78] J.L. Kenemans, P.C. Molenaar, M.N. Verbaten, and J.L. Slangen, "Removal of the ocular artifact from the EEG: A comparison of time and frequency domain methods with simulated and real data," *Psychophysiology*, vol. 28, no. 1, pp. 114 – 121, January 1991.

[79] S.M.M. Islam and M.S.U. Farid, "Denoising EEG signal using different adaptive filter algorithms, " *Int. J. Enhanced Research in Science, Tech. and Eng.*, vol. 4, no. 11, pp. 49 – 55, November 2015.

[80] A. Banerjee, K. Basu, and A. Chakraborty, "Prediction of EEG signal by digital filtering," *Proc. Inter. Conf. on Intelligent Sys. and Networks, India*, pp. 1 – 6, 2007.

[81] J.R. Hughes, "EEG in clinical practice," *J. Royal Society of Medicine,* 2nd Edition, Butterworth-Heinemann, vol. 88, September 1994.

[82] R.P. Schmidt and B.J. Wilder, *Epilepsy*. Philadelphia, USA: F.A. Davis Co., 1968.

[83] J.R.G. Carrie, "A hybrid computer technique for detecting sharp EEG transients," *Electroencephalography & Clinical Neurophysiology*, vol. 33, no. 3, pp. 336 – 338, September 1972.

[84] F.H. Lopes da Silve, K. Van Hulten, J.G. Lommen, W. StormVan Leeuwen, C.W. Van Veelen, and W. Vliegenthart, "Automatic detection and localization of epileptic foci.," *Electroencephalography & Clinical Neurophysiology*, vol. 43, no. 1, pp. 1 – 13, July 1977.

[85] B. Saltzberg, L.S. Lustick, and R.G. Heath, "Detection of focal depth spiking in the scalp EEG of monkeys," *Electroencephalography & Clinical Neurophysiology*, vol. 31, no. 4, pp. 327 – 333, October 1971.

[86] J. Gotman and P. Gloor, "Automatic recognition and quantification of interictal epileptic activity in the human scalp EEG," *Electroencephalography & Clinical Neurophysiology*, vol. 41, no. 5, pp. 513 – 529, November 1976.

[87] N. Mtetwa and L.S. Smith, "Smoothing and thresholding in neuronal spike detection," *Neurocomputing*, vol. 69, no. 10, pp. 1366 – 1370, June 2006.

[88] K. Vijayalakshmi and A.M. Abhishek, "Spike detection in epileptic patients EEG data using template matching technique," *Int. of Computer Applications*, vol. 2, no. 6, pp. 5 – 8, June 2010.

[89] R.C. Gonalez and R.E. Woods, *Digital Image Processing*. 2nd Edition, Reading, MA: Addison-Wesley Pub. Co., 1987.

[90] M. Abeles and M.H. Goldstein, "Multispike train analysis," *Proc. IEEE*, vol. 65, no. 5, pp. 762 – 773, May 1977.

[91] M. El-Gohary, J. McNames, and S. Elsas, "User-guided interictal spike detection," *Proc. IEEE 30th Annual Int. Conf. Eng. in Medicine and Biology Society*, Vancouver, BC, pp. 821 – 824, August 2008.

[92] Z. Ji, T. Sugi, S. Goto, and X. Wang, "Multi-channel template extraction for automatic EEG spike detection," *Proc. IEEE Int. Conf. Complex Medical Eng. (CME)*, Harbin, China, pp. 179 – 184, May 2011.

[93] N. Acir and C. Guzelis, "Automatic spike detection in EEG by a two-stage procedure based on support vector machines," *Computers in Biology and Medicine*, vol. 34, no. 7, pp. 561 – 575, October 2004.

[94] A.B. Barreto, J.C. Principe, and S.A. Reid, "STL: A spatio-temporal characterization of focal interictal events," *Springer, Brain Topogr*, vol. 5, no. 3, pp. 215 – 228, March 1993.

[95] M. Adjouadi, M. Cabrerizo, M. Ayala, D. Sanchez, I. Yaylali, P. Jayakar, and A. Barreto, "Detection of interictal spikes and artifactual data through orthogonal transformations," *J. Clinical Neurophysiology*, vol. 22, no. 1, pp. 53 – 64, February 2005.

[96] S. Mukhopadhyay and G.C. Ray, "A new interpretation of the nonlinear energy

operator and its efficacy in spike detection," *IEEE Trans. Biomed. Eng.*, vol. 45, no. 2, pp. 180 – 187, February 1998.

[97] P. Garcia, C.P. Suarez, J. Rodriguez, and M. Rodriguez, "Unsupervised classification of neural spike with a hybrid multilayer artificial neural network," *J. Neurosci. Methods*, vol. 82, no. 1, pp. 59 – 73, July 1998.

[98] G. Xu, J. Wang, Q. Zhang, S. Zhang, and J. Zhu, "A spike detection method in EEG based on improved morphological filter," *Comput. Biol. Med.*, vol. 37, no. 11, pp. 1674 – 1652, November 2007.

[99] A. Juozapavicius, G. Bacevicius, D. Bugelskis, and R. Samaitiene, "EEG analysis-automatic spike detection," *Nonlinear Analysis: Modelling and Control*, vol. 16, no. 4, pp. 375 – 386, December 2011.

[100] G. Xu, J. Wang, Q. Zhang, and J. Zhu, "An automatic EEG spike detection algorithm using morphological filter," *Proc. IEEE Int. Conf. Automation Science and Eng. (CASE)*, Shanghai, pp. 170 – 175, October 2006.

[101] S. Altunay, Z. Telatat, and O. Erogul, "Epileptic EEG detection using the linear prediction error energy," *Elsevier, Expert Sys. with Applications*, vol. 37, no. 8, pp. 5661 – 5665, August 2010.

[102] S. Shahid, J. Walker, and L.S. Smith, "A new spike detection algorithm for extracellular neural recordings," *IEEE Trans. Biomed. Eng.*, vol. 57, no. 4, pp. 853 – 866, April 2010.

[103] S. Shahid and J. Walker, "Cepstrum of bispectrum – A new approach to blind system reconstruction," *Signal Process.*, vol. 88, no. 1, pp. 19 – 32, January 2008.

[104] J.R. Smith, "Automatic analysis and detection of EEG spikes*," IEEE Trans. Biomed. Eng.*, vol. BME-21, no. 1, pp.1 – 7, January 1974.

[105] K. Arakawa, D.H. Fender, H. Harashima, H. Miyakawa, and Y. Saitoh, "Separation of a nonstationary component from the EEG by a nonlinear digital filter," *IEEE Trans.*

Biomed. Eng., vol. BME-33, no. 7, pp. 724 – 726, July 1986.

[106] E. Soto, E. Manjarrez, and R. Vega, "A microcomputer program for automated neuronal spike detection and analysis," *Int. J. Medical Informatics*, vol. 44, no. 3, pp. 203 – 212, May 1997.

[107] P.Y. Ktonas, "Automated spike sharp wave (SSW) detection," *In: Gevins, A. S. Remond, A., (Ed)., Methods of analysis of Brain electrical and magnetic signals, Elsevier*: Amsterdam, pp. 211 – 241, 1987.

[108] R.C. Eberhart and R.W. Dobbins, *Neural Network PC Tools- A Practice Guide*: *Chapter 10*. San Diego, California: Academic Press, Inc., 1990.

[109] O. Ozdamar, I. Yaylali, P. Jayakar, and C.N. Lopez, "Multilevel neural network system for EEG spike detection," *Proc. IEEE 4th Annual Symposium Computer based Medical Systems*, pp. 272 – 279, May 1991.

[110] O. Ozdamar, G. Zhu, I. Yaylali, and P. Jayakar, "Real-time detection of EEG spikes using neural networks," *IEEE EMBS 14th Annual Conf. Proc.*, vol. 3, pp. 1022 – 1023, November 1992.

[111] T. Kalayci and O. Ozdamar, "Wavele processing for automated neural network detection of EEG spikes," IEEE Engineer. in Med. and Bio. Mag., vol. 14, no. 2, pp. 160 – 166, March/April 1995.

[112] O. Ozdamar and T. Kalayci, "Detection of spikes with artificial neural networks using raw EEG," *Comput. and Biomed. Research*, vol. 31, no. 2, pp. 122 – 142, April 1998.

[113] D.E. Rumelhart, G.E. Hinton, and R.J. Williams, "Learning interval representations by back-propagating errors," *Nature Publishing Group*, vol. 323, no. 9, pp. 533 – 536, October 1986.

[114] R.C. Eberhart, R.W. Dobbins, and W.R.S. Webber, "CaseNet: A neural network tool for EEG waveform classification," *Proc. IEEE 2nd Annual Symp. Computer based Medical systems*, Minneapolis, MN, pp. 60 – 68, June 1989.

[115] J.C. Principe and A.M.P. Tome, “Performance and training strategies in feedforward neural networks: An application to sleep scoring,” *Proc. Int. Joint Conf. Neural Networks (IJCNN)*, pp. 341 – 346, 1989.

[116] B.H. Jansen, “Artificial neural nets for K-complex detection,” *IEEE Eng. Med. Biol. Mag.*, vol. 9, no. 3, pp. 50 – 52, September 1990.

[117] D. Alpsan and O. Ozdamar, “Backpropagation network for classifying auditory brainstem evoked potentials: input level biasing, temporal and spectral inputs and learning patterns,” *Proc. IEEE Int. Joint Conf. Neural Networks*, Washington, USA, December 1989.

[118] D. Alpsan and O. Ozdamar, “Brainstem auditory evoked potential classification by backpropagation networks,” *Proc. IEEE Int. Joint Conf. on Neural Networks*, vol. 2, pp. 1266 – 1271, November 1991.

[119] D. Alpsan and O. Ozdamar, “Auditory brainstem evoked potential classification for threshold detection by neural networks. I. Network design, similarities between human-expert and network classification feasibility,” *Automedica*, vol. 15, no. 1, pp. 67 – 82, December 1992.

[120] R.C. Eberhart and R.W. Dobbins, “Neural network design considerations for EEG spike detection,” *Proc. Northeast Bio. Eng., 15th Annual Conf.*, Boston, MA, pp. 97 – 98, March 1989.

[121] S.Y. Tseng, F.C. Chong, R.C. Chen, and T.S. Kuo, “Neural network for automatic detection of EEG spikes,” *Proc. IEEE 15th Annual Int. Conf. Eng. in Medicine and Biology Society*, pp. 461 – 462, 1993.

[122] F. Vaz and J.C. Principe, “Neural networks for EEG signal decomposition and classification,” *Proc. IEEE 17th Annual Int. Conf. Eng. in Medicine and Biology Society (EMBS) and CMBEC Signal Process.*, vol. 1, pp. 793 – 794, October 1995.

[123] Y.U. Khan and L. Tarassenko, “Detection of interictal epileptic events in EEG using

ANN," *Proc. IEE 5th Int. Conf. Artificial Neural Networks*, Cambridge, vol. 440, pp. 318 – 322, July 1997.

[124] C.J. James, R.D. Jones, P.J. Bones, and G.J. Carroll, "Spatial analysis of multi-channel EEG recordings through a fuzzy-rule based system in the detection of epiletiform events," *Proc. IEEE 20th Annual Int. Conf. Eng. in Medicine and Biology Society*, Hong Kong, vol. 20, no. 4, pp. 2175 – 2178, November 1998.

[125] S.B. Wilson and R. Emerson, "Spike detection: a review and comparison of algorithms," *Clinical Neurophysiology*, vol. 113, no. 12, pp. 1873 – 1881, January 2002.

[126] N. Acir, "Automated system for detection of epileptiform patterns in EEG by using a modified RBFN classifier," *Elsevier, Expert Syst. with Applications*, vol. 29, no. 2, pp. 455 – 462, August 2005.

[127] A.C. Walbran, C.P. Unsworth, A.J. Gunn, and L. Bennet, "A semi-automated method for epileptiform transient detection in the EEG of the fetal sheep using time-frequency analysis," *Proc. IEEE 31st Annual Int. Conf. Eng. in Medicine and Biology Society (EMBS)*, Minneapolis, Minnesota, USA, pp. 17 – 20, September 2009.

[128] Sharanreddy and P.K. Kulkarni, "EEG signal classification for epilepsy seizure detection using improved approximate entropy," *Int. J. Public Health Science (IJPHS)*, vol. 2, no, 1, pp. 23 – 32, March 2013.

[129] T. Kalayci and O. Ozdamar, "Wavelet preprocessing for automated neural network detection of EEG spikes," *IEEE Eng. Medicine and Biology Magazine*, vol. 14, no. 2, pp. 160 – 166, March/April 1995.

[130] M. Ganesan, E.P. Sumesh, and R. Vidhyalavanya, "Multi-stage, multi-resolution method for automatic characterization of epileptic spikes in EEG," *Int. J. Signal Process., Image Process. and Pattern Recognition*, vol. 3, no. 2, pp. 33 – 40, June 2010.

[131] N.J. Huan and R. Palaniappan, "Neural network classification of autoregressive features from electroencephalogram signals for brain-computer interface design," *J. Neural Eng.*, vol. 1, no. 3, pp. 142 – 150, August 2004.

[132] A.J. Casson and E. Rodriguez-Villegas, "Utilizing noise to improve an interictal spike detector," *Elsevier, J. Neuroscience Methods*, vol. 201, no. 1, pp. 262 – 268, September 2011.

[133] U. Melia, F. Claria, M. Vallverdu, and P. Caminal, "Removal of peak and spike noise in EEG signals based on the analytic signal magnitude," *Proc. IEEE 34th Annual Int. Conf. EMBS*, San Diego, California USA, pp. 3523 – 3526, August/September 2012.

[134] X. Yang and S.A. Shamma, "A totally automated system for the detection and classification of neural spikes," *IEEE Trans. Biomed. Eng.*, vol. 35, no. 10, pp. 806 – 816, October 1998.

[135] Z. Nenadic and J.W. Burdick, "Spike detection using continuous wavelet transform," *IEEE Trans. Biomed. Eng.*, vol. 52, no. 1, pp. 74 – 87, January 2005.

[136] G. Zouridakis and D.C. Tam, "Multi-unit spike discrimination using wavelet transforms," *Comput. Biol. Med.*, vol. 27, no. 1, pp. 9 – 18, February 1997.

[137] J.C. Letelier and P.P. Weber, "Spike sorting based on discrete wavelet transform coefficients," *J. Neurosci. Methods*, vol. 101, no. 2, pp. 93 – 106, September 2000.

[138] K.H. Kim and S.J. Kim, "A wavelet-based method for action potential detection from extracellular neural signal recording with low signal-to-noise ratio," *IEEE Trans. Biomed. Eng.*, vol. 50, no. 8, pp. 999 – 1011, August 2003.

[139] Y. Song and J. Zhang, "Automatic recognition of epileptic EEG patterns via extreme learning machine and multiresolution feature extraction," *Expert Syst. with Appl.*, vol. 40, no. 14, pp. 5477 – 5489, October 2013.

[140] L.S. Smith, S. Shahid, A. Vernier, and N. Mtetwa, "Finding events in noisy signals," *Proc. IET Conf. Irish Signals Syst. (ISSC)*, Derry, pp. 31 – 35, September 2007.

[141] K.P. Nayak, T.K. Padmashree, S.N. Rao, and N.U. Cholayya, "Artificial neural network for the analysis of electroencephalogram," *Proc. IEEE 4th Conf. Intelligent Sensing and Inf. Process., (ICISIP)*, Bangalore, pp. 170 – 173, December 2006.

[142] M. Nuh, A. Jazidie, and M.A. Muslim, "Automatic detection of epileptic spikes based on wavelet neural network," *Proc. IEEE Asia-Pacific Conf. Circuits and Systems (APCCAS)*, vol. 2, pp. 483 – 486, October 2002.

[143] G. Calvagno, M. Ermani, R. Rinaldo, and F. Sartoretto, " A multiresolution approach to spike detection in EEG," *Proc. IEEE Int. Conf. Acoustics, Speech, and Signal Processing, (ICASSP)*, Istanbul, pp. 3582 – 3585, June 2000.

[144] K.H. Kim and S.J. Kim, "Neural spike sorting under nearly 0-dB signal-to-noise ratio using nonlinear energy operator and artificial neural-network classifier," *IEEE Trans. Biomed. Eng.*, vol. 47, no. 10, pp. 1406 – 1411, October 2000.

[145] P. Maragos, J.F. Kaiser, and T.F. Quatieri, "On amplitude and frequency demodulation using energy operators," *IEEE Trans. Signal Process.*, vol. 41, no. 4, pp. 1532 – 1550, April 1993.

[146] Y.C. Liu, C.C.K. Lin, J.J. Tsai, and Y.N. Sun, "Model-based spike detection of epileptic EEG data," *Sensors*, vol. 13, no. 9, pp. 12536 – 12547, September 2013.

[147] B. Boashash, M. Mesbah, and H. Hassanpour, "SVD based technique for enhancing the time-frequency representation of signals," *Fourth Workshop Signal Process. Appl.*, Brisbane, Australia, pp. 113 – 116, December 2002.

[148] B. Boashash and M. Mesbah, "A time-frequency approach for newborn seizure detection," *IEEE-EMBS Mag.*, vol. 20, no. 5, pp. 54 – 64, September/October 2001.

[149] H. Hassanpour, W. Williams, M. Mesbah, and B. Boashash, "Time-frequency extraction of EEG spike events for seizure detection in neonate," *IEEE 6th Int. Symp. Signal Process. and its App. (ISSPA)*, Kuala Lumpour, Malaysia, vol. 1, pp. 246 – 249, August 2001.

[150] H. Hassanpour, M. Mesbah, and B. Boashash, "Time-frequency feature extraction of newborn seizure using SVD-based technique," *J. Applied Signal Processing (EURASIP)*, vol. 16, pp. 2544 – 2554, December 2004.

[151] H. Hassanpour, M. Mesbah, and B. Boashash, "A time-frequency approach for spike detection," *Proc. IEEE 10th Int. Conf. Electronics, Circuits and Systems (ICECS)*, vol. 1, pp. 56 – 59, December 2003.

[152] S.R. Mousavi, M. Niknazar, and B.V. Vahdat, "Epileptic seizure detection using AR model on EEG signals," *Proc. IEEE Int. Biomed. Eng. Conf.*, Cairo, pp. 1 – 4, December 2008.

[153] H.S. Liu, T. Zhang, and F.S. Yang, "A multistage, multimethod approach for automatic detection and classification of epileptiform EEG," *IEEE Trans. Biomed. Eng.*, vol. 49, no. 12, pp. 1557 – 1566, December 2002.

[154] D.M. Ward, R.D. Jones, P.J. Bones, and G.J. Carroll, "Enhancement of deep epileptiform activity in the EEG via 3-D adaptive spatial filtering," *IEEE Trans. Biomed. Eng.*, vol. 46, no. 6, pp. 707 – 716, June 1999.

[155] J. Pardey, S. Roberts, and L. Tarassenko, "A review of parametric modelling techniques for EEG analysis," *Med. Eng. Phys.*, vol. 18, no. 1, pp. 2 – 11, February 1996.

[156] D.A. Campbell, "Adaptive EEG transient event discrimination using dynamic LMS filter weight leakage," *Proc. IEEE 5th Int. Symp. Signal Process. and its Applications (ISSPA)*, Brisbane, Australia, vol. 1, pp. 359 – 362, August 1999.

[157] V.P. Oikonomou, A.T. Tzallas, and D.I. Fotiadis, "A Kalman based methodology for EEG spike enhancement," *Computer methods and Programs in Biomedicine*, vol. 85, no. 2, pp. 101 – 108, February 2007.

[158] G. Gomez-Herrero, W.D. Clercq, H. Anwar, O. Kara, K. Egiazarian, S.V. Huffel, and W.V. Paesschen, "Automatic removal of ocular artifacts in the EEG without an EOG

reference channel," *Proc. 7th Nordic Signal Process. Symposium (NORSIG)*, pp. 130 – 133, June 2006.

[159] A. Schlogl, C. Keinrath, D. Zimmermann, R. Scherer, R. Leeb, and G. Pfurtscheller, "A fully automated correction method of EOG artifacts in EEG recordings," *Clinical Neurophysiology*, vol. 118, no. 1, pp. 98 – 104, January 2007.

[160] T. Elbert, W. Lutzenberger, B. Rockstroh, and N. Birbaumer, "Removal of ocular artifacts from the EEG – A biophysical approach to the EOG," *Electroencephalogr Clinical Neurophysiology*, vol. 60, no. 5, pp. 455 – 463, May 1985.

[161] G. Gratton, M.G.H. Coles, and E. Donchin, "A new method for off-line removal of ocular artifact," *Electroencephalogr Clinical Neurophysiology*, vol. 55, no. 4, pp. 468 – 484, April 1983.

[162] O.G. Lins, T.W. Picton, P. Berg, and M. Scherg, "Ocular artifacts in EEGs and event-related potentials II: source dipole and source components," *Springer, Brain Topography*, vol. 6, no. 1, pp. 65 – 78, February 1993.

[163] R.J. Croft and R.J. Barry, "EOG correction: Which regression should we use?" *Psychophysiology*, vol. 37, no.1, pp. 123 – 125, January 2000.

[164] R.J. Croft and R.J. Barry, "Removal of ocular artifact from the EEG: A review," *Clinical Neurophysiology*, vol. 30, no. 1, pp. 5 – 19, February 2000.

[165] A.G. Correa, E. Laciar, H.D. Patino, and M.E. Valentinuzzi, "Artifact removal from EEG signals using adaptive filters in cascade," *J. Phys: Conf. Series*, vol. 90, no. 1, pp. 1 – 10, December 2007.

[166] S. Karimi, B. Molaee-Ardekani, M.B. Shamsollahi, C. Leroy, and P. Derambure, "Automatic ocular correction in EEG recordings using maximum likelihood estimation," *IEEE Int. Symposium Signal Process. and Inf. Tech. (ISSPIT)*, pp. 1 – 7, December 2013.

[167] P.M. Quilter, B.B. MacGillivray, and D.G. Wadbrook, "The removal of eye

movement artifacts from EEG signal using correlation techniques, random signal analysis," *IEEE Conf. Publication*, vol. 159, pp. 93 – 100, 1977.

[168] R.J. Croft and R.J. Barry, "EOG correction: a new aligned-artifact average solution," *Electroencephalogr Clinical Neurophysiology*, vol. 107, no. 6, pp. 395 – 401, December 1998.

[169] R.N. Vigario, "Extraction of ocular artifacts from EEG using independent component analysis," *Electroencephalography and Clinical Neurophysiology*, vol. 103, no. 3, pp. 395 – 404, September 1997.

[170] T.P. Jung, S. Makeig, C. Humphries, T.E-Won Lee, M.J. Mckeown, V. Iragui, and T.J. Sejnowski, "Removing electroencephalographic artifacts by blind source separation," *Psychophysiology*, vol. 37, no. 2, pp. 163 – 178, March 2000.

[171] S. Romero, M.A. Mananas, and M.J. Barbanoj, "Quantitative evaluation of automatic ocular removal from simulated EEG signals: regression vs. second order statistics methods," *Proc. IEEE 28th Annual Int. Conf. Eng. Medicine and Bio. Society (EMBS)*, New York City, USA, pp. 5495 – 5498, August/September 2006.

[172] S.S. Patil and M.K. Pawar, "EOG artifact correction from EEG signals for biomedical analysis," *Int. J. Computer Applications*, vol. 57, no. 9, pp. 35 – 40, November 2012.

[173] Z. Tiganj, M. Mboup, C. Pouzat, and L. Belkoura, "An algebraic method for eye blind artifacts detection in single channel EEG recordings," *Proc. 17th Int. Conf. Biomagnetism Advances in Biomagnetism*, vol. 28, no. 6, pp. 175 – 178, March 2010.

[174] W.D. Chang, J.H. Lim, and C.H. Im, "An unsupervised eye blink artifact detection method for real-time electroencephalogram processing," *Physiol. Meas.*, vol. 37, no. 3, pp. 401 – 417, March 2016.

[175] W.D. Chang, H.S. Cha, K. Kim, and C.H. Im, "Detection of eye blink artifacts from single prefrontal channel electroencephalogram," *Comput. Methods Programs Biomed.*, vol. 124, pp. 19 – 30, February 2016.

[176] S. Kim and J. McNames, “Automatic spike detection of based on adaptive template matching for extracellular neural recordings,” *J. Neurocsi. Methods*, vol. 165, no. 2, pp. 165 – 174, September 2007.

[177] P.S. Kumar, R. Arumuganathan, K. Sivakumar, and C. Vimal, “Removal of ocular artifacts in the EEG through wavelet transform without using an EOG reference channel,” *Int. J. Open Problems Compt. Math.*, vol. 1, no. 3, pp. 188 – 200, December 2008.

[178] V. Krishnaveni, S. Jayaraman, S. Aravind, V. Hariharasudhan, and K. Ramadoss, “Automatic identification and removal of ocular artifacts from EEG using wavelet transform,” *Measurement Science Review*, vol. 6, no. 4, pp. 45 – 57, 2006.

[179] V. Krishnaveni, S. Jayaraman, L. Anitha, and K. Ramadoss, “Removal of ocular artifacts from EEG using adaptive thresholding of wavelet coefficients,” *J. Neural Eng.*, vol. 3, no. 4, pp. 338 – 346, November 2006.

[180] V.D. Sanaja and V.P. Patel, “An adaptive filtering approach for removal of ocular artifact from EEG signal,” *Int. J. Innovative Research in Tech. (IJIRT)*, vol. 1, no. 11, pp. 218 – 223, 2014.

[181] Q. Zhao, B. Hu, Y. Shi, Y. Li, P. Moore, M. Sun, and H. Peng, “Automatic identification and removal of ocular artifacts in EEG – Improved adaptive predictor filtering for portable applications,” *IEEE Trans. Nano Bioscience*, vol. 13, no. 2, pp. 109 – 117, June 2014.

[182] P.A. Babu and K.V.S.V.R. Prasad, “Removal of ocular artifacts from EEG signals by fast RLS algorithm using wavelet transform,” *Int. J. Comp. App.*, vol. 21, no. 4, pp. 1 – 5, May 2011.

[183] R. Romo-Vazquez, R. Ranta, V. Lois-Dorr, and D. Maquin, “EEG ocular artifacts and noise removal,” *Proc. IEEE 29th Annual Int. Conf. Eng. Medicine and Biology Society*, pp. 5445 – 5448, August 2007.

[184] K.S. Yoo, T. Basa, and W.H. Lee, "Removal of eye blink artifacts from EEG signals based on cross-correlation," *Proc. IEEE Int. Conf. Convergence Inf. Tech.*, pp. 2005 – 2008, November 2007.

[185] G.L. Wallstrom, R.E. Kass, A. Miller, J.F. Cohn, and N.A. Fox, "Automatic correction of ocular artifacts in the EEG: a comparison of regression-based and component-based methods," *Elsevier, Int. J. Psychophsiology*, vol. 53, no. 2, pp. 105 – 119, July 2004.

[186] L. Astolfi, F. Cincotti, D. Mattia, F. Babiloni, M.G. Marciani, F.D.V. Fallani, M. Mattiocco, F. Miwakeichi, Y. Yamaguchi, P. Martinez, S. Salinari, A. Tocci, H. Bakardjian, F.B. Vialatte, and A. Cichocki, "Removal of ocular artifacts for high resolution EEG studies: simulation study," *Proc. IEEE 28th Annual Int. Conf. Eng. Medicine Biology Society (EMBS)*, pp. 976 – 979, August/September 2006.

[187] O.G. Lins, T.W. Picton, P. Berg, and M. Scherg, "Ocular artifacts in EEG and event-related potentials I: scalp topography," *Springer, Brain Topography*, vol. 6, no. 1, pp. 51 – 63, February 1993.

[188] J.L. Whitton, F. Lue, and H. Moldofsky, "A spectral method for removing eye movement artifact from the EEG," *Electroencephalogr Clinical Neurophysiology*, vol. 44, no. 6, pp. 735 – 741, June 1978.

[189] J.C. Woestenburg, M.N. Verbaten, and J.L. Slangen, "The removal of the eye-movement artifact from the EEG by regression analysis in the frequency domain," *Biological Psychology*, vol.16, no. 1 – 2, pp. 127 – 147, February 1983.

[190] T.D. Lagerlund, F.W. Sharbrough, and N.E. Busacker, "Spatial filtering of multichannel electroencephalographic recordings through principal component analysis by singular value decomposition," *J. Clinical Neurophysiol.*, vol. 14, no. 1, pp. 73 – 82, January 1997.

[191] L. Shoker, S. Sanei, W. Wang, and J.A. Chambers, "Removal of eye blinking artifact

from the electro-encephalogram, incorporating a new constrained blink source separation algorithm," *Med. Bio. Eng. Comput.*, vol. 43, no. 2, pp. 290 – 295, April 2005.

[192] C.A. Joyce, I.F. Gorodnitsky, and M. Kutas, "Automatic removal of eye movement and blink artifacts from EEG data using blind component separation," *Psychophysiology Research*, vol. 41, no. 2, pp. 313 – 325, March 2004.

[193] A. Erfanian and B. Mahmoudi, "Real-time ocular artifact suppression using recurrent neural network for electroencephalogram based on brain-computer interface," *Med. Biol. Eng. Comput.*, vol. 43, no. 2, pp. 296 – 305, April 2005.

[194] B. Noureddin, P.D. Lawrence, and G.E. Birch, "Effects of Task and EEG-based reference signal on performance of on-line ocular artifact removal from real EEG," *Proc. IEEE/EMBS 4th Int. Conf. Neural Eng.,* Antalya, Turkey, pp. 614 – 617, April/May 2009.

[195] S. Selvan and R. Srinivasan, "Removal of ocular artifacts from EEG using an efficient neural network based adaptive filtering technique," *IEEE Signal Process. Letters*, vol. 6, no. 12, pp. 330 – 332, December 1999.

[196] A. Erfanian and B. Mahmoudi, "Real-time eye blink suppression using neural adaptive filters for EEG-based brain computer interface," *Proc. IEEE Conf. 2nd Joint Eng. Medicine and Biology, Biomedical Society (EMBS/BMES)*, Houston, Tx., USA, vol. 1, pp. 44 – 45, October 2002.

[197] A. Zhang and W. Li, "Adaptive noise cancellation for removing cardiac and respiratory artifacts from EEG recordings," *Proc. IEEE, 5th World Congress Intelligent Control and Automation (WCICA)*, Hangzhou, P.R., China, vol. 6, pp. 5557 – 5560, June 2004.

[198] W. Chen, Z. Wang, K.F. Lao, and F. Wan, "Ocular artifact removal from EEG using ANFIS," *Proc. IEEE, Int. Conf. Fuzzy Systems*, Beijing, China, pp. 2410 – 2417, July

2014.

[199] B. Noureddin, P.D. Lawrence, and G.E. Birch, "Time-frequency analysis of EEG blinks and saccades in EOG for EEG artifact removal," *Proc. IEEE/EMBS, 3rd Int. Conf. Neural Eng.*, Kohala Coast, Hawaii, USA, pp. 564 – 567, May 2007.

[200] A. Cohen, *Biomedical Signal Processing*. Boca Raton, Fla: CRC Press, 1986.

[201] I. DiMatteo, C.R. Genovese, and R.E. Kass, "Bayesian curve-fitting with free-knot splines," *Biometrika*, vol. 88, no. 4, pp. 1055 – 1071, May 2001.

[202] G.L. Wallstrom, R.E. Kass, A. Miller, J.F. Cohn, and N.A. Fox, "Correction of ocular artifacts in the EEG using Bayesian adaptive regression splines," *Springer - Verlog, Bayessian Statistics*, *New York*, vol. 6, pp. 353 – 367, 2002.

[203] P. He, G. Wilson, C. Russell, and M. Gerschutz, "Removal of ocular artifacts from EEG: a comparison between time-domain regression method and adaptive filtering method using simulated data," *Med. Bio. Eng. Comput.*, vol. 45, no. 5, pp. 495 – 503, May 2007.

[204] W. Philips, "Adaptive baseline correction EEGs using warped polynomials," *Proc. IEEE-EMBC and CMBEC*, *Theme 4: Signal Process*., vol. 2, pp. 853 – 854, 1995.

[205] S. Mehrkanoon, M. Moghavvemi, and H. Fariborzi, "Real-time ocular and facial muscle artifacts removal from EEG signals using LMS adaptive algorithm," *Int. Conf. Intelligent and Advanced Sys.*, pp. 1245 – 1250, November 2007.

[206] P.T. Kavitha, C.T. Lau, and A.B. Premkumar, "Modified ocular artifact removal technique from EEG by adaptive filtering," *Proc. IEEE, 6th Int. Conf. Information, Commun. and Signal Process. (ICICS)*, pp. 1 – 5, December 2007.

[207] H. Shahabi, S. Moghimi, and H. Zamiri-Jafarian, "EEG eye blink artifact removal by EOG modeling and Kalman filter," *5th Int. Conf. BioMedical Eng. Informatics (BEMI)*, pp. 496 – 500, October 2012.

[208] G. Bodenstein and H.M. Praetorious, "Feature extraction from the

electroencephalogram by adaptive segmentation," *Proc. IEEE,* vol. 65, no. 5, pp. 642 – 652, May 1977.

[209] A.C. Guyton, *Text Book of Medical Physiology.* 7th Edition, Philadelphia, PA: Saunders, Chs. 11 and 59, 1986.

[210] V. Bajaj and R.B. Pachori, "Epileptic seizure detection based on the instantaneous area of analytic intrinsic mode functions of EEG signals," *Springer, Biomed. Eng. Lett.*, vol. 3, no. 1, pp. 17 – 21, March 2013.

[211] G. Garg, V. Singh, J.R.P. Gupta, and A.P. Mittal, "Wrapper based wavelet feature optimization for EEG signals," *Springer, Biomed. Eng. Lett.*, vol. 2, no. 1, pp. 24 – 37, March 2012.

[212] Y. Kumar, M.L. Dewal, and R.S. Anand, "Relative wavelet energy and wavelet entropy based epileptic brain signals classification," *Springer, Biomed. Eng. Lett.*, vol. 2, no. 3, pp. 147 – 157, September 2012.

[213] A.T. Tzallas, V.P. Oikonomou, and D.I. Fotiadis, "Epileptic spike detection using a Kalman filter based approach," *Proc. IEEE Int.28th Conf. EMBS*, NY, USA, pp. 501 – 504, August/September 2006.

[214] T.P. Exarchos, A.T. Tzallas, D.I. Fotiadis, S. Konitsiotis, and S. Giannopoulos, "EEG transient event detection and classification using association rules," *IEEE Trans. Inform. Technol. Biomedicine*, vol. 10, no. 3, pp. 451– 457, July 2006.

[215] W.D. Penny and S.J. Roberts, "Dynamic models for nonstationary signal segmentation," *Elsevier, Comput. & Biomedical Res.*, vol. 32, no. 6, pp. 483 – 502, December 1999.

[216] A. Potamianos and P. Maragos, "A comparison of the energy operator and the Hilbert transform approach to signal and speech demodulation," *Elsevier, Signal Processing*, vol. 37, no. 1, pp. 95 – 120, May 1994.

[217] J.F. Kaiser, "On a simple algorithm to calculate the 'energy' of a signal," *Proc. IEEE*

Int. Conf. Acoustic Speech and Signal Processing, Albuquerque, NM, vol. 1, pp. 381–384, April 1990.

[218] J.F. Kaiser, "On Teager's energy algorithm and its generalization to continuous signals," *Proc. IEEE 4th Digital Signal Processing Workshop,* Mohonk (New Paltz), NY, September 1990.

[219] J.G. Proakis and D.G. Manolakis, *Digital Signal Processing: Principles, Algorithms and Applications*. 3rd Edition, USA: Pearson Education, 1996.

[220] H. Semmaoui, J. Drolet, A. Lakhssassi, and M. Sawan, "Setting adaptive spike detection threshold for smoothed TEO based on robust statistics theory," *IEEE Trans. Biomed. Eng.*, vol. 59, no. 2, pp. 474 – 482, February 2012.

[221] A. Papoulis, *Probability Random Variables and Stochastic Processes.* 3rd Edition, USA: McGraw-Hill, 1984.

[222] A.M. White, P.A. Williams, D.J. Ferraro, S. Clark, S.D. Kadam, F.E. Dudek, and K.J. Staley, "Efficient unsupervised algorithms for the detection of seizures in continuous EEG recordings from rats after brain injury," *Elsevier, J. Neuroscience Methods*, vol. 152, no. 1-2, pp. 255 – 266, April 2006.

[223] R.Q. Quiroga, A. Kraskov, T. Kreuz, and P. Grassberger, "Performance of different synchronization measures in real data: A case study on electroencephalographic signals," *The American Physical Society, Physical Review E*, vol. 65, no. 041903, pp. 1 – 14, March 2002.

[224] R.Q. Quiroga, T. Kreuz, and P. Grassberger, "Event synchronization: A simple and fast method to measure synchronicity and time delay patterns," *The American Physical Society, Physical Review E*, vol. 66, no. 041904, pp. 1 – 9, October 2002.

[225] C. Shao, S. Li, and J. Fan, "EEG spike detection based on qualitative modeling of visual observation," *Proc. IEEE 4th Int. Conf. on Fuzzy Systems and Knowledge Discovery,* Haikou, vol. 2, pp. 745 – 748, August 2007.

[226] S. Aydin, “Comparison of power spectrum predictors in computing coherence functions for intracortical EEG signals,” *Annals of Biomed. Eng. society*, vol. 37, no. 1, pp. 192 – 200, January 2009.

[227] N. Acir, I. Oztura, M. Kuntalp, B. Baklan, and C. Guzelis, “Automatic detection of epileptiform events in EEG by a three-stage procedure based on artificial neural networks,” *IEEE Trans. Biomed. Eng.*, vol. 52, no. 1, pp. 30 – 40, January 2005.

[228] M. Arnold, W.H.R. Miltner, H. Witte, R. Bauer, and C. Braun, “Adaptive AR modeling of nonstationary time series by means of Kalman filtering,” *IEEE Trans. Biomed. Eng.*, vol. 45, no. 5, pp. 553 – 562, May 1998.

[229] S. Dandapat, and G.C. Ray, “Spike detection in biomedical signals using midprediction filter,” *IEEE Trans. Medical and Biological Eng. and Computing*,” vol. 35, no. 4, pp. 354 – 360, July 1997.

[230] P.J. Durka, “Adaptive time-frequency parameterization of epileptic spikes,” *Physical Review E*, vol. 69 (051914), no. 5, pp. 1 – 5, May 2004.

[231] G.M. Friesen, T.C. Jannett, M.A. Jadallah, S.L. Yates, S.R. Quint, and H.T. Nagle, “A comparison of the noise sensitivity of nine QRS detection algorithms,” *IEEE Trans. Biomed. Eng.*, vol. 37, no. 1, pp. 85 – 98, January 1990.

[232] J.D. Frost, P. Kellaway, R.A. Hrachovy, D.G. Glaze, and E.M. Mizrahi, “Changes in epileptic spike configuration associated with attainment of seizure control,” *Ann Neurology*, vol. 20, no. 6, pp. 723 – 726, December 1986.

[233] H.K. Garg and A.K. Kohli, “Nonstationary-epileptic-spike detection algorithm in EEG signal using SNEO,” *Springer, Biomed. Eng. Lett.*, vol. 3, no. 2, pp. 80 – 86, June 2013.

[234] D. Godard, “Channel equalization using a Kalman filter for fast data transmission” *IBM J. Res. and Develop.*, vol. 18, no. 3, pp. 267 – 273, May 1974.

[235] M.S. Grewal and A.P. Andrews, *Kalman Filtering: Theory and Practice*. USA:

Prentice-Hall, Englewood Cliffs, 1993.

[236] M.S. Grewal and A.P. Andrews, *Kalman Filtering Theory and Practice using MATLAB.* 3rd Edition, USA: John Wiley & Sons, 2008.

[237] H. Hassanpour, M. Mesbah, and B. Boashash, "EEG spike detection using time-frequency signal analysis," *Proc. IEEE Int. Conf. Acoustics, Speech and Signal Proc. (ICASSP)*, vol. 5, pp. 421 – 424, May 2004.

[238] C.J. James, M.T. Hagan, R.D. Jones, P.J. Bones, and G.J. Carroll, "Multireference adaptive noise canceling applied to the EEG," *IEEE Trans. Biomed. Eng.*, vol. 44, no. 8, pp. 775 – 779, August 1997.

[239] S.M. Kay, *Fundamentals of Statistical Signal Processing Estimation Theory*. USA: Prentice-Hall, Englewood Cliffs, 1993.

[240] M.B. Malarvili, H. Hassanpour, M. Mesbah, and B. Boashash, "A histogram-based electroencephalogram spike detection," *Proc. 8th International Symp. on Signal Processing & Its Applications*, Sydney, Australia, vol. 1, pp. 207 – 210, August 2005.

[241] R.K. Mehra, "On the identification of variances and adaptive Kalman filtering," *IEEE Trans. Automatic Control*, vol. AC-15, no. 2, pp. 175–184, April 1970.

[242] R.K. Mehra, "On-line identification of linear dynamic systems with applications to Kalman filtering," *IEEE Trans. Automatic Control*, vol. AC-16, no. 1, pp. 12 – 21, February 1971.

[243] R.K. Mehra, "Approaches to adaptive filtering," *IEEE Trans. Automatic Control*, vol. 17, no. 5, pp. 693 – 698, October 1972.

[244] D.L. Schomer and F.L.D. Silva, *Niedermeyer's Electroencephalography: Basic Principles, Clinical Applications, and Related Fields*. 6th Ed., USA: Lippincott, 2012.

[245] C.C.C. Pang, A.R.M. Upton, G. Shine, and M.V. Kamath, "A comparison of algorithms for detection of spikes in the electroencephalogram" *IEEE Trans. Biomed. Eng.*, vol. 50, no. 4, pp. 521 – 526, April 2003.

[246] V. Parsa and P.A. Parker, “Multireference adaptive noise cancellation applied to somatosensory evoked potentials,” *IEEE Trans. Biomed. Eng.*, vol. 41, no. 8, pp. 792 – 800, August 1994.

[247] P.K. Sadasivan and D.N. Dutt, “ANC schemes for the enhancement of EEG signals in the presence of EOG artefacts,” *Comput. and Biomed. Res.*, vol. 29, no. 1, pp. 27 – 40, February 1996.

[248] F.H. Lopedasilva, A. Dijk, and H. Smits, “Detection of nonstationarities in EEG’s using autoregressive model – an application to EEG’s of epileptics,” *Computerized EEG Analysis*, G. Dolce and H. Kundel (Eds.), Stuttgart, Gustav Fischer Verlag, pp. 180 – 199, 1975.

[249] L. Tarassenko, Y.U. Khan, and M.R.G. Holt, Identification of inter-ictal spikes in the EEG using neural network analysis, *IEE Proc. Science, Measurement and Tech.*, vol. 145, no. 6, pp. 270 – 278, November 1998.

[250] M.P. Tarvainen, S.D. Georgiadis, P.O. Ranta-aho, and P.A. Karjalainen, “Time-varying analysis of heart rate variability with Kalman smoother algorithm,” *Physiological Measurement*, vol. 27, no. 3, pp. 225 – 239, January 2006.

[251] A.T. Tzallas, M.G. Tsipouras, D.G. Tsalikakis, E.C. Karvounis, L. Astrakas, S. Konitsiotis, and M. Tzaphlidou, “Automated epileptic seizure detection methods: A review study,” *Epilepsy-Histological, Electroencephalographic and Physiological Aspects*, pp. 75 – 99, February 2012.

[252] G. Yen and A.N. Michel, “A learning and forgetting algorithm in associative memories: Results involving pseudo-inverses,” *IEEE Trans. Circuit and Systems*, vol. 38, no. 10, pp. 1193 – 1205, October 1991.

[253] R. Verleger, T. Gasser, and J. Mocks, “Correction of EOG artifacts in event-related potentials of the EEG: Aspects of reliability and validity,” *Psychophysiology*, vol. 19, no. 4, pp. 472 – 480, July 1982.

[254] J.T. Connor, R. Martin, and L.E. Atlas, “Recurrent neural networks and robust time series prediction,” *IEEE Trans. Neural Netw.*, vol. 5, no. 2, pp. 240–254, March 1994.

[255] A.K. Kohli and D.K. Mehra, “Tracking of time-varying channels using two-step LMS-type adaptive algorithm,” *IEEE Trans. Signal Process.*, vol. 54, no. 7, pp. 2606 – 2615, July 2006.

[256] X.H. Yu, Z.Y. He, and Y.S. Zhang, “Time-varying adaptive filters for evoked potential estimation,” *IEEE Trans. Biomed. Eng.,* vol. 41, no. 11, pp. 1062 – 1071, November 1994.

[257] A. Rai and A.K. Kohli, “Adaptive polynomial filtering using generalized variable step-size least mean pth power (LMP) algorithm,” *Springer, Circuits, Systems and Signal Process.*, vol. 33, no.12, pp. 3931 – 3947, December 2014.

[258] X.H. Yu, Y.S. Zhang, and Z.Y. He, “Peak component latency-correlated average method for evoked potential waveform estimation,” *IEEE Trans. Biomed. Eng.,* vol. 41, no. 11, pp. 1072 – 1082, November 1994.

[259] Y.S. Cho, S.B. Kim, and E.J. Powers, “Time-varying spectral estimation using AR models with variable forgetting factors,” *IEEE Trans. Signal Process.,* vol. 39, no. 6, pp. 1422 – 1426, June 1991.

[260] K.T. Wagner and M. Doroslovacki, *Proportionate-Type Normalized Least Mean Square Algorithms*. NJ, USA: Johan Wiley & Sons Inc., 2013.

[261] https://www.physionet.org

[262] N. Tengtrairat, W.L. Woo, S.S. Dlay, and B. Gao, “Online noisy single-channel source separation using adaptive spectrum amplitude estimator and masking,” *IEEE Trans. Signal Process.*, vol. 64, no. 7, pp. 1881 – 1895, April 2016.

[263] R. Yadav, M.N.S. Swamy, and R. Agarwal, “Model-based seizure detection for intracranial EEG recordings,” *IEEE Trans. Biomedical Eng.*, vol. 59, no. 5, pp. 1419 – 1428, May 2012.

[264] J.K. Johannesen, J. Bi, R. Jiang, J.G. Kenney, and C-M.A. Chen, "Machine learning identification of EEG features predicting working memory performance in schizophrenia and healthy adults," *Neuropsychiatric Electrophysiology*, vol. 2, no. 3, pp. 1 – 21, February 2016.

[265] Y. Kumar, M.L. Dawal, and R.S. Anand, "Epileptic seizure detection using DWT based fuzzy approximate entropy and support vector machine, *Neurocomputing*, vol. 133, pp. 271 – 279, June 2014.

[266] S. Gazor, "Prediction in LMS-type adaptive algorithms for smoothly time varying environments," *IEEE Trans. on Signal Proccess.*, vol. 47, no. 6, pp. 1735 – 1739, June 1999.

[267] S. Venkataramanan, P. Prabhat, S.R. Choudhury, H.B. Nemade, and J.S. Sahambi, "Biomedical instrumentation based on electrooculogram (EOG) signal processing and application to a hospital alarm system," *IEEE Proc. Int. Conf. Intelligent Sensing and Information Process.*, pp. 535 – 540, November 2005.

[268] I. Saini, D. Singh, and A. Khosla, "QRS detection using k-nearest neighbor algorithm (KNN) and evaluation on standard ECG databases," *Elsevier, J. Advanced Research*, vol. 4, no. 4, pp. 331 – 344, July 2013.

[269] H.K. Garg and A.K. Kohli, "EEG spike detection technique using output correlation method - A Kalman filtering approach," *Springer, Circuits, Systems and Signal Process.*, vol. 34, no. 8, pp. 2643 – 2665, August 2015.

[270] D. Ko, C. Lee, E-J. Lee, S.H. Lee, and K.Y. Jung, "A dry and flexible electrode for continuous-EEG monitoring using silver balls based polydimethylsiloxane (PDMS)," *Springer, Biomed. Eng. Lett*., vol.2, pp. 18 – 23, February 2012.

[271] S. Kumar, A. Kumar, S. Anand, and A. Krishnan K., "Cumulative power spectrum of EEG – A predictor of awake and sleep state," *Int. J. Emerging Tech.*, vol. 1, no. 1, pp. 27 – 30, 2010.